SELECTIVE ENRICHMENT OF GLYCOPROTEINS USING MAGNETIC MICROSPHERES AND THEIR SENSITIVE DETECTION WITH SURFACE ENHANCED RAMAN SPECTROSCOPY

GLİKOPROTEİNLERİN MANYETİK MİKROKÜRELER KULLANILARAK SEÇİCİ ZENGİNLEŞTİRİLMESİ VE YÜZEY DESTEKLİ RAMAN SPEKTROSKOPİSİ İLE HASSAS TAYİNİ

BÜŞRA BİLGİÇ

ASST. PROF. DR. EDA ÇELİK AKDUR
Supervisor

Submitted to Graduate School of Science and Engineering of Hacettepe University
as a Partial Fulfillment to the Requirements
for the Award of the Degree of Master of Science
in Chemical Engineering

2018

This work named "**Selective Enrichment of Glycoproteins Using Magnetic Microspheres and Their Sensitive Detection with Surface Enhanced Raman Spectroscopy**" by **BÜŞRA BİLGİÇ** has been approved as a thesis for the Degree of **MASTER OF SCIENCE IN CHEMICAL ENGINEERING** by the below mentioned Examining Committee Members.

Prof. Dr. Tülin KUTSAL
Head .....

Asst. Prof. Dr. Eda ÇELİK AKDUR
Supervisor .....

Prof. Dr. Süleyman Ali TUNCEL
Member .....

Prof. Dr. Hülya YAVUZ ERSAN
Member .....

Prof. Dr. Pınar ÇALIK
Member .....

This thesis has been approved as a thesis for the Degree of **MASTER OF SCIENCE IN CHEMICAL ENGINEERING** by Board of Directors of the Institute for Graduate School of Science and Engineering.

Prof. Dr. Menemşe Gümüşderelioğlu
Director of the Institute of
Graduate School of Science and Engineering

YAYINLAMA VE FİKRİ MÜLKİYET HAKLARI BEYANI

Enstitü tarafından onaylanan lisansüstü tezimin/raporumun tamamını veya herhangi bir kısmını, basılı (kağıt) ve elektronik formatta arşivleme ve aşağıda verilen koşullarla kullanıma açma iznini Hacettepe üniversitesine verdiğimi bildiririm. Bu izinle Üniversiteye verilen kullanım hakları dışındaki tüm fikri mülkiyet haklarım bende kalacak, tezimin tamamının ya da bir bölümünün gelecekteki çalışmalarda (makale, kitap, lisans ve patent vb.) kullanım hakları bana ait olacaktır.

Tezin kendi orijinal çalışmam olduğunu, başkalarının haklarını ihlal etmediğimi ve tezimin tek yetkili sahibi olduğumu beyan ve taahhüt ederim. Tezimde yer alan telif hakkı bulunan ve sahiplerinden yazılı izin alınarak kullanması zorunlu metinlerin yazılı izin alarak kullandığımı ve istenildiğinde suretlerini Üniversiteye teslim etmeyi taahhüt ederim.

☐ **Tezimin/Raporumun tamamı dünya çapında erişime açılabilir ve bir kısmı veya tamamının fotokopisi alınabilir.**
(Bu seçenekle teziniz arama motorlarında indekslenebilecek, daha sonra tezinizin erişim statüsünün değiştirilmesini talep etseniz ve kütüphane bu talebinizi yerine getirse bile, tezinin arama motorlarının önbelleklerinde kalmaya devam edebilecektir.)

☒ **Tezimin/Raporumun 11/02/2021 tarihine kadar erişime açılmasını ve fotokopi alınmasını (İç Kapak, Özet, İçindekiler ve Kaynakça hariç) istemiyorum.**
(Bu sürenin sonunda uzatma için başvuruda bulunmadığım taktirde, tezimin/raporumun tamamı her yerden erişime açılabilir, kaynak gösterilmek şartıyla bir kısmı ve ya tamamının fotokopisi alınabilir)

☐ **Tezimin/Raporumun ..... tarihine kadar erişime açılmasını istemiyorum, ancak kaynak gösterilmek şartıyla bir kısmı veya tamamının fotokopisinin alınmasını onaylıyorum.**

☐ **Serbest Seçenek/Yazarın Seçimi**

11 / 02 / 2018

Büşra BİLGİÇ

Öğrencinin Adı Soyadı

ETHICS

In this thesis study, prepared in accordance with the spelling rules of Institute of Graduate Studies in Science of Hacettepe University,

I declare that

- all the information and documents have been obtained in the base of the academic rules
- all audio-visual and written information and results have been presented according to the rules of scientific ethics
- in case of using others Works, related studies have been cited in accordance with the scientific standards
- all cited studies have been fully referenced
- I did not do any distortion in the data set
- and any part of this thesis has not been presented as another thesis study at this or any other university.

05/02/2018

Büşra BİLGİÇ

ABSTRACT

Selective Enrichment of Glycoproteins Using Magnetic Microspheres and Their Sensitive Detection with Surface Enhanced Raman Spectroscopy

Büşra BİLGİÇ

Master of Science, Department of Chemical Engineering

Supervisor: Asst. Prof. Dr. Eda ÇELİK AKDUR

February 2018, 77 pages

Glycoproteins play critical roles including cell−cell interaction; signal transduction, protein folding, molecular recognition and host-pathogen interactions in metabolism. Glycoproteins are also widely used in pharmaceutical industry because of effectiveness in drug stability, pharmacokinetic and immunogenicity. Antibodies and antibody-derived molecules are the leading family of biopharmaceuticals. One of the most popular antibody is Immunoglobulin G (IgG) and its production at high levels of purity is an important process necessity.

In the first part of this study, a magnetic silica based sorbent was used to purify IgG glycoprotein from complex serum media. The sorbent was functionalized with amino phenyl boronic acid (APBA) group to obtain pH-dependent diol-sensitive system for IgG purification. Adsorption-desorption mechanism was observed and optimum conditions were studied. 0.05 M HEPES buffer, pH 8.5, was used as binding buffer. IgG adsorption behavior was found compatible with Langmuir model; it shows that adsorption has occurred as a single layer and homogeneously. Maximum adsorption capacity of IgG was calculated as 84 $mg.g^{-1}$. After the adsorption process, optimization of the desorption media was performed. Optimum isolation of IgG was obtained with 5 mg sorbent in 1 M Tris-Cl (pH 8.5) with 0.2 M NaCl. After the purification process, IgG in serum was concentrated 4-fold and IgG was found approximately 80% purity in elution buffer.

In the second part of this study, after the effective purification step of glycoproteins, sensitive and fast detection of these glycan structures were investigated for possible use in pathogen detection, early diagnosis of today's important disorders like cancer, diabetes and effective pharmaceuticals production. For this purpose, Surface Enhanced Raman Spectroscopy (SERS)

technique was used with diol sensitive mercapto phenyl boronic acid (MPBA) functionalized Ag nanoshell coated magnetic polymethyacrylate microspheres (MPBA-Ag@MagPMMS). As model proteins, much similar RNase A protein (negative control) and RNase B glycoprotein were used with this special sandwich system. Characterization and quantification of adsorbed glycoproteins were realized with this technique. RNase B concentrations down to 0.1 ng/mL, nearly 10^{-15} M, could be detected with this method effectively.

Keywords: Boronate Affinity Chromatography, Glycoprotein Enrichment, IgG, SERS, RNase A, RNase B

ÖZET

Glikoproteinlerin Manyetik Mikroküreler Kullanılarak Seçici Zenginleştirilmesi ve Yüzey Destekli Raman Spektroskopisi ile Hassas Tayini

Büşra BİLGİÇ

Yüksek Lisans, Kimya Mühendisliği Bölümü

Tez Danışmanı: Yrd. Doç. Dr. Eda ÇELİK AKDUR

Şubat 2018, 77 sayfa

Glikoproteinler metabolizmada hücre-hücre etkileşimi, sinyal iletimi, protein katlanması, molekül tanıma ve konakçı-patojen etkileşimi gibi konularda kritik rol oynamaktadır. Ayrıca, ilaç endüstrisinde ilacın kararlılığı, farmokokinetik ve imunojenik özellikleri üzerindeki etkisi sebebiyle glikoproteinler sıklıkla kullanılmaktadır. Antikor ve antikor türevli moleküller ilaç endüstrisinin başlıca üyelerindendir. Antikorların en popülerlerinden biri de İmmunoglobulin G (IgG) glikoproteini olup, yüksek saflıkta üretimi önemlidir.

Çalışmanın ilk bölümünde, kompleks serum ortamından IgG glikoproteinini saflaştırmak için manyetik, silika temelli bir sorbent kullanılmıştır. IgG saflaştırmak amacıyla pH-bağımlı diol gruplarına seçimli bağlanmayı sağlayan bir sistem olarak sorbent, amino fenil boronik asit (APBA) grubu ile fonksiyonalize edilmiştir. Adsorpsiyon-desorpsiyon mekanizmaları incelenmiş ve optimum koşullar araştırılmıştır. Bağlayıcı tampon çözelti olarak 0.05 M pH 8.5 HEPES kullanılmıştır. IgG adsorpsiyon davranışı Langmuir modeli ile uyumlu bulunmuştur; bu da adsorpsiyonun tek tabaka halinde ve homojen olarak gerçekleştiğini göstermektedir. IgG maksimum adsorpsiyon kapasitesi 84 $mg.g^{-1}$ olarak hesaplanmıştır. Adsorpsiyon işleminden sonra glikoproteini saflaştırmak için en iyi desorpsiyon ortamı incelenmiştir. IgG'nin optimum izolasyonu 0.2 M NaCl içeren 1 M Tris-Cl (pH: 8.5) desorpsiyon ortamında 5 mg sorbent kullanarak elde edilmiştir. Saflaştırma işleminden sonra serum içerisindeki IgG glikoproteini 4 kat konsantre edilmiş olup, elüsyonlarda 80% saflığında IgG gözlenmiştir.

Çalışmanın ikinci kısmında ise, etkili bir saflaştırma işleminden sonra; patojen tanısı, kanser, diyabet gibi günümüz hastalıklarının erken teşhisi ve etkili

farmasötiklerin geliştirilmesi kapsamında önemli bir araç olan glikan yapıların hassas ve hızlı tayini incelenmiştir. Bu amaçla, diol gruplarına seçimli olarak bağlanmayı sağlayan merkapto fenil boronik asit (MPBA) ile fonksiyonalize edilmiş gümüş kabuğa sahip manyetik polimetakrilat mikroküreler (MPBA-Ag@MagPMMS) yardımıyla Yüzeyce Zenginleştirilmiş Raman Spektroskopisi (SERS) tekniği kullanılmıştır. Model protein olarak birbirine oldukça benzer yapıda olan RNase A proteini (negatif kontrol) ve RNase B glikoproteini bu özel sandviç sistemiyle kullanılmıştır. Adsorplanan glikoproteinlerin karakterizasyonu ve nicel ölçümü bu teknikle gerçekleştirilmiştir. Bu yöntemle, 0.1 ng/mL, yaklaşık 10^{-15} M, derişim seviyesine kadar RNase B tayini kolaylıkla yapılabilmiştir.

Anahtar Kelimeler: Boronat Afinite Kromatografisi, Glikoprotein Saflaştırma, IgG, SERS, RNase A, RNase B

ACKNOWLEDGMENTS

I would like to express my greatest appreciation to my supervisor Asst. Prof. Dr. Eda ÇELIK AKDUR for her helpful criticism, guidance and patience in the progress and preparation of this thesis.

I especially want to send my thanks to Prof. Dr. Süleyman Ali TUNCEL for his creative ideas, technical supports and facilities. I am also grateful to Lab 12 members, especially Dr. Kouroush SALİMİ, Dr. Çiğdem KİP and Duygu Deniz USTA for their endless cooperation and kindness to improve my studies.

I specially want to send my greatest thanks to my lab-mates Khaliunsarnai TSOGTBAATAR, Kübra ÇALIŞIR, Ayfer KOYUNCU, İlkay KOÇER, Murat AKDOĞAN and Ece ANTURAN for their friendship, assistance and encouragement.

The moral support and opportunities supplied by TÜBİTAK SAGE especially in the experimental studies and preparation of thesis have an important place in my studies so I am also grateful to my institution.

I want to express my gratitude to my precious family Nimet BİLGİÇ, Necati BİLGİÇ and Berk BİLGİÇ for their implicit, explicit and complimentary help, support, encouragement and understanding, not only during my thesis, but also throughout my life.

TABLE OF CONTENTS

FIGURES

TABLES

SYMBOLS AND ABBREVIATIONS

Symbols

%	Percentage
°C	Centigrate Degree
µL	Microliter
Ag	Silver
A_T	Temkin isotherm equilibrium binding constant(L/g)
Au	Gold
B	Maximum adsorption process heat related constant
b_T	Temkin isotherm constant
C_0	Initial concentration of adsorbent (mg/L)
C_e	Equilibrium concentration of adsorbent (mg/L)
Cu	Copper
E	Energy
fmol	femtomole
kDa	Kilodalton
K_D	Dissociation constant
K_f	Freundlich isotherm constant
K_L	Langmuir adsorption constant (L/mg)
m	Mass
mg	Miligram
min	Minute
mL	Mililitre
mM	Milimolar
mW	Miliwatt
n	Adsorption density constant
nm	Nanometer
R	Gas constant (8.314 J/mole/K)
R^2	Variation Constant
s	Second
T	Temperature (K)

V	Volume
q_e	Adsorbed quantity by unit adsorbent at equilibrium concentration (mg/g)
q_m	Maximum adsorption capacity of adsorbent (mg/g)

Abbreviations

APBA	Amino phenyl boronic acid
APTES	3-Aminopropyl triethoxysilane
BSA	Bovine serum albumin
CEA	Carcinoembryonic antigen
DMAB	Dimethylamino benzaldehyde
EDC.HCl	N-(3-Dimethylaminopropyl)-N′-ethylcarbodiimide hydrochloride
EMEA	European Medicines Agency
FDA	U.S. Food and Drug Administration
Fe_3O_4	Iron oxide
GMA	Glycdyl methacrylate
GNP	Glyconanoparticles
HC	Heavy Chain
HEPES	4-(2-Hydroxyethyl)piperazine-1-ethanesulfonic acid, N-(2-Hydroxyethyl)piperazine-N′-(2-ethanesulfonic acid)
IgG	Immunoglobulin G
LC	Light Chain
LPS	Lipopolysaccharide
LSPR	Localized Surface Plasmon Resonance
mAb	Monoclonal Antibody
MNP	Magnetic Nanoparticles
MPBA	Mercapto phenyl boronic acid
MS	Mass spectrometry
NaCl	Sodium chloride
NHS	N-hydroxysuccinimide
NIR	Near Infrared
NMR	Nuclear magnetic resonance
PATP	p-aminothiophenol

PBS	Phosphate buffered saline
PMMS	Polymethacrylate microspheres
PSA	Prostate specific antigen
PTM	Posttranslational modification
RNase	Ribonuclease
SAM	Self-assembled monolayers
SDS-PAGE	Sodium dodecyl sulfate polyacrylamide gel electrophoresis
SERS	Surface Enhanced Raman Spectroscopy
SiO_2	Silica
TEA	Triethanolamine
Tris-Cl	Tris chloride
UV	Ultraviolet
QD	Quantum dots

1. INTRODUCTION

Complex carbohydrates (glycans) bind to lipids and proteins as a result of “glycosylation” process. The glycans bound with this posttranslational modification play critical roles including cell−cell interaction, signal transduction, protein folding, molecular recognition and host-pathogen interactions [1-3]. It is known that differentiation in glycosylation is the reason of some diseases like cancer and retroviral infections [4, 5]. At the same time, rise in glycosylation level of proteins like albumin and hemoglobin is the reporter of diabetic disorders [6, 7].

Glycoproteins are also widely used in pharmaceutical industry because of effectiveness in drug stability, pharmacokinetic and immunogenicity [8]. Monoclonal antibodies (mAb) and antibody-derived molecules are the leading group of biopharmaceuticals considering therapeutic and market potential, with total sales expected to reach $70 billion in recent years [9]. Nowadays, more than 40 mAb-based drugs have been approved by regulatory agencies (EMEA, FDA) for the treatment of several diseases like cancer, multiple sclerosis and rheumatoid arthritis. As a result of the increasing patient population and relatively low capacity of mAbs, the need for production processes to produce consistently large amounts of pharmaceutical-grade mAbs arises [10].

The most abundant type of antibody is Immunoglobulin G (IgG). It protects against viral and bacterial infections and is also found in all body fluids. IgG is produced in a delayed response to an infection and can be retained in the body for some time. IgG is very useful for passive immunization because of the long half-life in serum. For these reasons, IgG is the principle antibody used in clinical diagnostics and immunological research.

The increasing demand for these therapeutic agents further demonstrates the need to establish economical and feasible production processes. Currently, almost all of the marketed therapeutic antibodies are produced in mammalian cells [11]. Since the latest improvements in cell culture productivity, the emphasis has now shifted to the downstream processing. Protein purification strategy is still a challenging topic in today’s technology. Currently, there are several methods to separate or enrich glycoproteins, majority of them being lectin-affinity

chromatography [12-15], hydrazide chemistry [16, 17], size exclusion [18] and hydrophilic interaction chromatography [19, 20].

In addition to these strategies, in recent decades, boronic acid-based affinity methods have become more and more popular and have been successfully applied in enrichment of glycoproteins [9, 21, 22]. The boronic acid groups can tightly form a covalent bond with biomolecules containing cis-1,2-diols moiety in an alkaline environment, while the five or six membered cyclic esters dissociate by switching to acidic solutions [23]. Boronic acid functionalized materials like iron oxide magnetic nanoparticles (MNP's) are commonly used in glycoprotein enrichment because they provide a quick and simple separation process by using an external magnetic field [9, 21, 24, 25]. However, there is still a need for micro-sized particles with high affinity and selectivity towards glycoproteins.

After the effective purification step of glycoproteins, sensitive and fast detection of these glycan structures is another important topic, especially for pathogen detection and early diagnosis of today's important disorders like diabetes and cancer [26]. Surface Enhanced Raman Spectroscopy (SERS) technique is one of the most powerful spectroscopic techniques used in determination of analytes due to some key advantages [27, 28]. SERS technique generates spectra specific to molecules with one molecule sensitivity by using metal nanoparticles as signal inducer surface for Raman scattering [29]. SERS is also preferred for non-destructive, cheap, fast, sensitive and quantitative detection of analytes.

In this study, firstly, purification of IgG glycoprotein from serum sample was aimed, using APBA@MagSiO2 microbeads. For effective enrichment of IgG, binding and elution conditions were optimized, where quantitative detection of the glycoprotein was realized using SDS-PAGE and spectrophotometric methods. In the second part, SERS technique was used for ultrasensitive detection of glycoproteins. For this purpose, diol sensitive MPBA-Ag@MagPMMS was used. As model proteins, much similar RNase A protein (negative control) and RNase B glycoprotein were preferred. The detection limit of RNase B glycoprotein was obtained at femtomolar levels.

2. LITERATURE SURVEY

2.1. Carbohydrate Structures in Organisms

Carbohydrates in nature are very broad class of biopolymers found as monosaccharides, oligosaccharides, polysaccharides and glycoconjugates, and are found in nearly all plants and animals. More common monosaccharides in organisms are glucose, fucose, mannose, galactose sialic acid, *N*-acetylglucosamine and *N*-acetylgalactosamine (Figure 2.1). These are joined together with loss of a molecule of water by using a glycosidic bond. It can be possible to form more than 10 million tetrasaccharides from combination of just nine monosaccharides, it is highly extraordinary [30].

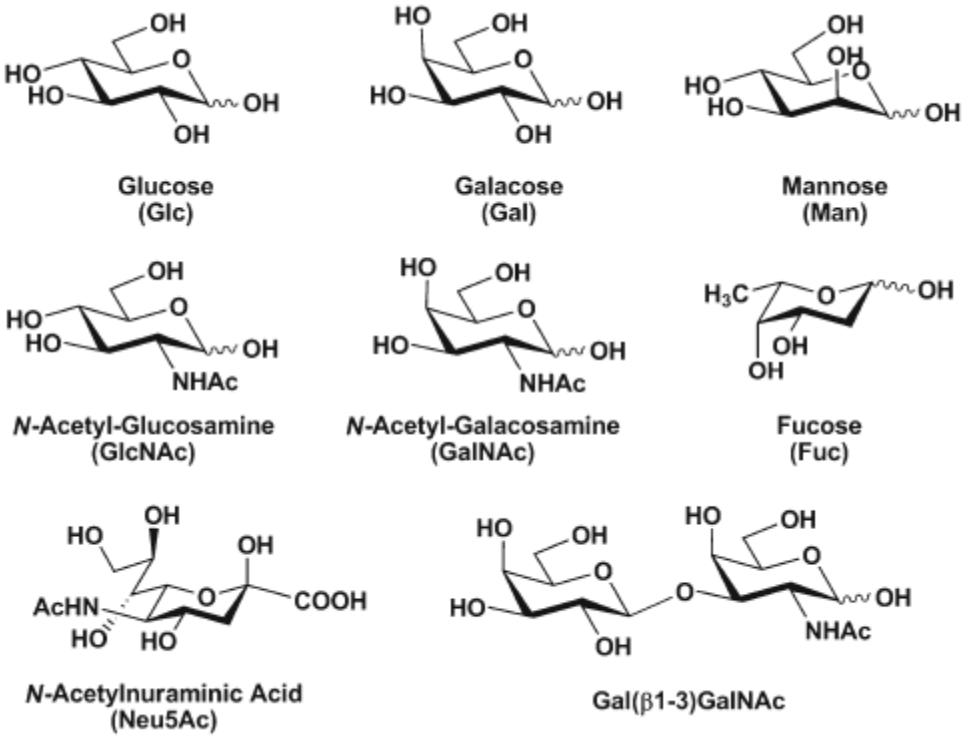

Figure 2.1 Examples of carbohydrate structures in organisms [31]

In recent decades, carbohydrates roles in cellular function and recognition has started to be exactly realized and understood [32-36]. Carbohydrates play key roles in cell-cell interaction , between constituents of the cellular environment and cells and can appear on cell surfaces as glycocalyx [37]. In the glycocalyx layer, carbohydrates are mainly bound to protein and lipid structures and they form complex carbohydrate units like glycoproteins [38] and glycolipids [39].

2.1.1. Glycosylation of Proteins and Roles of Glycans in Cells

Glycosylation is one of the most common posttranslational modifications of proteins which strengthens structural and functional roles of proteins on the cellular surfaces and within cells [31]. It is one of the major ways in which proteins are post-translationally modified and involves linking of monosaccharides via glycosidic bonds to form a glycan that is covalently attached to a biomolecule, such as a protein or a lipid. Over 50% of eukaryotic proteins are predicted to be glycosylated [40], although yeasts have fewer total glycoproteins than multicellular eukaryotes [41]. The importance of glycosylation is better understood by the fact that nearly 70% of therapeutic proteins that are either approved by US and European regulatory agencies or are in preclinical and clinical development are glycoproteins [42].

Glycosylation can occur at several amino acid residues, most commonly through asparagine (*N*-linked) and serine or threonine (*O*-linked). Although there are currently no established rules for predicting the effect of glycosylation on protein folding or function, empirical evidence reveals numerous roles for this protein modification. For example, glycans can influence folding, stability, molecular interactions, and quality control [43]. Extracellular display of glycans plays a role in cell–cell recognition, adhesion, and host immune responses to pathogens [44].

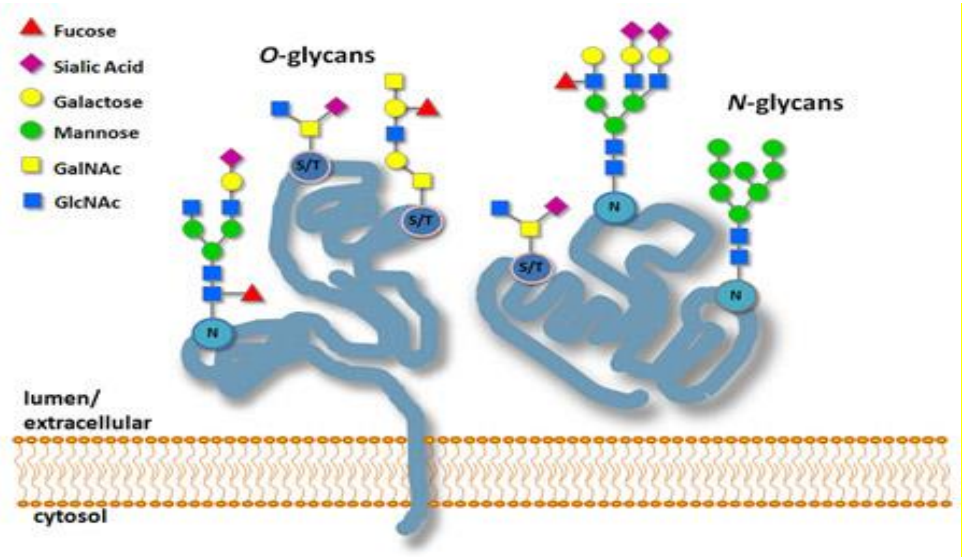

Figure 2.2 *N*-linked and *O*-linked glycosylation [45]

If compared with the normal tissues and cells, glycosylation level has altered in malignant cells and diseased tissues [46]. Additionally, complex carbohydrates behave as receptors for complementary binding proteins, typically lectins. Lectins are proteins and their interactions with polysaccharides are similar to the antibody–antigen and enzyme–substrate reactions [47].

Figure 2.3 shows carbohydrate–protein interactions at the cell surface like ligand–receptor recognition, cell-cell interaction, , typing of blood group, transportation of biological macromolecules, and immune recognition processes [13]. Carbohydrates present on cell surface play critical roles in many biological processes including leukocyte–endothelial cell adhesion [48-50], fatal diseases (inborn disorders of glycosylation [51, 52]) originated from a bacterial and viral infection, deficiency of glycosidases, and production of glycoproteins.

The synthetic glycoconjugates can be used as tools for the fundamental study of glycobiology and as candidates for future generation therapeutics [31]. Intentionally changing protein-associated carbohydrates can be used to tailor the pharmacokinetic properties of a protein, leading to drugs with enhanced *in vivo* activity, half-life, and resistance to proteolysis [43]. Glycosylation can also be used in production of specific therapeutic proteins [53] and to enhance their biological activities [54]. In an opposite manner, the inappropriate structure or position (on a protein backbone) of glycans can negatively affect pharmacokinetics, and in some

cases trigger immunogenic responses [55]. For these reason carbohydrate recognition has been located in the leading position of scientific research.

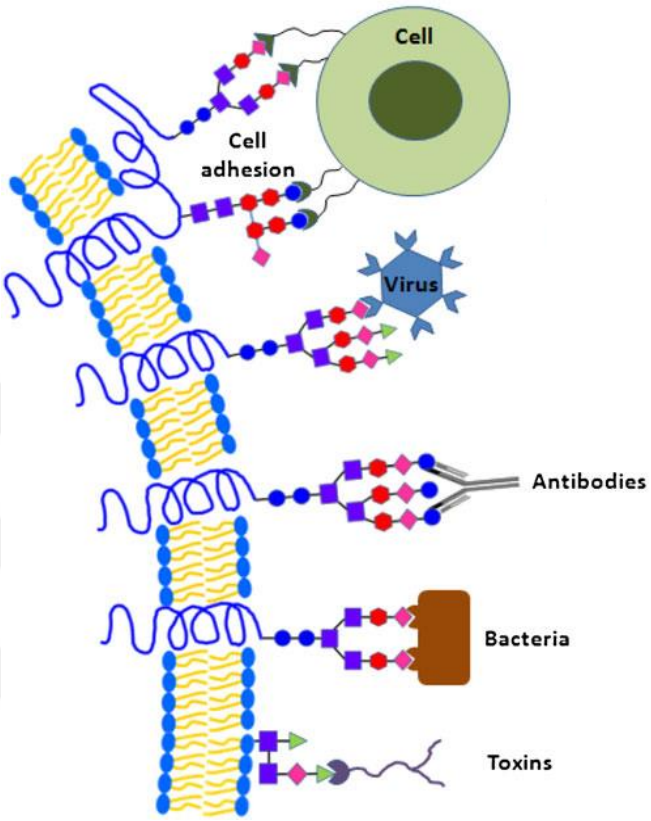

Figure 2.3 Protein–carbohydrate interactions at the cell surface (Figure modified from [31])

2.2. Analysis of Glycans as Biomarker

In the analysis of glycoprotein biomarkers or in glycoprofiling of intact, mainly cancerous cells, recognition of glycan has been utilized as part of the biomarker.

Protein glycosylation, which is the most common post-translational modification in higher organisms including human, means that a wide range of different glycoproteins can be used as disease biomarkers for early detection of pathological processes. This is a relatively new, yet very interesting approach with a potential to develop assays for the detection of diseases such as diabetes, rheumatoid arthritis, infection by a Dengue virus, as well as various types of cancer [56].

For instance, glycated hemoglobin is a marker of diabetes. In this disease, a continuously elevated concentration of glucose within the blood of patients with diabetes modifies the N-terminal valine of the β-chain of hemoglobin. Thus, monitoring of glycated hemoglobin can give information about a long-term progression of the disease, not influenced by a short-term variability in the glucose concentration. Also glycated albumin is used as an important biomarker for monitoring the long term glycemic history of diabetics [56], glycated albumins are not affected from changes in erythrocyte life times as a powerful feature, in contrast to glycated hemoglobin [7]. Glycated hemoglobin (HbA1c) in blood sample was detected quantitatively by using DCDR (drop coating deposition Raman) technique for clinical applications of glycemic control [6].

Antibodies (particularly immunoglobulins G, IgG) circulating in the blood contain complex type N-glycans of a biantennary structure [57]. IgG's glycan is in healthy individuals often terminated with N-acetylneuraminic acid, and in patients with rheumatoid arthritis this glycan can be terminated in galactose or N-acetylglucosamine. The severity of the rheumatoid arthritis correlates with the extent of the IgG's glycosylation change [14, 45]. Diluted serum samples from patients suffering from rheumatoid arthritis and healthy individual controls were analyzed by the EIS-based lectin biosensors. Three different lectins were covalently immobilized on SAM patterned gold surfaces to prepare three lectin biosensors for detection of sialic acid, galactose, and mannose/N-acetylglucosamine present on the surface of glycoproteins. The lectin biosensors could detect glycoproteins selectively down to the femtomolar level with the ability to distinguish between samples from healthy and sick individuals based on changes in the glycan composition on IgGs [14].

An early diagnosis of any type of cancer requires identification of cancer biomarkers, an effort feasible to be achieved only by a multidisciplinary approach relying on an array of strategies, technologies, and methods [58, 59]. Such studies revealed that in cancer tissues, glycan structures of glycoproteins are altered. There are only few cancer glycoprotein biomarkers approved by the U.S. Food and Drug Administration for diagnostics of various cancer types. For example PSA (prostate specific antigen) glycoprotein is a prostate cancer biomarker. Also CEA (carcinoembryonic antigen) is one of the most widely used tumor biomarkers

worldwide and the most often utilized biomarker of colorectal cancer. Although it was shown that CEA (or a CEA-like protein) is present in healthy people, its concentration in people affected by cancer is approximately 60-fold higher as compared to healthy individuals [60]. CEA is considered to be a biomarker also for other kinds of cancer including breast, lung, and pancreatic cancer [61]. For detecting of this antigen, attachment of glycan part of this protein can be used.

Recent studies, suggest that PSA from sera of patients with prostate cancer contain glycan with a higher amount of sialic acid as compared to PSA from healthy individuals or those having benign prostatic hyperplasia [61]. Moreover, it was shown that a relative abundance of glycosylated isoforms of PSA may provide useful additional information for clinically relevant investigations.

Graham et al. studied glycan expression for the identification of cancerous cell with confocal SERS mapping technique. Lectin functionalized silver nanoparticles were used for carbohydrate-lectin interactions in mammalian cells and as a result it was shown that prostate cancerous cells has higher amount of sialic acid residue composition according to noncancerous cell [4].

Chen et al. used SERS method with 4 MPBA functionalized AuNP, for detecting or visualizing glycans on live cells and detected cancerous cells [62]. In another new study, 4-mercaptophenylboronic acid (4-MPBA) functionalized, silver nanoparticle decorated silicon wafer was used as multifunctional chip based on SERS technique that effectively captures, discriminates, and inactivates pathogenic bacteria [63].

Bacteria can be categorized as Gram-negative and Gram-positive bacteria. Many diseases like pneumonia, meningitis, plague and diarrhea are caused by Gram-negative bacteria. Gram-negative bacteria pathogenicity is often related with their lipopolysaccharide (LPS) structure that covers 75% of the bacterial surface and is a highly complex glycolipid layer. LPS is essential for bacteria and there are many roles of LPS in host-pathogen interactions, so LPS analysis is important for truly understanding these interactions through infections. Additionally, by using these LPS-lectin interactions, detecting and isolating bacteria can be achieved more easily [64, 65]. With the aim of detecting and removal of Gram-negative bacteria *E. coli,* Wang et al. designed a lectin modified micro-engine and by using interactions

of lectin and O-antigens in glycan structure of *E. coli* cell surface, it was isolated easily [65].

2.3. Glycans in Biotechnology and the Pharmaceutical Industry

Protein-based biopharmaceuticals are highly popular therapeutics, and the necessity to these drugs within the pharmaceutical industry is rapidly increasing. Nowadays the number of recombinant proteins approved for use is over 50 and over 500 more are under development [66]. It is expected to increase developments in this field with stem cell technologies [67, 68]. Over one-third of these biopharmaceuticals have glycoprotein structure [69]. Glycosylation is the most common post-translational modification (PTM), occurring in up to one-half of all gene products [69]. Glycoproteins are also widely used in pharmaceutical industry because of effectiveness in drug stability, pharmacokinetic and immunogenicity [8].

Many well-known drugs, like anticancer therapeutic agents and antibiotics, have glycans naturally in their essential structure and/or as a sugar side chain (i.e., a glycoside). Natural products that have a glycan side chains are shown in Figure 2.4. In some synthetic drugs, glycan structures have also been modified. The most recent examples of these synthetic drugs are the small-molecule inhibitors of influenza virus neuraminidase [45].

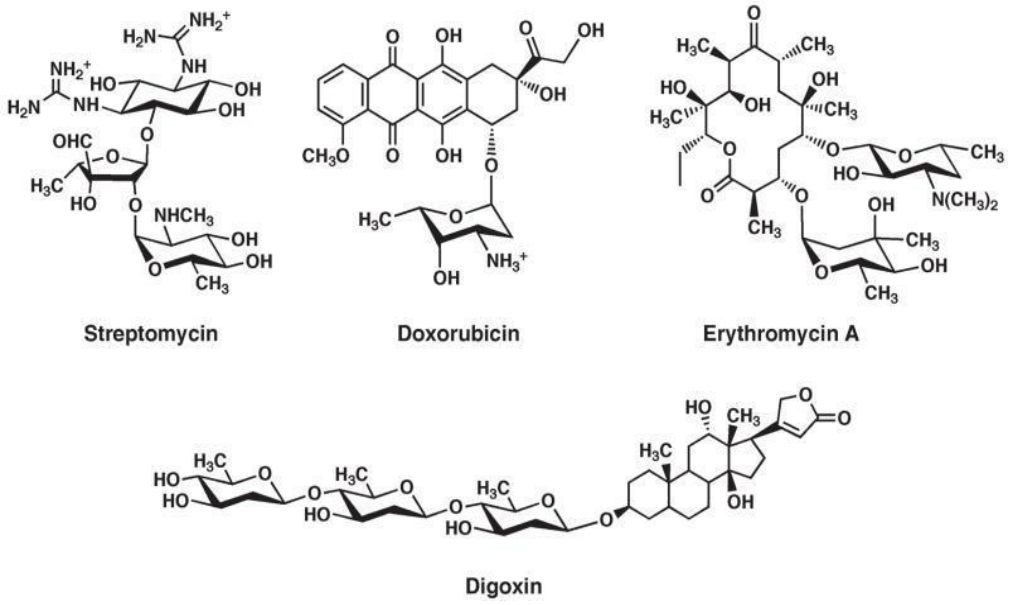

.

Figure 2.4 Examples of natural products which contain glycan components. Doxorubicin is chemotherapeutic drug, streptomycin and erythromycin A are antibiotics and digoxin is used to treat cardiovascular disease [45].

Glycosylation of naturally occurring molecules is often critical for their function and activity. Likewise, it is known that the action of therapeutic compounds might be significantly altered by glycosylation. Properties such as serum half-life, solubility, immunogenicity and binding specificity can be altered dramatically. Enzymatic remodeling of recombinant glycoproteins promises to be a useful tool for refining pharmacological activity. Thus it is possible to see many glycoconjugates as therapeutics. A classic example of a recombinant glycoprotein used in human therapy is erythropoietin which is used in treatment of anemia. Correct glycosylation of this glycoprotein is essential for activity as the incorrectly glycosylated molecule is rapidly cleared from circulation. Also, synthetically altered glycosylation can affect the selectivity, potency or action of drug, and may have beneficial or detrimental effects. In the case of morphine, artificial glycosylation has a beneficial effect and more effective than native one. Other glycocconjugate examples are antibiotics; altering their glycosylation may be a way of creating new antibiotics to overcome antibiotic resistance developed by pathogenic bacteria [70].

It is seen that clearly, glycoconjugates are abundant and effective in therapeutics and pharmaceutical industry. It is not enough to determine whether a protein is glycosylated, but also that the correct glycan has been attached truly and bound to the correct amino acid. Thus, biosensors are aimed to investigate glycosylation status in these pharmaceuticals easily and with high sensitivity.

In this respect, Goodacre et al., studied with model proteins, RNase A protein and RNase B glycoprotein, to investigate glycosylated therapeutics. RNase B glycosylation status was monitored and quantified, where its concentration was determined with Raman spectroscopic technique. This study lead to determine other glycoconjugates in drugs [8].

In another study, a boronate affinity sandwich assay was designed as an alternative to immunoassays for the determination of glycoproteins by using SERS method [71].

2.4. Glycomics

Similar to proteomics and genomics, glycomics shows the systematic methodology of the “glycome” (total of glycan structures) of a cell type or organism. However,

the glycome is more complex than the proteome or genome. Besides the extremely greater structural diversity in glycans, the dynamic changes occur during differentiation, development, malignancy, infection or inflammation. The other diversity originates from glycosylation alterations. Therefore, a large number of possible glycome states can be described for a given cell type in a given species. Today, glycomic analysis generally includes extracting complete cell types, organs, or organisms; releasing all the glycan chains from their linkages; and identifying them with detection techniques such as mass spectrometry [45].

The structural aspects of glycomics are being extensively addressed with the improvement in advanced profiling and structural characterization approaches, e.g., exoglycosidase digestions coupled high-resolution chromatography methods [72] and modern mass spectrometry (MS) analyses [73] and NMR [74]. However, understanding the involvements of carbohydrates in diverse recognition systems (often through their interactions with effector proteins) that participate in cell-cell communication and signaling still remain challenging [75].

Detailed analyses of carbohydrate-protein interactions present difficulties at all levels. First, only limited amounts of oligosaccharides (at submicromol levels) can typically be isolated from natural sources when released from proteins or lipids, and these are often highly heterogeneous. Second, the structural diversity of oligosaccharides leads to difficulties in their structural characterization; currently, there is a lack of an efficient means of automated assignment and the characterization is mainly reliant on expert interpretation by MS analyses. Third, the biosynthesis of oligosaccharides is not template driven, as for proteins and nucleic acids, and the diverse repertoire of oligosaccharides is difficult to access by chemical synthesis. Fourth, most carbohydrate-protein interactions are of low affinity, and there is a requirement for multivalent sites of carbohydrate ligands to detect the binding in microscale analysis. These challenges lead to new approaches to detect these interactions and structural analysis fast, easily and effectively.

2.5. Glycan Analysis Tools

The complexity and diversity of oligosaccharide structures and the physical similarity of the monosaccharides of which they are composed means that their analysis is technically difficult.

Lectins are useful tools for detecting of carbohydrates. They have biologically significant activity, including specific recognition of complex carbohydrate structures. [76]. Lectin affinity chromatography facilitates the purification of oligosaccharides an glycoconjugates from complex mixtures [12].

Another glycan purification method is boronate affinity chromatography. The specificity of boronate makes it an important ligand to separate cis-diol-containing compounds like glycoproteins, catechols, nucleic acids, nucleotides, nucleosides, and carbohydrates. The esterification process between boronate ligands and cis-diol groups is the basic interaction for boronate affinity chromatography. The process of esterification majorly requires that the two hydroxyl groups of a diol should be on adjacent carbon atoms and in an nearly coplanar configuration, that describes 1,2-cis-diol. Despite the interaction of boronate with cis-inositol, 1,3-cis-diols or triethanolamine, the strongest boranate ester bond forms with 1,2-cis-diols [77].

The other technique and the most common method for the analysis of proteins is SDS-PAGE. Different concentrations of acrylamide are incorporated into the electrophoretic gel matrix and the resulting differences in crosslinking enable gels to be constructed which separate proteins ranging in molecular mass from 10 to 200 kDa. For some heavily glycosylated proteins that do not migrate adequately in SDS-PAGE, borate buffer is used. Boric acid binds to the monosaccharides and enables the glycoproteins to migrate in the electric field. Following their separation, proteins are visualized with some stains like Coomassie Brilliant Blue or silver stain [78].

Another powerful technique is Western Blotting. It is the process by which (glyco)proteins, first separated by SDS-PAGE, are transferred to an inert membrane that can then be probed with lectins or antibodies to identify oligosaccharides on the protein of interest [79].

Unlike proteins, monosaccharides and oligosaccharides only weakly absorb light in the ultraviolet (UV) range. Furthermore, the immense diversity of oligosaccharide structures means that they are often resent only in tiny quantities. This has caused the development of alternative reliable, sensitive techniques for detection of oligosaccharides.

There are so many techniques for detection of glycans. The sensitivities of the different approaches to glycan analysis are compared in Table 2.1.

Table 2.1 The sensitivity of different methods for oligosaccharide analysis. The amount of protein required has been based on 20% oligosaccharide w/w protein [57]

Analysis Method	Starting amount of protein	Approximate oligosaccharide detection levels
Nuclear magnetic resonance (NMR)	100 µg	nmol
Matrix assisted laser desorption ionization/time of flight (MALDI/TOF)	10s of µg	pmol
Electrospray mass spectrometry (MS)	10s of µg	10 pmol
Fast atom bombardment MS	10s of µg	10 pmol
Gel electrophoresis separation of glycans (FACE)	0.5-1 µg	100 fmol
HPLC with fluorescent label	0.5-1 µg	10 fmol
High pH anion exchange chromatography (HPAEC)	100 µg	nmol
Native glycans labelled with fluorophore	0.5-1 µg	sub-pmol

It is seen that from Table 2.1, to improve detection levels of oligosaccharides have included labelling of mono- and oligosaccharides. The development and validation of fluorescent labels has also enabled improved sensitivity in detection of oligosaccharides. It is now possible to detect oligosaccharides in quantities as small as 10 fmol. It provides higher detection limit but makes it harder and noisier to detect these structures because of extra substance (label). In addition to these, carbohydrates or proteins labeling with fluorescence needs additional steps. The presence of the labels may cause additional interferences to the binding process.

These reasons lead to label-free glycan detection techniques [31]. Many techniques have been attempted to study carbohydrate–protein interactions, including isothermal titration calorimetry (ITC) [80], surface plasmon resonance (SPR) [81], capillary electrophoresis (CE) [82], nuclear magnetic resonance (NMR) [83], quartz crystal microbalance (QCM) [84], fluorescence spectroscopy [85], and atomic force microscopy (AFM) [86].

Raman spectroscopy is also another technique used in glycan analysis studies [8, 87]. It is easy, useful, simple and cost effective, but at the same time because of lower detection limit inherently weak technique [88].

In recent years, to improve sensitivity, nanoparticle based tools are used. For example, as a special case of SPR, Localized Surface Plasmon Resonance (LSPR) technique is used. It realizes on the metallic nanoparticle surface providing real-time assays and because of using simple instrumentation, good reproducibility in a cost-effective way can be possible [89].

Another nanoparticle based tool is Surface-Enhanced Raman Spectroscopy (SERS) technique. As different from the other techniques, concurrent analysis of multiple components in a single sample is possible with SERS technique; it provides a distinctive vibrational fingerprint spectrum so it causes an important increase in sensitivity. SERS is a versatile technique which can be used sensitively in many studies, including microorganism recognition [90], the monitoring of biological interactions [91], and also as a tool for detection of cancereous cell [92-94]. In this study, SERS is used because of its key advantages, so more detailed information on the technique is given in Section 2.10.

2.6. Affinity Chromatography and Glycoprotein Purification

Biomolecules are purified using several chromatographic techniques according to differences in specific properties, as given in Figure 2.5.

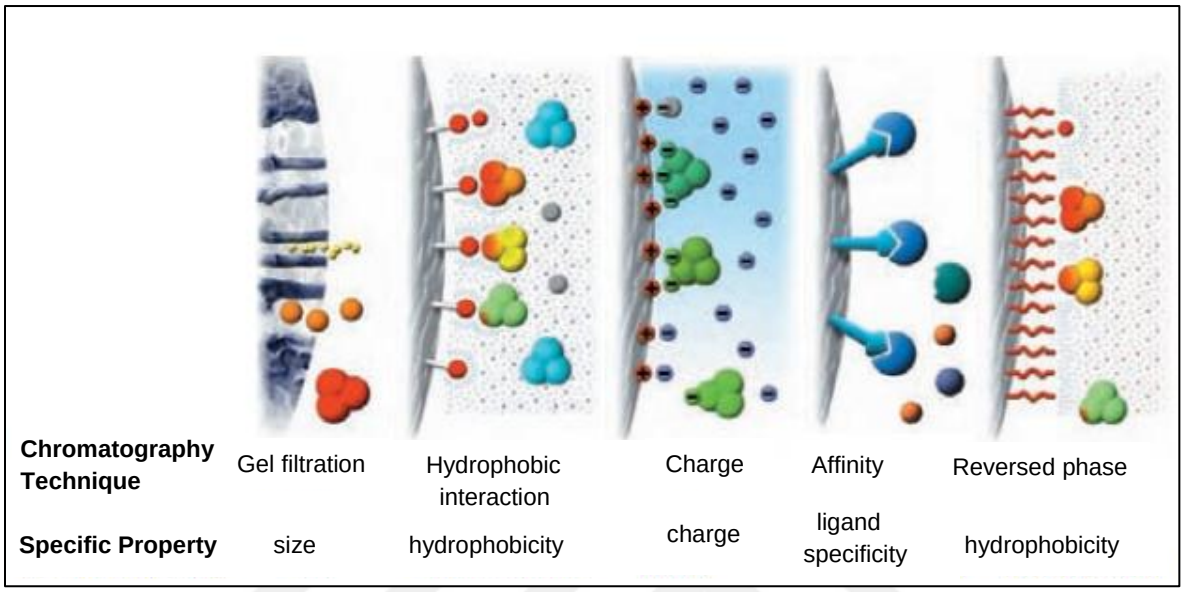

Figure 2.5 Separation principles in chromatographic purification (Figure modified from [95])

Separations of proteins are realized with affinity chromatography by using reversible interaction between a protein and a specific ligand in a chromatography matrix. This technique is suitable for capturing or it can be an intermediate step in a purification process and used when a complementary ligand is available for the target protein(s). Because of high selectivity, high capacity and high resolution, it is possible to achieve high recovery of active material. Also target protein(s) is obtained in a purified and concentrated form.

In this technique by using hydrophobic or electrostatic interactions, van der Waals' forces and/or hydrogen bonding, biological interactions between ligand and target molecule can be realized. After the interaction step, to isolate the target molecule elution from the affinity medium realizes with reversing the interaction, by changing the pH, ionic strength or polarity and using a competitive ligand.

Affinity purification can provide immense time-saving process compared to less selective multistep procedures. Large volumes can be processed because of concentrating effect. Target molecules can be isolated from complex biological

samples and biological material in low level can be purified from high amounts of contaminating substances.

In the basis of successful affinity purification process, there is a biospecific ligand that covalently attaches to a chromatography matrix. The specific binding affinity of coupled ligand must be retained for the target molecules and, after washing step of non-specific unbound material, the binding process must be reversible between the ligand and target molecule to elute the target molecules in an active form. Any material can be used as a ligand to purify its complementary partner. Some typical examples of biological interactions widely used in affinity chromatography are antibody-antigen, enzyme-substrate, glycoprotein-lectin, metal ions-poly(His) fusion protein pairs.

Purification of glycoproteins by selectively capturing the glycan component is commonly done using affinity chromatography. The most common nonspecific binding of saccharides can be realized with boronate affinity matrices, whereas immobilized lectins are used for specific binding of carbohydrates.

The difference of glycated proteins from non-glycated proteins is attachment of sugar moieties at diverse binding sites via a ketoamine bond. Glycated proteins therefore have 1,2-cis-diol groups that is not found in non-glycated proteins; boronate affinity chromatography uses this difference to separate glycated and non-glycated constituents [96]. Boronate affinity systems mimic lectins and they have synthetic lectin-like carbohydrate receptors.

2.6.1. Lectin-Based Biosensors for Detecting Carbohydrates

Carbohydrates and lectins are interacted reversibly with each other's predominant in different biological and pathological processes, like cell proliferation, cell-cell interaction, tumor metastasis, apoptosis, fertilization and immune responses.

Lectins bind to cell surfaces includes specific carbohydrate-containing receptor sites [97]. To analyze glycoproteins and carbohydrates, highly specific lectins are used as bioreceptors for biosensor applications.

Common immobilization techniques of lectin range from non-covalent to covalent immobilization onto a wide variety of substrates. In a study, as an example of non-covalent immobilization, ConA lectin is attached reversibly to polymyxin B surface with hydrophobic interactions [98]. In addition, the immobilization of lectins, like

ConA, on gold NPs generally occurs via electrostatic interactions. With the aim of make more efficient immobilization process, Oliveira et al. utilized gold and polyvinyl butyral (PVB) NPs for the development of an immunosensor [99]. PVB entraps the protein–NP aggregate on the electrode surface.

As an another technique, covalent immobilization of a lectin was obtained by flow-injection assay of the pathogenic enterobacteria via a lectin-based QCM biosensor [100]. In here, lectin ConA was the biosensing element and immobilized onto the gold surface of a quartz crystal electrode.

Lectins have oligomeric structure with several glycan binding sites and there are abundant carbohydrate structures on bacterial cell surface. Thus, in a study, a carbohydrate–lectin sensor, by using binding affinity of a lectin to both lipopolysaccharide structures of bacterial cell surface and a carbohydrate sensing element that is immobilized onto the Au transducer surface, has been developed [101].

In another lectin-based sensor study, Wang et al., by alkanethiol lectin conjugation method, lectin modified microengine was designed and used for *E. coli* isolation and release strategy [65]. For the lectin conjugation, alkane thiols are commonly used molecules because of higher affinity of S-bonding to surface.

In another example, Graham et al, synthesized lectin functionalized silver nanoparticles by using EDC·HCl and sulfo NHS coupling chemistry. The linker molecule was modified with each lectin and then they were bound to citrate reduced silver nanoparticles. In here, amine coupling method was applied again [4].

Although lectin based biosensors provides high specificity and power in carbohydrate detection, in case of some disadvantages and limitations about this technique, by mimicking lectins, synthetic materials based sensors are revealed and highly used in recent years. These types of sensors are explained in depth in the next section below.

2.6.2. Sensors Using Boronic Acid Derivatives to Detect Carbohydrates

Natural sources are utilized in order to isolate most of the lectins so affinity of lectins can decrease after purification process. Some lectins can also be cross-specific; it means they bind multiple glycan structures. Furthermore, there

are some disadvantages about lectin-based systems like the short lifetimes and lack of stability, thus they need renewal because of their intrinsic protein nature. In an alternative way, some molecular structures have been recently used in the development of lectin-like carbohydrate receptors.

The most widely used one among lectin-like carbohydrate receptors is boronic acid-containing compounds. They're covalent interaction-based carbohydrate receptors [102]. Because of low mammalian toxicity of boronic acids and their unique interactions with diol groups, the boronic acid-containing receptors are frequently used: cyclic esters are formed with interaction of boronic acid and diol groups in water more readily compared to many other acids.

In recent years, studies with boronic acids are realized for use in glucose sensors [103], membrane transport agents [104], cell surface imaging and recognition [105], and catalysts and protective agents in synthesis [106]. The variety of substrate affinity and selectivity is studied with boronic acid-based receptors, containing multiple binding sites. [107].

In another example to enable the oriented immobilization, boronic acid containing, O-cyanate chain-end functionalized polymer has been synthesized. This system offers a three-dimensional expression of a carbohydrate receptor as shown in Figure 2.6. Briefly, as a multivalent carbohydrate receptor a boronic acid-containing polymer (boropolymer) was oriented and immobilized to surface using isourea bond formation. In order to increase binding affinity and specificity of boropolymer surface, carbohydrates were linked to AuNPs which provided multivalent carbohydrate group to increase the response signal [31].

In another study, Zhang et al., synthesized boronic acid modified magnetic nanoparticles with thiol–ene click chemistry for selective enrichment of glycoproteins from complex bio-samples. In here, as boronic acid containing compound, 4-mercaptophenyl boronic acid (4-MPBA) was used as a glycan structures probe [21].

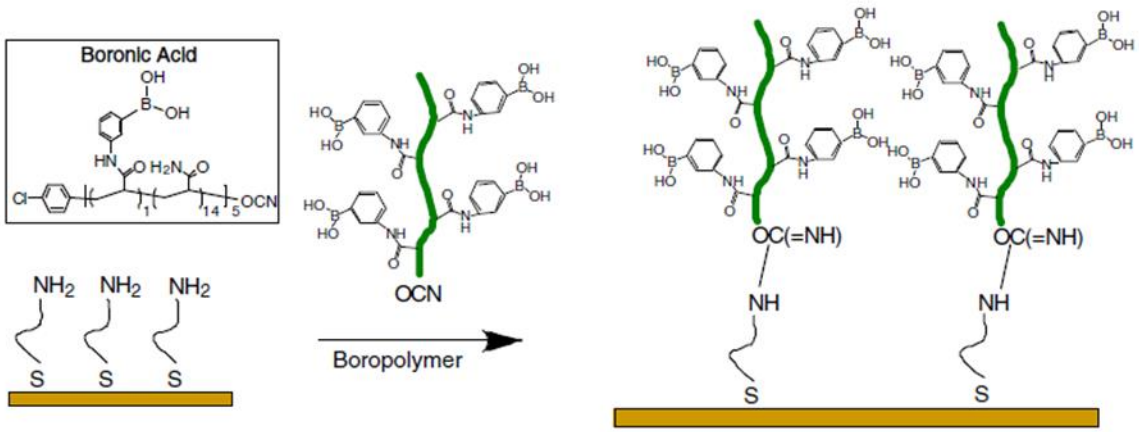

Figure 2.6 Boronic acid containing**,** O-Cyanate chain-end functionalized polymer and its immobilization on amine surface with isourea bond formation as carbohydrate receptor [31]

Yu et al., studied an important issue of today's world and reported specific, sensitive and accurate detection of fructose for diabetic symptoms, in protein solutions using SERS by forming a mixed self-assembled monolayer (SAM), where the fructose probe was 4-mercaptophenylboronic acid (4-MPBA) [108].

In this thesis study, for selection of glycan structures in model protein samples and detection of glycosylation level in glycoprotein samples, magnetic polymeric microbeads functionalized with 4-MPBA were used as synthetic material in SERS-based method.

2.7. Adsorption Equilibria

When the adsorbate and adsorbent are interacted with each other long enough, equilibrium will be established, which is characterized by adsorption isotherms. An adsorption isotherm is related to the equilibrium concentration of a solute on the adsorbent surface, q_e, to the concentration of the solute in the liquid, C_e, with which it is in direct contact. The adsorption isotherm is also related to the amount of solute adsorbed onto the surface of an adsorbent and the equilibrium concentration of the solute in solution at a given temperature.

For calculation of q_e values, equation below is used.

$$q_e = \frac{(C_0 - C_e).V}{m} \qquad (2.1)$$

In this equation; q_e, adsorbed quantity by unit adsorbent at equilibrium concentration (mg/g); C_0, initial concentration of adsorbent (mg/L); C_e, equilibrium concentration of adsorbent (mg/L); V, volume of adsorbent solution (L) and m, mass of adsorbent (g).

2.8. Adsorption Isotherms

Equilibrium study on adsorption process informs about the capacity of the adsorbent. An adsorption isotherm is described by certain constant values provides the information about affinity of the adsorbent, surface properties and can also be utilized to compare the adsorption capacities of the adsorbent for different conditions. Equilibrium data is processed to analyze adsorption behavior using commonly known adsorption models. The characterization of experimental data of adsorption isotherms can be realized via several mathematical models. The Langmuir, Freundlich and Temkin models were used to analyze the adsorption behavior that happened in the glycoprotein purification experiments.

2.8.1. Langmuir Model

This isotherm developed by Irving Langmuir is the best model that expresses chemical adsorption. Single layer is formed on outer surface of adsorbent by adsorbed matter and after the layer forms, adsorption process ends. This isotherm is explained by Equation 2.2 [109].

$$q_e = \frac{q_m.K_L.C_e}{1+K_L.C_e} \tag{2.2}$$

When this equation is converted to linearized form, Equation 2.3 is formed.

$$\frac{1}{q_e} = \frac{1}{q_m} + \frac{1}{q_m.K_L.C_e} \tag{2.3}$$

In this equation, q_m, maximum adsorption capacity of adsorbent (mg/g) and K_L, Langmuir adsorption constant (L/mg) and these values are calculated with slope and intercept values of linear curve from the graph plotted for $1/C_e$ versus $1/q_e$.

2.8.2. Freundlich Model

Freundlich isotherm is mostly preferred to determine adsorption characteristics of heterogenic surfaces. This isotherm is explained with Equation 2.4 [110].

$$q_e = K_f.C_e^{\frac{1}{n}} \tag{2.4}$$

In this equation, K_f, Freundlich isotherm constant and n, adsorption density constant. When Equation 2.4 is linearized, Equation 2.5 is formed.

$$\ln q_e = \ln K_f + \frac{1}{n}.\ln C_e \quad (2.5)$$

ln C_e versus ln q_e graph is plotted. n value is calculated with slope of the curve and intercept of the curve is used for calculation of K_f value.

2.8.3. Temkin Model

Temkin isotherm assumes that decrease in the heat of adsorption is linear with increasing coverage. This isotherm is expressed in Equation 2.6 and Equation 2.7 [109].

$$q_e = \frac{R.T}{b_T}.\ln A_T + \left(\frac{R.T}{b_T}\right).\ln C_e \quad (2.6)$$

$$q_e = B.\ln A_T + B.\ln C_e \quad (2.7)$$

In these equations A_T, Temkin isotherm equilibrium binding constant (L/g); b_T, Temkin isotherm constant; B = $\frac{RT}{b_T}$, constant related with adsorption heat (J/mol); R, gas constant (8.314 J/mol/K); T, heat (298 K).

ln C_e versus q_e graph is plotted. A_T and B values are calculated from intercept of the curve and slope of the curve, respectively.

2.9. Raman Spectroscopy

The phenomena of inelastic light scattering, called as the Raman effect was discovered by physicist Chandrashekhara Venkata Raman, in 1928. This phenomena expresses the wavelength shift of a small fraction of radiation scattered by molecules, its frequency is different from the frequency of incident beam [111]. There is a relationship between the shift in wavelength and the chemical structure of the molecules responsible for the scattering. This relation used by Raman spectroscopy provides information about the symmetry, structure, bonding and electronic environment of the molecule, so it provides the quantitative and qualitative analysis of the every single compound [112].

The irradiation of a molecule sourced by monochromatic light causes inelastic or elastic or light scattering. If elastic scattering occurs, photon frequency,

wavelength and energy do not change. In other scenario, if inelastic scattering occurs, there is shift in photon frequency and wavelength because of deactivation or excitation of molecular vibrations in which either the photon may lose or gain some amount of energy [113]. Thus, three types of phenomena can occur when the light reaches a molecule as shown in Figure 2.7 [114]; elastic scattering, also known as Rayleigh scattering, inelastic scatterings called as Stokes and Anti-Stokes Raman Scattering.

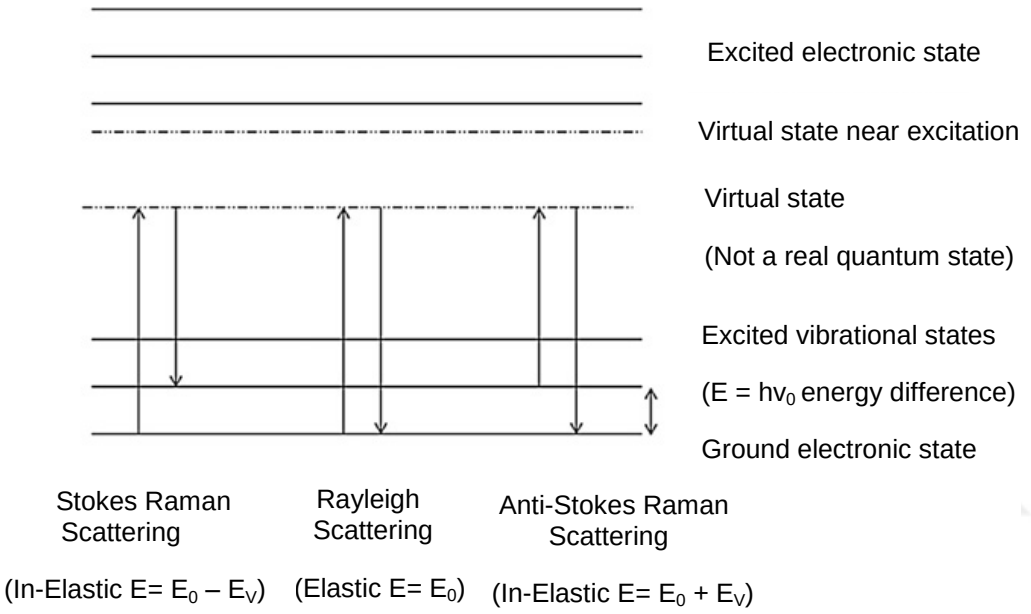

Figure 2.7 Raman scattering mechanisms [115]

A typical Raman spectrometer contains light source, monochromator, sample holder and detector. There are a few factors which affect the analysis on Raman spectra. These can be high signal-to-noise ratio, satisfied resolution and instrument stability [116]. In a typical Raman instrument like in Figure 2.8, firstly a laser beam in the near infrared (NIR), ultraviolet (UV) or visible (Vis) range is sent from light source to sample. Scattered light is collected by aid of a lens and finally a Raman spectrum of a sample is obtained from interference filter or spectrophotometer.

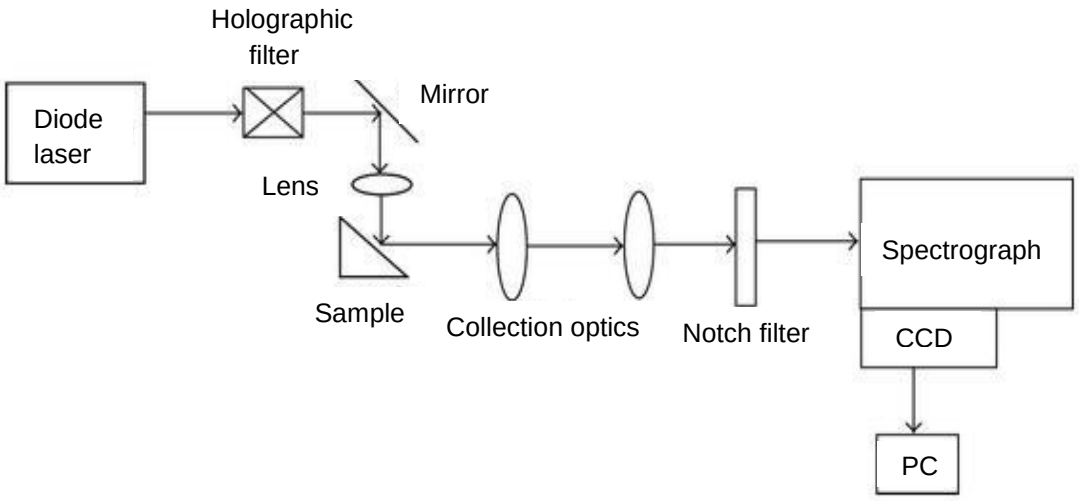

Figure 2.8 Diagram of a typical Raman instrumentation [115]

Separation of spontaneous Raman scattering from intense Rayleigh scattering is hard process. In here, the major problem is not only the Rayleigh scattering itself, in the close proximity to the laser wavelength, the intensity of stray light from the Rayleigh scattering may be pretty higher than the intensity of the useful Raman signal. Generally to solve this problem, spectral range of ± 80-120 cm^{-1} from the laser line are cut-off by using interference (notch) filters. This method is efficient but its important disadvantage is not allowing the detection of low-frequency Raman modes in the range below 100 cm^{-1}.

In the beginning, single-point detectors like photon-counting Photomultiplier Tubes (PMT) were mainly used. However, a single Raman spectrum acquired with a PMT detector is a time consuming process and slows down research based on Raman analytical technique. In these times, multi-channel detectors such as Photodiode Arrays (PDA) or Charge-Coupled Devices (CCD) are used to detect the Raman scattered light. Efficiency and sensitivity of CCD detectors are rapidly getting better with improvements. Currently, CCD is the preferred detector for Raman spectroscopic analyses.

On its own, Raman technique is normally not quite well because of weakness of Raman signal. To keep up with developing technology, Raman spectroscopy techniques are also improved step by step. Many different methods of preparation and illumination of sample or detection of scattered light were developed to

increase the intensity of Raman signal. The important and strongest one of these ways is SERS.

2.10. Surface-Enhanced Raman Spectroscopy (SERS)

SERS is a highly sensitive tool to detect adsorbate molecules on roughened metal surfaces that enhances Raman scattering signal like showed in Figure 2.9 schematically. This enhancement phenomena was investigated independently by Jeanmaire et al. [117] and Albrecht et al. [118], and they both explained this observed enhancement with a different mechanism. According to them, there are two effective factors to increase the Raman signals: (i) Electromagnetic enhancement (EM), related with the roughness of the metal surface [117]; (ii) Chemical enhancement (CHEM), related with the electronic coupling of adsorbed molecules on the roughened metal surfaces which contains changes of the electronic state of the molecules adsorbed because of the bond formation between analytes and metal surface or chemisorption of the analyte [118].

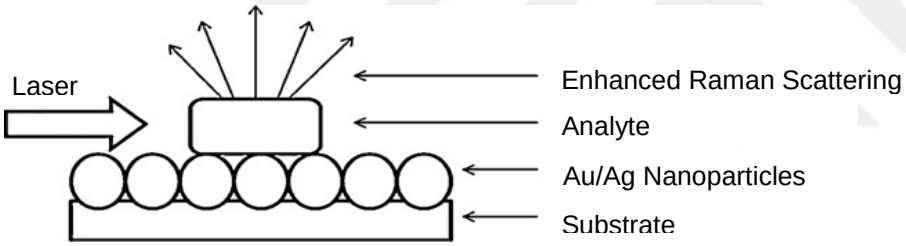

Figure 2.9 Surface enhanced Raman scattering [115]

When compared with each other's, the electromagnetic effect is more dominant, thus also known as the "first-layer effect," due to necessity of direct contact between the metal surface and analyte [119, 120]. These enhancement factors can be understood by the concept of surface plasmon, found in the metals such as Cu (copper), Au (gold) and Ag (silver). Strong scattering forms when this plasmon oscillate perpendicular to the surface of the metal, reflects the roughness of the surface sourced from nano/micro particles or a physical roughness [121-123]. As mentioned above due to weak signals sourced from normal Raman scattering, to get more detectable or enhanced signals, SERS technique is used. This technique can be informative about molecules interacting with surfaces of the adsorbate, even in very low analyte concentrations. The intensity of the Raman signal is

increased by using these specially prepared metal surfaces such as copper, silver and gold up to 10^4-10^6 folds. This signal enhancement provides more sensitive, faster and higher accuracy detection of chemical and biological samples [124].

2.10.1. SERS Materials

Au and Ag are air stable materials so they're most often used as SERS substrates, while Cu is more reactive. As shown in Figure 2.10, these three metals have LSPRs cover most of the near infrared and visible wavelength range. Most of the Raman measurements take place in this range and it makes these metals more popular and suitable for SERS applications.

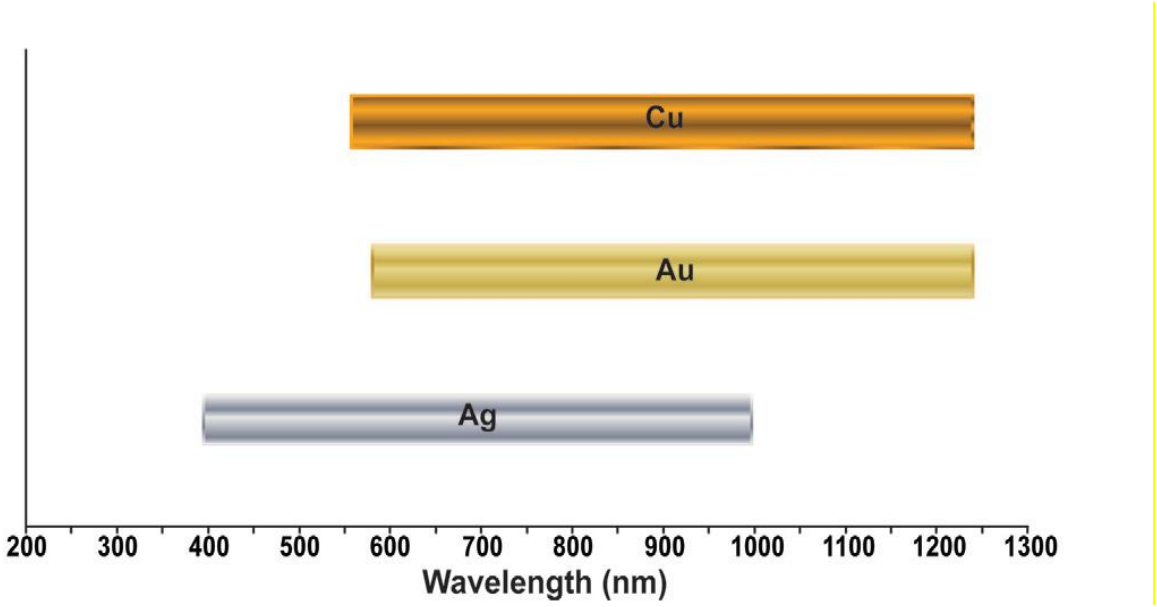

Figure 2.10 Approximate wavelength ranges where Cu, Ag, and Au used as SERS materials [125]

In the last 30 years, to improve enhancement factors, it is tried to optimize substrate structure and configuration. To contribute to SERS's enhancement, new plasmonic materials are discovered as well as different shapes [126-128].

SERS is increasingly used to detect some biomolecules as biosensor and it is preferred because of importance of low detection limit in biomarker or biomolecule analyses [129-131]. In this thesis study, the powerful SERS technique is utilized for detecting model proteins. To detect low concentration biomolecules with SERS method, various particles are used. These particles and their application areas will be discussed in the next section.

2.10.1.1. Micro and Nanoparticles

Metallic nanoparticles (NPs) have been widely used and preferred in biological processes for developing different kinds of biosensors due to their unique optical, electronic and catalytic properties. Biomolecule coupled metal NPs are very popular probes because they can bind easily with thiolated molecules to the surface of the adsorbent. It has been realized many improvement in development of bioassay strategies because of the broad applications of metal NPs, include colorimetric detection methods [132], localized surface-plasmon resonance (LSPR) technique [3], electrochemical methods, and surface-enhanced Raman scattering (SERS) technique [4].

Due to its unique optical (for example; surface plasmon resonance absorption and resonance light scattering) and catalytic properties gold nanoparticles (AuNPs) are popular in bioanalysis. Also due to their nontoxic and biocompatible structures, they are used in many areas like fotonic, diagnostic and therapy [91, 133-135]. Especially the usage of functionalized gold nanoparticles with ultrasensitive diagnostic and imaging methods in biology and pharmacology, makes these materials popular in biodiagnostic platform for researchers [136, 137]. In addition to these, by modifying of AuNP's with various biofunctional groups, they gain multidirectional properties [138]. Amphilic polymers, silanes, sugars and nucleic acids are some of these groups [139-141]. Also gold surfaces have strong affinity to thiol groups and they're used often in literature [22]. By using these nanoparticles, with properties shortly given above, chemical sensor and imaging studies are sustained in analytical and biological sciences [134].

For example, to image proteins in biological samples, antibody conjugated gold nanoparticles are fairly used in light and electron microscope. Maieret et. al. developed immunochip biosensor in the basis of optical trapping near resonance to detect allergens. With this method, by forming sandwich structure and no need to reading apparatus, immunochemical binding is monitored easily and quickly [142].

The most important point for AuNP's is low particle dimension distribution and synthesis with desired shape and size. In this respect, different mechanisms are suggested for their synthesis with different shape and size. The most common

method is classic Turkevich-Frens method in the base of citrate reduced gold salts [143, 144]. With this method, the size of gold nanoparticle is easily controlled by adjusting ratio between reducing/ stabilizer agent (trisodium citrate) and gold salt derivatives. This method was also used for the particles used in this thesis.

In addition to this common method above, alternatively by using microemulsion [145], copolymer micelle [146], reverse micelle [147], and surfactant amphilic components, gold nanoparticles are synthesized. Alternatively to chemical methods to help synthesis of gold controlled nanoparticles, physical methods like photochemistry (ultraviolet (UV), NIR) [148], sonochemistry [149], radiolysis [150] and thermolysis [151] are used. In another study, Rubinstein et al., developed a sensitive and effective LSPR transducer with carbohydrate-modified Au-film to study carbohydrate-protein interactions [152]. This interaction informs about biological process types in organisms and also it enables development of biomedical agents according to type of processes. The carbohydrate-protein interactions have a central importance for this thesis study.

Because of their strong characteristics, easy synthesis and biocompatibility factors, AuNP's are used in intracellular diagnostic applications [134]. Medley et al., determined cancer cells directly with colorimetric method. AuNP's functionalized with aptamers showed high affinity to cancer cells interacted with target cells, a distinct color change occured; but for the noncancerous cells it was not observed [153]. Other strong and mainly used metallic nanoparticles are silver nanoparticles (AgNPs). Graham et al., designed an on/off SERS aggregation system to investigate carbohydrate-lectin interactions with AgNPs. Silver nanoparticles were preferred in this study because of the 10-fold increase in scattering efficiency in comparison to AuNPs. SERS is chosen in here as a surface-sensitive technique, where, Raman signal is enhanced by adsorbed molecules on rough metal surfaces. This enhancement can be as high as 10^{10}–10^{11}. The lectin Con A was detected at picomolar levels [92].

Silver has plasmonic properties and can also be used in many applications with gold. Methods given in synthesis of gold particles are almost applied for silver. The most used approach similar to Turkevich-Frens method is Lee-Meisel method [154]. Only difference in application is usage of silver salts instead of gold ones. In

this thesis, silver nanoshell coated particles are formed with seed mediated growth method onto gold.

In recent studies, as sensitive and efficient biosensor, graphene and carbon nanotubes (CNTs) have been used successfully for sensitive detection of carbohydrate-related biomolecules [155, 156]. These materials are widely used because of their high surface area-to-volume ratio, unique carrier mobility, versatile chemistry and outstanding robustness. Chen et al. reviewed the strategies for non-covalent and covalent functionalization of carbon nanostructures with glycans, as well as their applications in biomedicine and biosensing [157].

As semiconductor nanocrystals, quantum dots (QDs) have unique electronic and optical properties; it makes QDs more attractive in analytical chemistry. A QD immunofluorescence coupled microfluidic platform was designed for monitoring and determination of the expression of glycans on the cell surface. The QD-based immunofluorescence probe showed greater stability and higher brightness against photobleaching, when compared with equivalents [158].

Another type of attractive material is magnetic nanoparticles (MNPs). They are used in magnetic resonance imaging, sensing and separation applications because of their special magnetic properties. In addition to simple, rapid magnetic separation advantages, MNPs provide fast assay procedure and prevent target molecule damage and the potential risks of contamination during the time consuming and difficult purification process. There are various methods for synthesis of magnetic nanoparticles, such as hydrothermal [159], thermal degradation [160, 161], microemulsion [162], sol-gel synthesis [163], sonochemical reaction [164], flow injection synthesis [165] and electrospray synthesis [166]. Dual precipitation technique is the easiest and most effective method in production of magnetic nanoparticles. Iron oxides (Fe_2O_3 or Fe_3O_4) are prepared by formation of stoichiometric mixtures of ferric and ferrous salts in aqueous solutions. Chemical reaction of Fe_3O_4 formation can be shown in below:

$$Fe^{2} + Fe^{3+} + 8OH^{-} \rightarrow Fe_3O_4 + 4H_2O \quad (2.8)$$

Dual-precipitation method materializes in two steps [167, 168]. In first step, when concentrations of iron solutions reach to critical extreme saturation, nucleation occurs in short time. In second step, with diffusion of solute onto crystal surface,

slow growth of seed in other words crystal growth occurs. During synthesis, by adjusting pH, ionic strength, temperature, natural salts (perchlorates, chlor, sulfate, nitrates) or Fe_2/Fe_3 ratio parameters; dimension, magnetic and surface properties is controlled [168]. In our study, this method is also used. Magnetic nanoparticles usage in medical application areas like magnetic storage [169], biosensor applications [24, 170, 171], drug delivery [172, 173], gene delivery [174], bioseperation [175], immunoserologic method [11] and magnetic resonance imaging (MRI) [176, 177] are studied by researchers. Behra et al. also described a microparticle system that provides selective detection and easy removal of bacteria from contaminated solutions with introducing super-paramagnetic iron-oxide NPs to microbeads [25].

Polymeric particles are also used widely in above applications. For this thesis, poly glycdyl methacrylate poly (GMA) microspheres are produced with dispersion polymerization of GMA monomer. Then, monodisperse and porous formed polymethacrylate microspheres are obtained with multiple steps microsuspansion polymerization method [178]. Moreover, there are also various composite nanoparticles to integrate all other unique nanoparticle properties. For instance, self-propelled, template-based, nickel/gold/ platinum/polyaniline (Ni/Au/Pt/PANI) microtubular engines, functionalized with the Con A bioreceptor, provides rapid, real-time isolation of *E. coli* bacteria from food, clinical and fuel-enhanced environmental samples that are contaminated [65].

In the basis of these particles, analysis tools and application areas, in this thesis, a multi directional system was designed, to unify all strong properties of nanoparticles, a novel microbead design was used. The novel microbead gold core AgNP nanoshell coated magnetic polymeric microbeads functionalized with 4-MPBA and it was used for selective enrichment and detection of glycan structures in model protein samples, using SERS.

3. MATERIALS AND METHODS

3.1. APBA Functionalized, Monodisperse-Porous Magnetic Silica Microspheres

Amino phenyl boronic acid (APBA) functionalized, monodisperse-porous magnetic silica (APBA@$MagSiO_2$) microspheres were kindly supplied by Prof. Dr. S. Ali Tuncel and Dr. Çiğdem Kip at the Laboratory 12, Chemical Engineering Department, Hacettepe University, Ankara, Turkey.

3.2 Glycoprotein Adsorption and Isolation Process via APBA Functionalized Magnetic Silica Microspheres

Optimization of various experimental parameters was realized with adsorption and desorption processes of different types of glycosylated and non-glycosylated proteins. Model glycoprotein (IgG) isolation in complex media was succeeded via magnetic silica microbeads at the optimized conditions.

3.2.1. Effects of Initial Protein Concentration and Sorbent Mass

Firstly, to see the effect of binding buffer pH to adsorption capacity, HEPES buffer at pH 7.5, 8, 8.5, 9.0 and 9.5 was used. 1 mg/mL IgG glycoprotein solution was prepared and added to 2 mg sorbent. According to adsorption capacity and isolation yield results, 50 mM HEPES buffer at pH 8.5 was chosen as binding buffer. IgG adsorption kinetics was also studied to determine the saturation point. 1 mg/mL IgG was added to 2 mg sorbent in adsorption medium and while IgG and sorbent were interacting with each other, adsorption quantity of IgG was measured, in different time periods. Required time period to reach saturation point was determined. After these data following, initial protein concentration and sorbent mass effects on adsorption capacity were studied.

APBA@$MagSiO_2$ microspheres were suspended in binding buffer (50 mM HEPES buffer, pH: 8.5). This stock solution was vortexed to obtain homogeneous sorbent. 2 mg of sorbent was pipetted and allocated to micro-centrifuge tubes, washed with binding buffer two times, followed by magnetic separation. Protein stock solutions (0.5, 1, 2, 2.5, 3, 3.5, 4 mg/mL) were prepared in binding buffer. 0.1 mL stock solution was added to micro-centrifuge tubes (1.5 mL) containing sorbent and incubated at room temperature for 1h by shaking. Glycoprotein adsorbed

APBA@MagSiO$_2$ microspheres were settled via magnet and washed three times to remove non-specifically adsorbed proteins. To investigate the effect of sorbent mass, APBA@MagSiO$_2$ microspheres suspended in binding buffer was aliquoted as 1, 5, 10, 20 and 40 mg to micro-centrifuge tubes and the same procedure was followed using 2 mg/mL protein stock solution. All stock solutions and supernatants (flow through, washes) were stored at 4°C and analyzed to calculate equilibrium adsorption capacity of microbeads.

By using initial concentration of IgG glycoprotein and equilibrium adsorption capacity values, by using drawn linearized adsorption isotherms, adsorption behavior of IgG glycoprotein onto magnetic APBA functionalized silica microbeads and compatibility with Langmuir, Freundlich and Temkin adsorption isotherms were investigated.

3.2.2. Desorption Process of Specifically Adsorbed Proteins

After adsorption process of glycoproteins, for effective desorption of IgG glycoprotein pH, ionic strength and glucose effects were studied with different concentrations of these parameters. Optimized desorption buffer was chosen and desorption was realized with 0.1 mL of Tris-Cl buffer (1M, pH: 8.5) with 0.2 M NaCl. Following the washing of microbeads, desorption buffer was added onto microbeads in micro-centrifuge tubes contains adsorbed proteins. This solution was shaken for 30 minutes at room temperature by vortex shaker. Eluted proteins were collected three times and collected eluates were stored at 4°C to use in analysis of desorption and isolation yields of proteins.

3.2.3. Isolation Process of Glycoproteins from Complex Media

In addition to optimized conditions above, effect of NaCl concentration in wash buffer for high isolation yield of IgG glycoprotein in complex media was investigated. By using all of these knowledges, isolation process in complex media was realized at optimized conditions.

To simulate complex media, firstly, equimolar solution of IgG glycoprotein and BSA non-glycosylated protein were used. 1 mg/mL IgG and BSA proteins solution (0.1 mL) was incubated and then adsorbed proteins were eluted from microspheres with 0.8 mL of elution buffer with same procedures above.

Rabbit serum (Sigma-Aldrich Co., U.S.A.) was also used as complex media, IgG glycoprotein was purified via functionalized magnetic microbeads. 50-fold diluted serum solution (0.5 mL) was added onto 5 mg sorbent and incubated. All the steps were performed as described above. Adsorption capacity, desorption and isolation yields of proteins were determined with methods specified in following sections.

3.3. Analysis

3.3.1. Total Protein Concentration

Total protein concentration in an eluate solution was determined spectrophotometrically in duplicates using Bradford reagent (Sigma). The absorbance was read at 595 nm by UV-spectrophotometer. The calibration curve was obtained using BSA or IgG in the concentration range of 0-1 mg/mL. Protein concentration was also verified spectrophotometrically at 268 nm (NanoDrop 1000, Thermo Scientific).

3.3.2 SDS-Polyacrylamide Gel Electrophoresis (SDS-PAGE)

Sample mixture, purified proteins and non-adsorbed proteins (supernatants) were analyzed by using sodium dodecyl sulfate polyacrylamide gel electrophoresis (SDS-PAGE) including a protein ladder. Separated proteins were stained with coomassie stain and visualized by GelDoc EZ Imaging System (BioRad). The protein purification parameters like desorption yield and isolation yield were calculated by using Image Lab 5.1 software (BioRad), based on total protein concentration and analysis of the PAGE image.

The desorption yield for the target protein was defined as weight ratio of eluted target protein from sorbent to adsorbed target protein onto sorbent. The isolation yield for the target protein was defined as weight ratio of eluted target protein from sorbent to initial target protein loaded to sorbent [179].

3.4. SERS Analysis

3.4.1. p-aminothiophenol (PATP) and MPBA-attached Ag shell-coated magnetic polymethacrylate microspheres as SERS substrate

Diol sensitive MPBA-Ag@MagPMMS were kindly supplied by Prof. Dr. S. Ali Tuncel, Dr. Kouroush Salimi and Duygu Deniz Usta at the Laboratory 12, Chemical Engineering Department, Hacettepe University, Ankara, Turkey.

3.4.2. Attachment of RNase A non-glycosylated and/or RNase B glycosylated model proteins onto MPBA-Ag@MagPMMS

The lyophilized form of RNase A and RNase B proteins were dissolved in HEPES buffer at pH 8.5 (50 mM, 5 mL) by gently mixing. Then these solutions were aliquoted to micro-centrifuge tubes as 1 mg/mL stock solution, stored at -20°C.

Typically, MPBA-Ag@MagPMMS (2 mg) was precipitated from the HEPES buffer by means of a magnet. The sample solution (5 mL, 50 mM HEPES buffer, pH 8.5) containing RNase A and/or RNase B at a certain concentration was added to precipitated MPBA-Ag@MagPMMS (2 mg). The new dispersion was mixed and shaken for 2 h at room temperature. The sample solutions containing RNase A/B with concentrations ranging from 0.1 to 1000 ng/mL were used for the adsorption of the respective diol carrying agent onto MPBA-Ag@MagPMMS. RNase B glycoprotein in sample was substantially captured by MPBAAg@MagPMMS via the formation of a cyclic boronate ester between MPBA and diol groups of glycosyl moieties on RNase B. RNase B-bound MPBA-Ag@MagPMMS was extensively washed with HEPES buffer (50 mM, pH 8.5) using an external magnet and finally dispersed in HEPES buffer (50 mM, pH 8.5) by vortexing.

3.4.3. Construction of Diol-Sensitive Sandwich System

The RNase B-bound SERS tag was incubated with the colloidal solution of PATP:MPBA (2:1 mol/mol)-attached Ag NPs (PATP/MPBA@Ag NPs) in HEPES buffer (0.1 mg in 5 mL, 50 mM, pH 8.5) for 2 h. Then, a certain fraction of PATP/MPBA@Ag NPs were bound onto the RNase B present on MPBA-Ag@MagPMMS by the formation of cyclic boronate ester between the glycosyl residues on bound RNase B and MPBA ligand on Ag NPs. The unbound PATP/MPBA@Ag NPs were removed with the supernatant obtained by the precipitation of RNase B@MPBA-Ag@MagPMMS carrying bound fraction of

PATP/ MPBA@Ag NPs (i.e., the sandwich system, PATP/MPBA@AgNPs@ RNase B@MPBA-Ag@MagPMMS) by an external magnet. The sandwich system was washed three times with fresh HEPES buffer (50 mM, pH 8.5) to remove any physically adsorbed constituents. The washed microspheres were redispersed within the fresh HEPES buffer (5 mL, 50 mM, pH 8.5) for SERS measurements.

3.4.4. SERS Measurements

An aliquot (50 µL) of the sandwich system-bound and RNase B-attached SERS tag dispersion was deposited on a glass substrate, and a cast film of the SERS tag was obtained by evaporation of the liquid at room temperature. SERS measurements were made using the cast film of the SERS tag. All SERS measurements were performed using the WITEC Alpha 300S Confocal Raman spectrometer module. A NIR laser with 785 nm wavelength was used for excitation. Laser power was measured using an optical power and energy meter console (Thorlabs, PM100D, USA). For single Raman measurements, 50× objective, 20 s integration time, and 0.67 mW excitation power were used [180] .

4. RESULTS AND DISCUSSION

In the first part of this thesis study, 3-aminophenyl boronic acid (APBA) functionalized monodisperse, porous, magnetic silica microbeads were used to isolate glycoproteins selectively from complex media. IgG was selected as the model glycoprotein.

First, binding buffer selection was done according to maximum adsorption capacity of proteins. Then, effect of initial protein concentration and sorbent mass on adsorption-desorption process and isolation yield was determined. Afterwards, elution buffer was chosen and optimum conditions were determined for pH, ionic strength and glucose concentration. Glycoprotein isolation from complex serum media was realized successfully by using the optimized conditions and verified with SDS-PAGE analysis.

After isolation of glycoproteins, SERS method was used for ultrasensitive detection of glycoproteins with a sandwich system containing MPBA-functionalized silver nanoshell-coated magnetic, monodisperse polymethacrylate microspheres (MPBA-Ag@MagPMMS). By using SERS spectra, another model glycoprotein (RNase B) was detected at femtomolar levels and calibration curves were formed for determination of glycoprotein concentrations.

4.1. The Effect of Binding Buffer pH

For more stable boronic acid and cis-diols interaction, HEPES buffer is generally preferred as the binding buffer. To see the effect of binding buffer pH to adsorption capacity, HEPES buffer at pH 7.5, 8, 8.5, 9.0 and 9.5 was used. 1 mg/mL IgG glycoprotein solution was prepared and added to 2 mg sorbent.

The maximum adsorption capacity, 29 mg IgG/g-sorbent was obtained using 0.05 M HEPES binding buffer with 8.5 pH value, as shown in Figure 4.1-A. Also, the desorption yield of IgG glycoprotein was relatively higher when binding buffer at pH 8.5 was used (Figure 4.1-B).

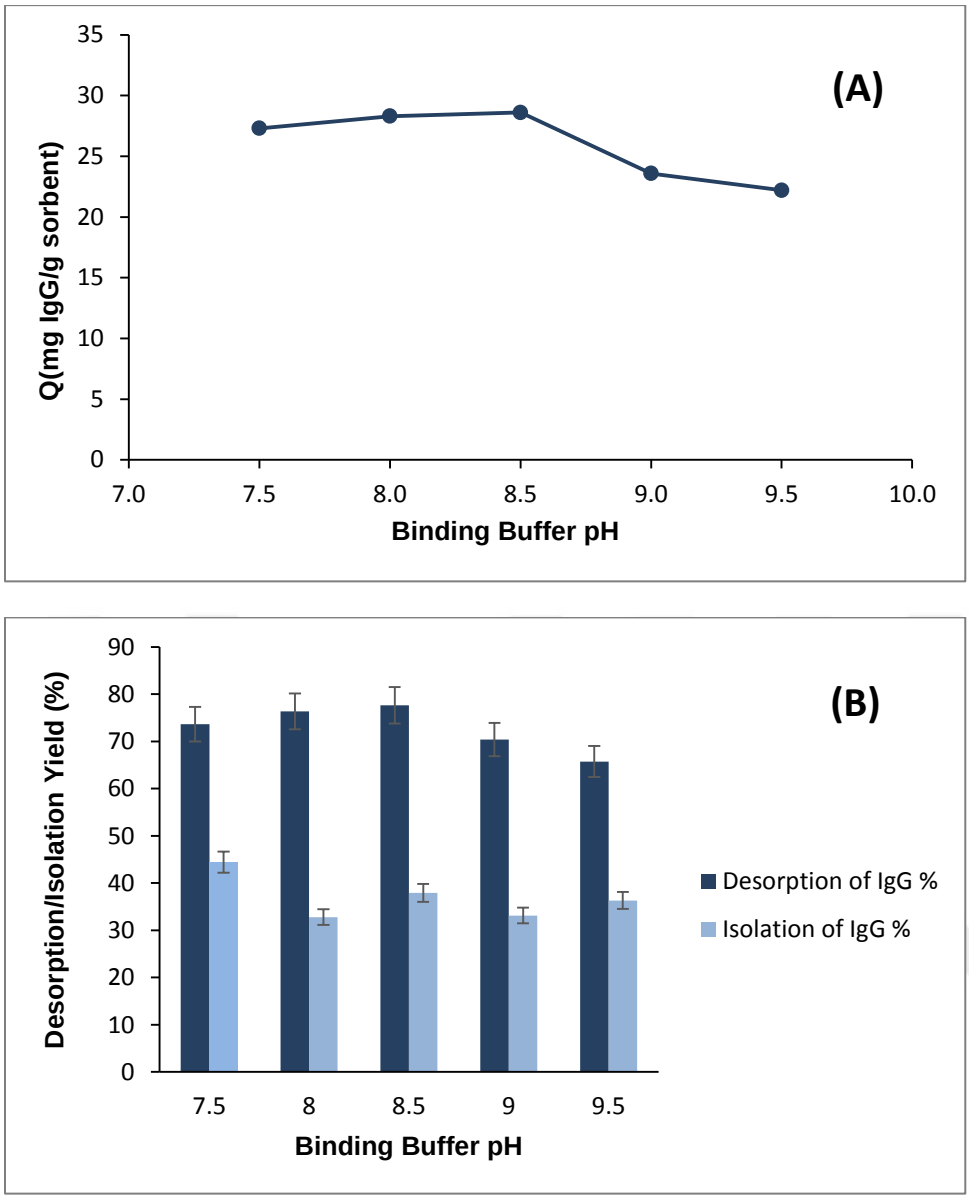

Figure 4.1 (A) Adsorption capacity change of IgG glycoprotein to APBA attached magnetic silica microbeads with pH of binding buffer. Binding buffer: 0.05 M HEPES, IgG concentration: 1 $mg.mL^{-1}$, Adsorption medium: 0.1 mL.

(B) Relative desorption and isolation yield change of IgG glycoprotein with pH of binding buffer. Desorption buffer: 1 M Tris-Cl with 0.2 M NaCl, Desorption medium: 0.08 mL.

Boronate normally has a trigonal coplanar geometry but in aqueous solution, under basic conditions it is hydroxylated, forming a tetrahedral boronate anion. Then, this anion can form five- or six-membered cyclic esters binding covalently with cis-diols. Boronate ester is “trapped” in its more stable tetrahedral form at

higher pH, because of high hydroxide concentrations. The reverse reaction takes place under acidic conditions with hydrolyzing of cyclic diester [23].

4.2. The effect of initial protein concentration

Initial protein concentration effect on adsorption capacity of sorbent was studied with 0.5, 1, 2, 3, 4 and 5 mg/mL concentrations of proteins. In here, IgG glycoprotein and BSA non-glycated protein were preferred as model proteins. These proteins were added to 2 mg sorbent in 0.1 mL adsorption buffer. Also with this study, it is aimed to see the effect of initial protein concentration for isolation of the desired glycoprotein in mixture. Effect of initial protein concentration on adsorption capacity before and after wash treatment is shown in Figure 4.2.

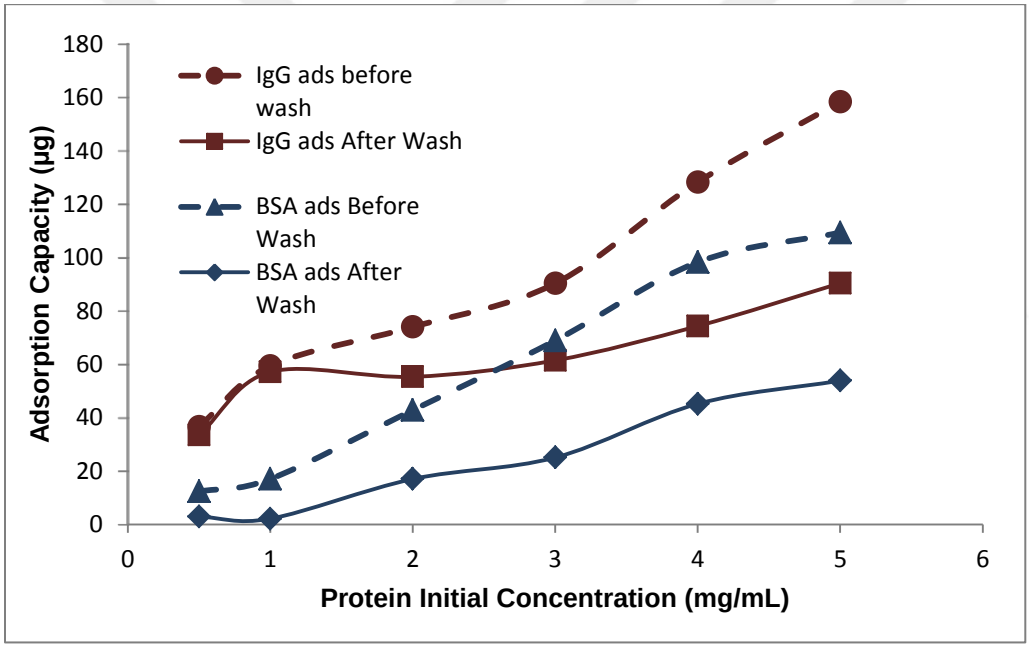

Figure 4.2 Adsorption capacity of Immunoglobulin G (IgG) glycoprotein and bovine serum albumin (BSA) non-glycoprotein onto 2mg APBA functionalized magnetic silica microbeads before and after wash, according to their initial concentrations. Adsorption buffer: 0.05 M HEPES pH 8.5, adsorption medium: 0.1 mL.

IgG is a glycoprotein that contains cis-diol groups. BSA has been used as negative control, it is a non-glycoprotein, so according to boronic acid-diol interaction mechanism, it is expected that only IgG glycoprotein is bound chemically to APBA functionalized silica microbeads. As expected, with increasing concentration of IgG

glycoprotein, its adsorption capacity also increased then became saturated. The equilibrium adsorption capacity of IgG was observed as 46 $mg.g^{-1.}$ On the other hand, before the wash treatment, non-glycated BSA protein adsorption capacity was high because of non-specific physical interactions between particles and BSA protein. After wash treatment, it is shown that this interaction decreased and with increasing initial protein concentration, the same saturation curve was obtained but in low level according to IgG glycoprotein, as expected. Even for 1 mg/mL protein, adsorption capacity difference between IgG glycoprotein and BSA non-glycoprotein was highest; BSA was nearly not adsorbed in this concentration.

4.3. Adsorption Kinetic

IgG adsorption kinetics was also studied to determine the saturation point. 1 mg/mL IgG was added to 2 mg sorbent in adsorption medium and while IgG and sorbent were interacting with each other, adsorption quantity of IgG was measured, in different time periods. Initially adsorption capacity increased with a high rate, then IgG adsorption rate decreased and eventually the sorbent was saturated. The equilibrium adsorption capacity was reached within 30-40 minutes (Figure 4.3).

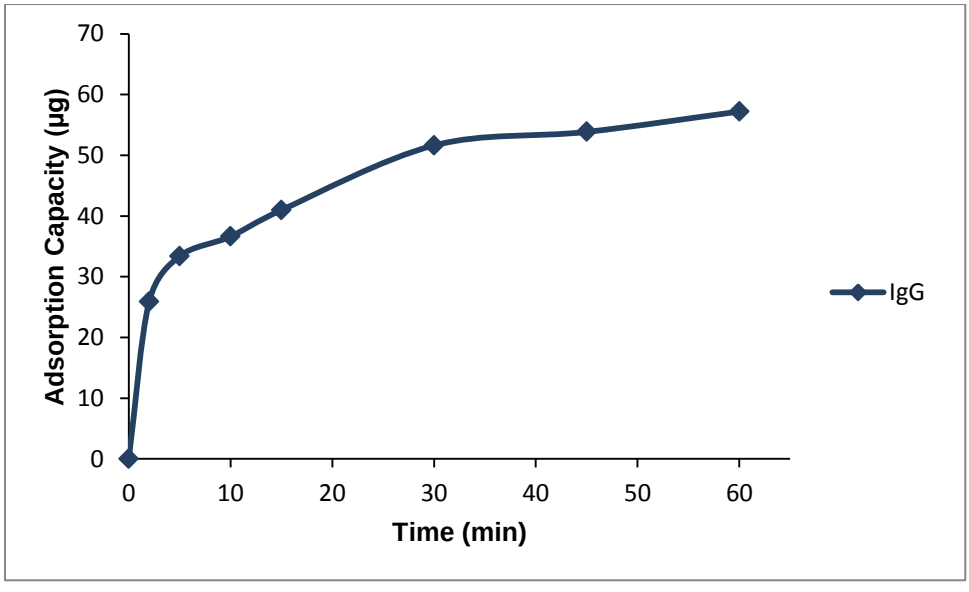

Figure 4.3 Effect of stirring time on adsorption of IgG glycoprotein with concentration of 1 $mg.mL^{-1}$. Adsorption medium 0.1 mL, sorbent 2 mg.

4.4. Adsorption Isotherms

By using initial concentration of IgG glycoprotein and equilibrium adsorption capacity values, linearized adsorption isotherms have been drawn. These adsorption data were used to determine adsorption behavior of IgG glycoprotein onto magnetic APBA functionalized silica microbeads and compatibility with Langmuir, Freundlich and Temkin adsorption isotherms. In Figure 4.4, Figure 4.5 and Figure 4.6 linearized adsorption isotherms are shown and calculated isotherm constants are given in Table 4.1. When R^2 values for each fit are compared (Table 4.1), IgG adsorption behavior is seen to be more compatible with Langmuir model. This shows that adsorption has occurred as single layer and homogeneously [160].

In Figure 4.4 by using slope and intercept of the line, maximum adsorption capacity of the IgG (Q_m) and Langmuir adsorption constant (K_L) were calculated (Table 4.1). The maximum theoretical adsorption capacity of IgG was calculated as 84 $mg.g^{-1}$. From Figure 4.5, by using slope and intercept of the line, adsorption density (n) and Freundlich adsorption constant (K_F) were calculated respectively (Table 4.1). In Figure 4.6 by using slope and intercept of the line, maximum adsorption process heat related constant (B) and binding constant at equilibrium concentration (A_T) were calculated and shown in Table 4.1.

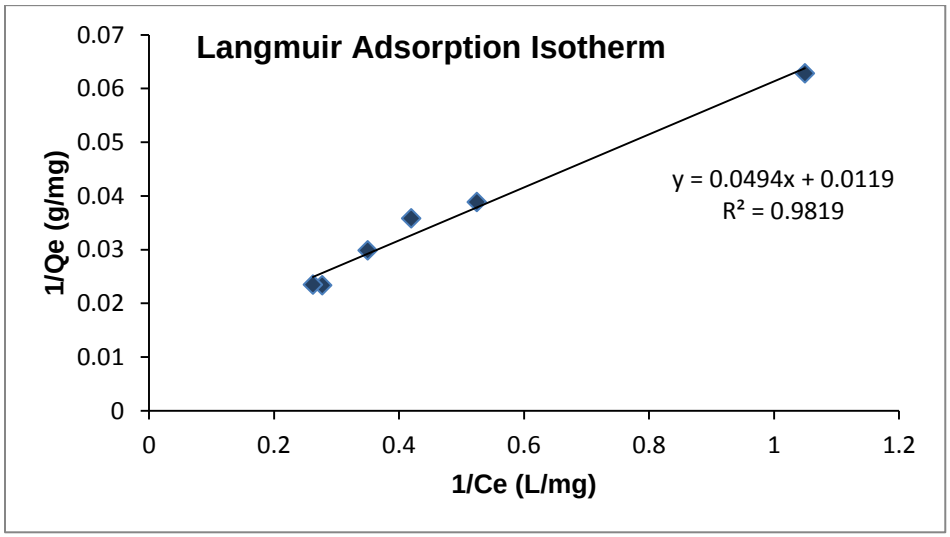

Figure 4.4 Langmuir Adsorption Isotherm of IgG glycoprotein onto APBA functionalized magnetic silica microbeads. Adsorption buffer 0.05 M HEPES pH 8.5, adsorption medium 0.1 mL.

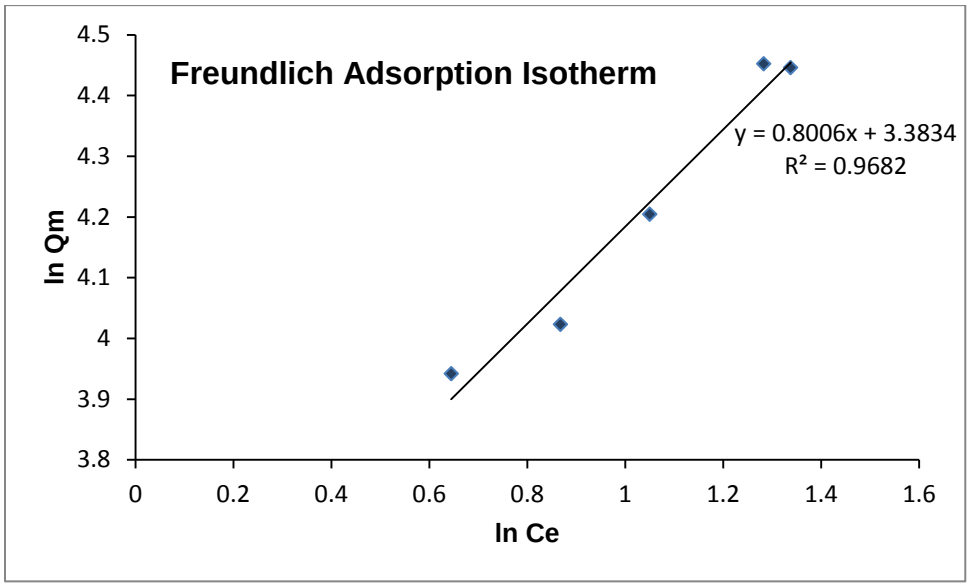

Figure 4.5 Freundlich Adsorption Isotherm of IgG glycoprotein onto APBA functionalized magnetic silica microbeads. Adsorption buffer 0.05 M HEPES pH 8.5, adsorption medium 0.1 mL.

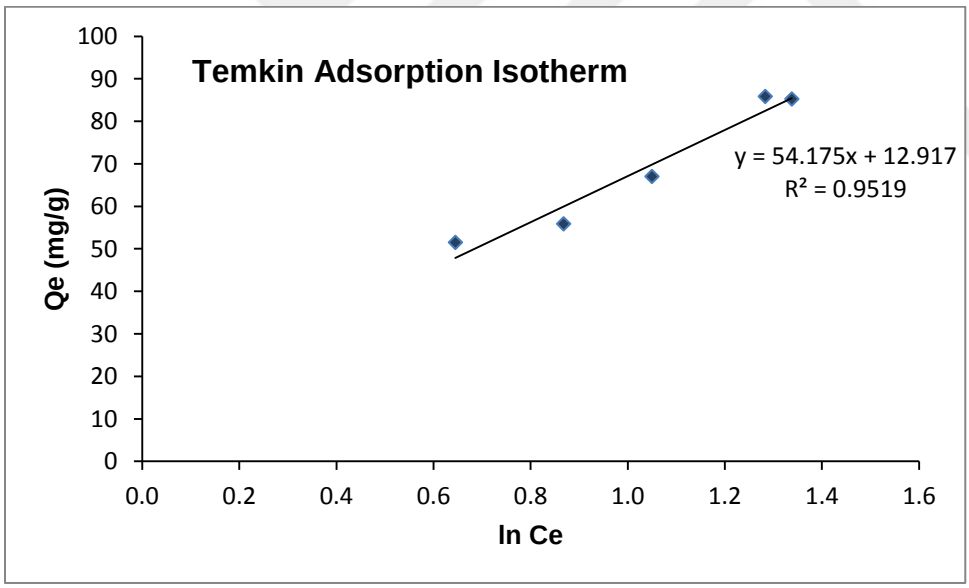

Figure 4.6 Temkin Adsorption Isotherm of IgG glycoprotein onto APBA functionalized magnetic silica microbeads. Adsorption buffer 0.05 M HEPES pH 8.5, adsorption medium 0.1 mL.

When R^2 values for each fit are compared (Table 4.1), IgG adsorption behavior is seen to be more compatible with Langmuir model. This shows that adsorption has occurred as single layer and homogeneously [181].

Table 4.1 Langmuir, Freundlich and Temkin Adsorption Isotherm Constants and R^2 Values for IgG Equilibrium Adsorption onto magnetic silica microbeads

LANGMUIR			**FREUNDLICH**			**TEMKIN**		
q_m (mg/g)	**k_L (L/mg)**	**R^2**	**n**	**k_f (mg/g)**	**R^2**	**B (J/mol)**	**A_T (L/mg)**	**R^2**
84.034	0.241	0.982	1.249	29.471	0.968	54.175	1.269	0.952

4.5. Effect of Elution Buffer

Adsorption capacity of proteins on magnetic silica microbeads were shown in previous figures. After adsorption process, isolation of these proteins is also an important topic. To see effect of elution buffer type and pH value, three types of elution buffer seen often in literature were used.

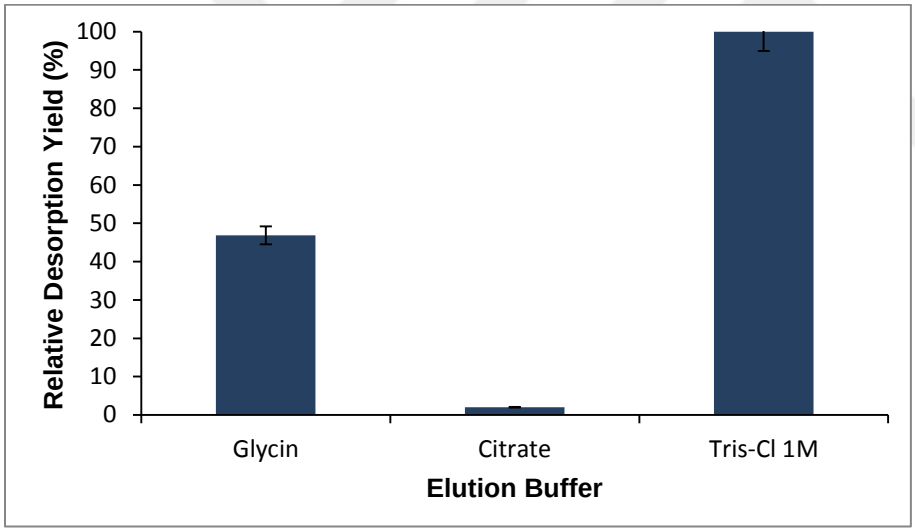

Figure 4.7 Effect of elution buffer type to desorption yield of IgG glycoprotein (0.1 M Glycine Buffer pH 2.2, 0.1 M citrate buffer pH 3, 1 M Tris-Cl buffer pH 8.5).

In here, 0.1 M glycine (pH: 2.2), 0.1 M citrate (pH: 3.0) and 1 M Tris-Cl (pH: 8.5) buffers were used to see effect of pH value on desorption yield. It is clearly seen that desorption yield was higher with 1 M Tris-Cl buffer (Figure 4.7), being 72% with Tris-Cl buffer, 33% with glycine buffer and 1.5% with citrate buffer, respectively. Actually to break the boronic acid-diol group bond, acidic conditions are generally preferred but in here, because of the low molarity of acidic buffers,

Tris-Cl buffer was more effective. On the other hand, more concentrated acidic conditions can be harsh for reusability of the sorbent.

4.5.1. Effect of Elution Buffer Molarity

In order to show elution buffer concentration effect on desorption yield, Tris-Cl buffer was used at different concentrations. Desorption yield of IgG increased with increasing molarity of Tris-Cl buffer, reaching 72% with 1 M Tris-Cl, 37.5% with 0.5 M Tris-Cl, 14.5% with 0.2 M Tris-Cl and 5% with 0.1 M Tris-Cl elution buffers, respectively (Figure 4.8).

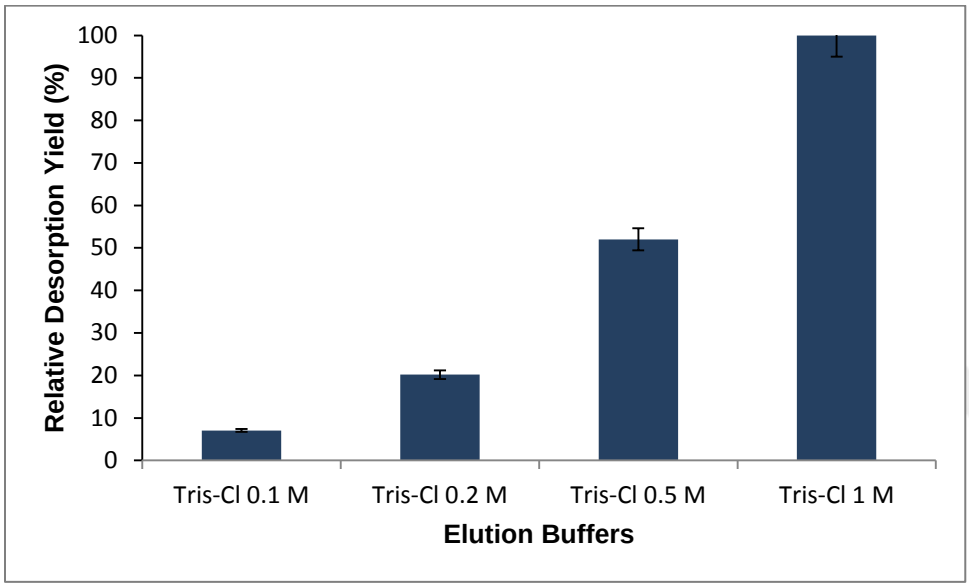

Figure 4.8 Effect of molarity of elution buffer (0.1, 0.2, 0.5, 1 M Tris-Cl buffer pH 8.5) to desorption yield.

4.5.2. Effect of sorbitol molarity in elution buffers

Addition of high amount of sorbitol to desorption media can cause ligand competition between sorbitol and glycan structures in IgG so this mechanism can increase desorption yield. Therefore, Tris-Cl buffer with different sorbitol concentrations were used to show effect of sorbitol on desorption of IgG.

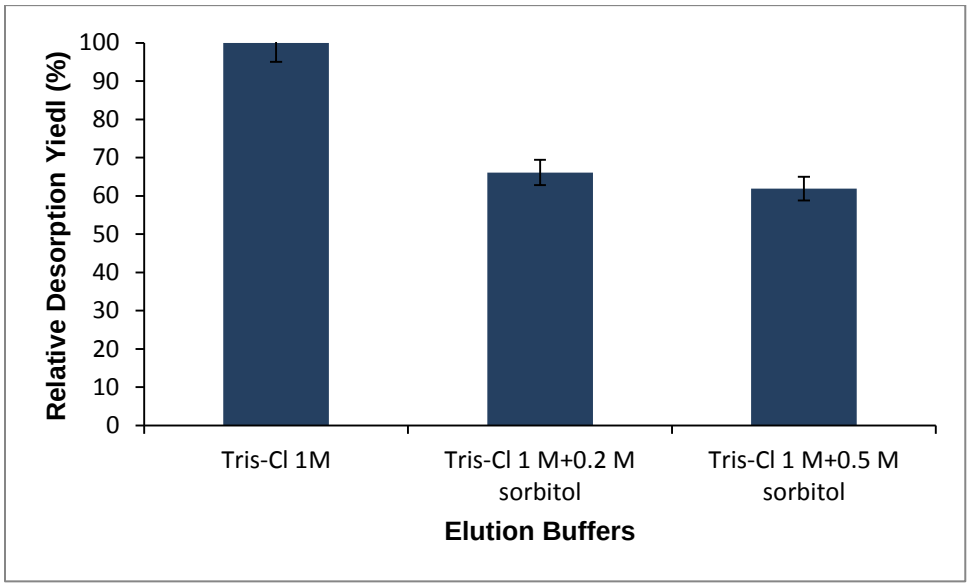

Figure 4.9 Effect of sorbitol concentration (0, 0.2, 0.5 M sorbitol) in elution buffer to desorption yield.

Contrary to belief, Figure 4.9 shows that sorbitol had negative effect in Tris-Cl buffer for desorption of IgG. Thus, elution buffer was preferred with no glucose nor its derivatives.

4.5.3. Effect of NaCl molarity in elution buffers

The effect of ionic strength on desorption yield is shown in Figure 4.10. For this purpose, NaCl salts were used in 1 M Tris-Cl buffer with different concentrations. Desorption yield of IgG glycoprotein increased with increasing ionic strength. Maximum desorption percentage of IgG glycoprotein, 88% was obtained using 1 M Tris-Cl buffer with 0.2 M NaCl.

4.5.4. Effect of Elution Buffer pH

In order to see the effect of pH on desorption yield of IgG glycoprotein, 1 M Tris-Cl elution buffers were used with different pH values, 7.5, 8, 8.5 and 9. The maximum desorption yield was obtained at pH 9 (Figure 4.11).

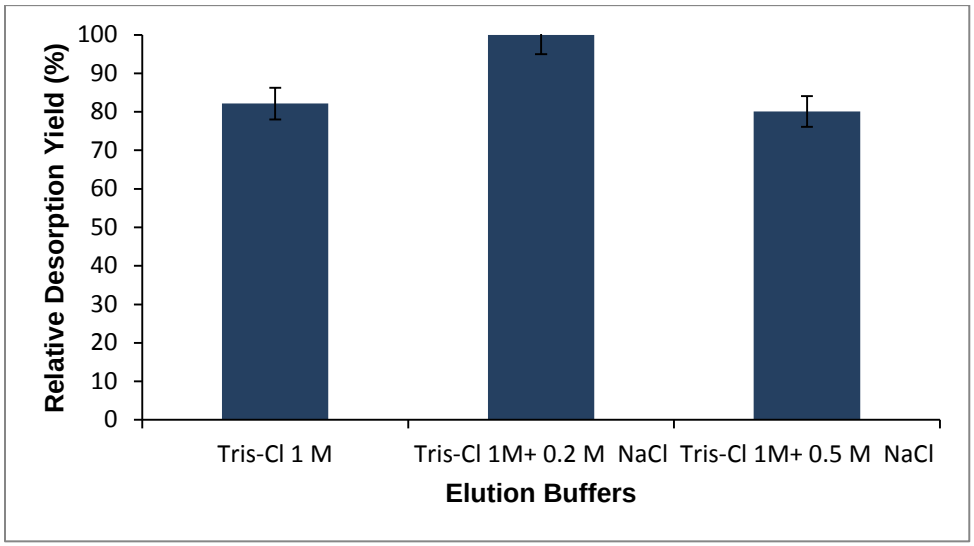

Figure 4.10 Effect of NaCl concentration (0, 0.2, 0.5 M NaCl) in elution buffer to desorption yield.

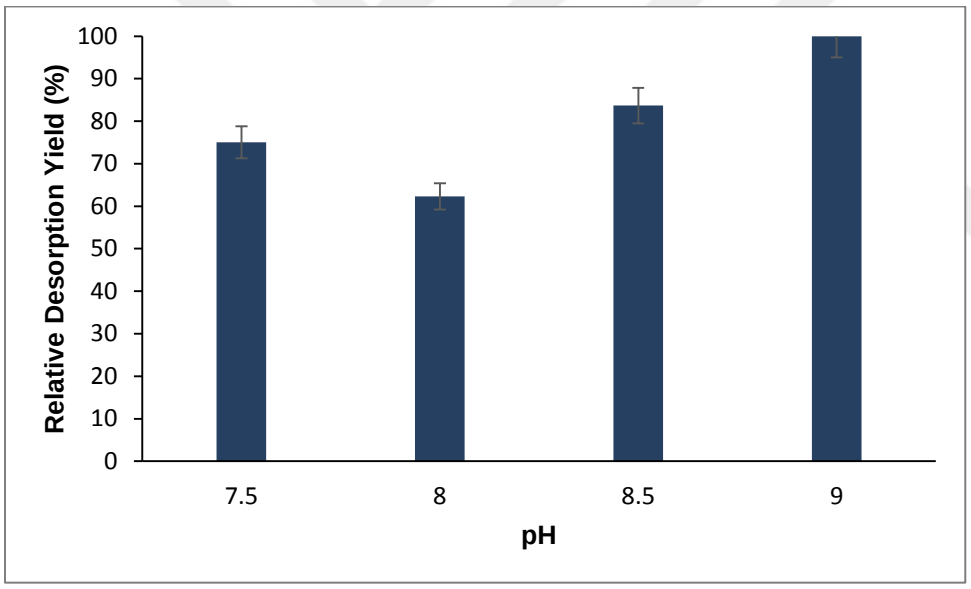

Figure 4.11 Effect of elution buffer pH (7.5, 8, 8.5, 9) to desorption yield.

4.6. Effect of NaCl concentration in binding buffer

The effect of NaCl concentrations in binding buffer on adsorption and isolation of glycosylated proteins in complex media was studied under this topic. For this purpose, a protein sample was prepared by using IgG glycoprotein and BSA non-glycated protein in same ratio. It was aimed to investigate ionic strength effect on isolation of IgG glycoprotein.

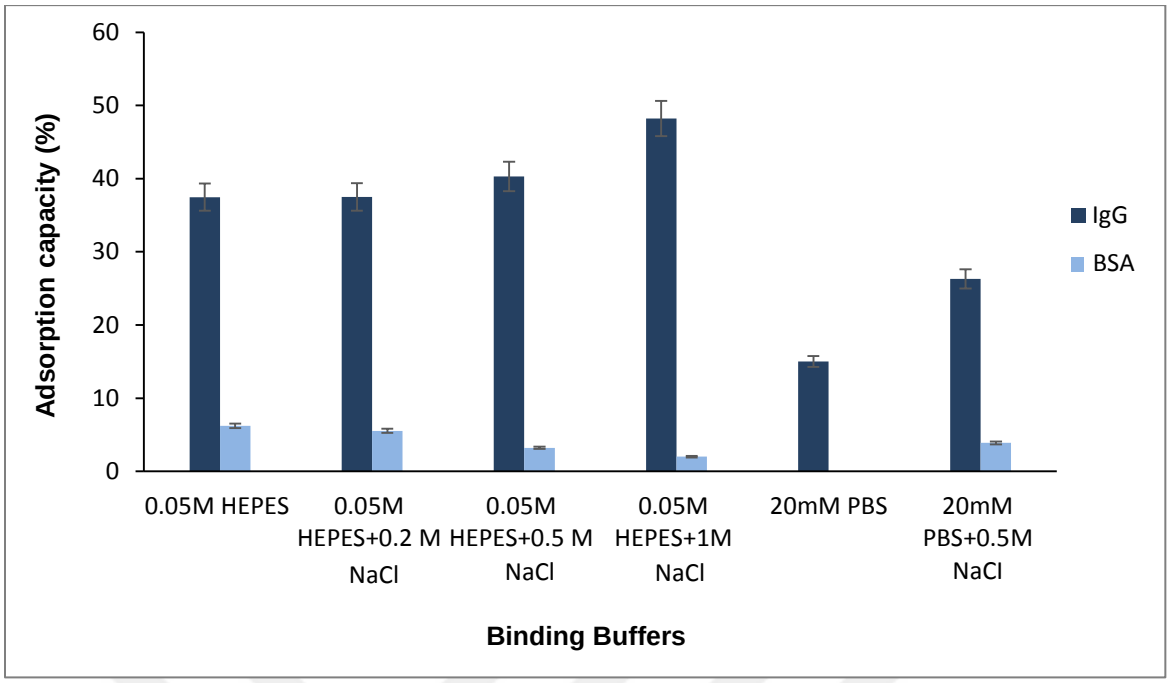

Figure 4.12 Effect of NaCl concentration in binding buffer for isolation of IgG glycoprotein in complex media.

In this experiment, in addition to NaCl concentration variations, different binding buffer type was used and its effect on adsorption process was studied (Figure 4.12). Firstly, when binding buffers were compared, it was clearly seen that HEPES buffer was more successful than PBS for adsorption process. When ionic strength effect on adsorption process was compared, adsorption yield of IgG glycoprotein in mixture increased with increasing of NaCl concentration. 0.05 M HEPES with 1 M NaCl had higher efficiency than others. Also with increasing NaCl concentration, undesired BSA adsorption was minimized and isolation of IgG glycoprotein was maximized (Figure 4.12). Although BSA adsorption realized in low level, adsorption yield of IgG glycoprotein was also in low level. Before the binding process, ionic strength effect on adsorption capacity was minimal, thus ionic strength effect was studied after binding process, in wash treatment.

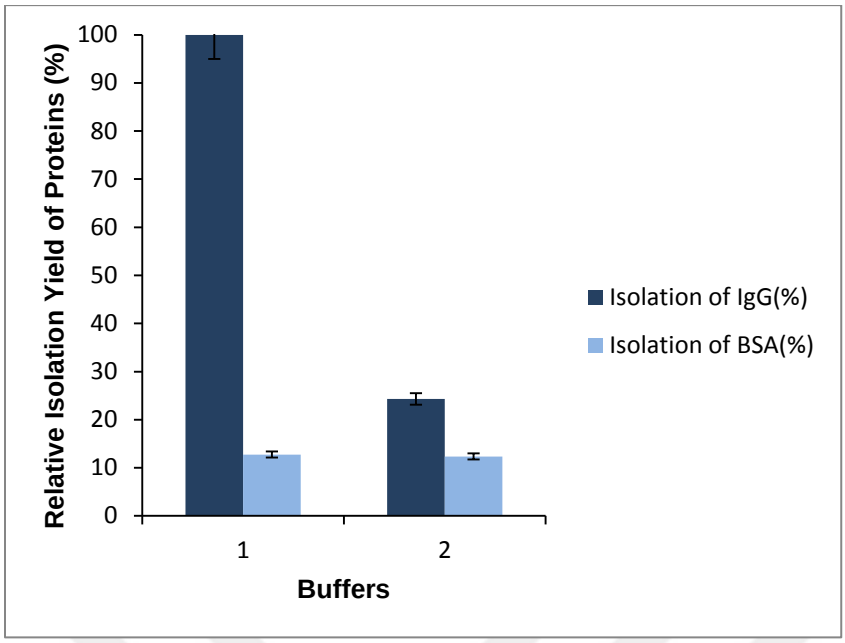

Figure 4.13 Effect of NaCl concentration in wash buffer to isolation yield of IgG glycoprotein in complex media. (1) Binding Buffer 0.05 M HEPES, Wash Buffer 0.05 M HEPES+1 M NaCl (2) Binding and wash buffer 0.05 M HEPES+1 M NaCl.

In previous figure, effect of NaCl in binding buffer to isolation of IgG was studied. With this condition adsorption capacity was low, thus the effect of NaCl existence in wash buffer (0.05 M HEPES) on isolation of IgG glycoprotein in complex media was observed (Figure 4.13). It is seen that, with the presence of NaCl in wash buffer, isolation yield of IgG glycoprotein increased relatively more compared to other condition, also negative control BSA protein's adsorption yield decreased. As a result, IgG purity level became higher.

4.7. Effect of NaCl concentration in wash buffer

Ionic strength effect in wash buffer on isolation of glycosylated protein was shown in previous figure. In order to see NaCl concentration effect on isolation efficiency of IgG glycoprotein in complex media, wash buffer with different concentration of NaCl were used.

Figure 4.14 shows that effect of NaCl concentration in wash buffer to isolate IgG glycoprotein in complex media. Optimum results were obtained by using 0.05 M HEPES with 0.5 M NaCl as wash buffer. Isolation yield of IgG glycoprotein increased; besides this, adsorbed quantity of the non-glycated protein BSA decreased as expected.

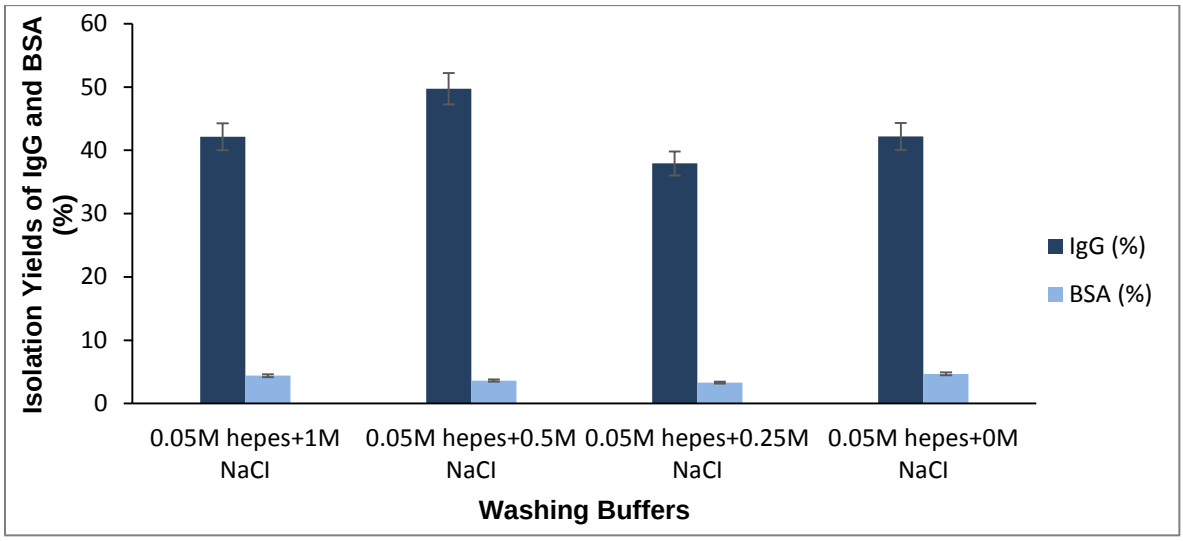

Figure 4.14 Effect of NaCl concentration in wash buffer to isolation yield of IgG glycoprotein in rabbit serum media. Wash buffers: 50 mM HEPES + 1 M NaCl, 50 mM HEPES + 0.5 M NaCl, 50 mM HEPES + 0.25 M NaCl, 50 mM HEPES, respectively.

4.8. Enrichment of IgG from serum media

Rabbit serum is composed of various glycated and non-glycated proteins. IgG purification steps with APBA functionalized magnetic silica microbeads (original sample, washes and eluted proteins, respectively) was investigated next.

SDS-PAGE analysis of purified IgG glycoprotein from rabbit serum is given in Figure 4.15. After purification with APBA functionalized silica microbeads, IgG glycoprotein was seen clearly in elution lanes (E1, E2, E3), with negligible amounts in wash lanes (W1, W2, W3). It showed successful purification process of IgG glycoprotein.

4.8.1. Effect of ionic strength in wash buffer for IgG purification

SDS-PAGE analysis of purified IgG glycoprotein from rabbit serum by using different concentrations of NaCl in wash buffer is given in Figure 4.16. According to wash buffer types, IgG in serum sample (in the middle band of the figure) was purified how was shown in elution bands. After purification with APBA functionalized silica microbeads, IgG glycoprotein isolation yield changes with different concentrations of NaCl in wash buffer (50 mM HEPES, pH: 8.5) was seen clearly in elution lanes (E1, E2).

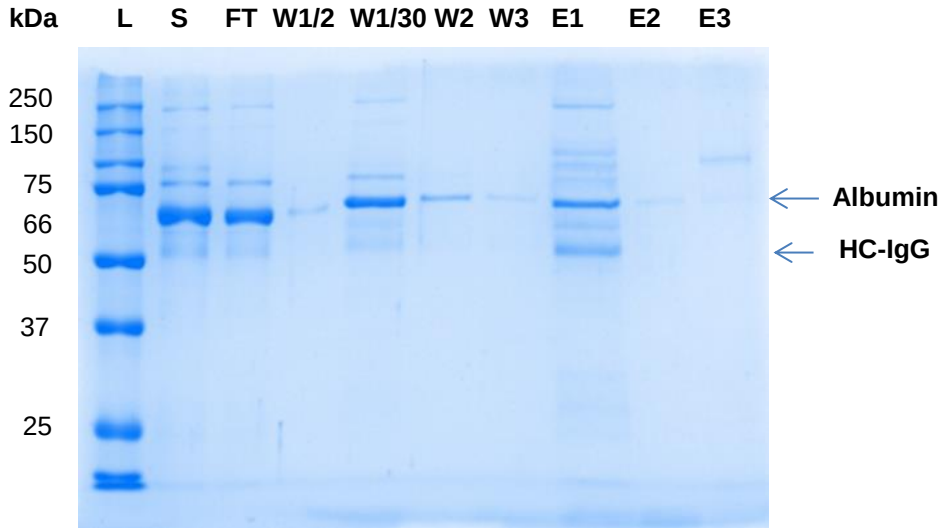

Figure 4.15 SDS-PAGE analysis of affinity purification steps of IgG glycoprotein from rabbit serum complex media flow-through loading 2 ul to well (FT), wash 1 loading 2 ul to well (W1/2), wash1 loading 30 ul to well (W1/30), wash 2 loading 30 ul to well (W2), wash 3 loading 30 ul to well (W3), elutions 1-3 loading 30 ul to well (E1-E3), using 5 mg of sorbent in 0.5 mL of adsorption medium(0.05 M HEPES pH 8.5) and 1 M Tris-Cl with 0.2 M NaCl elution buffer.

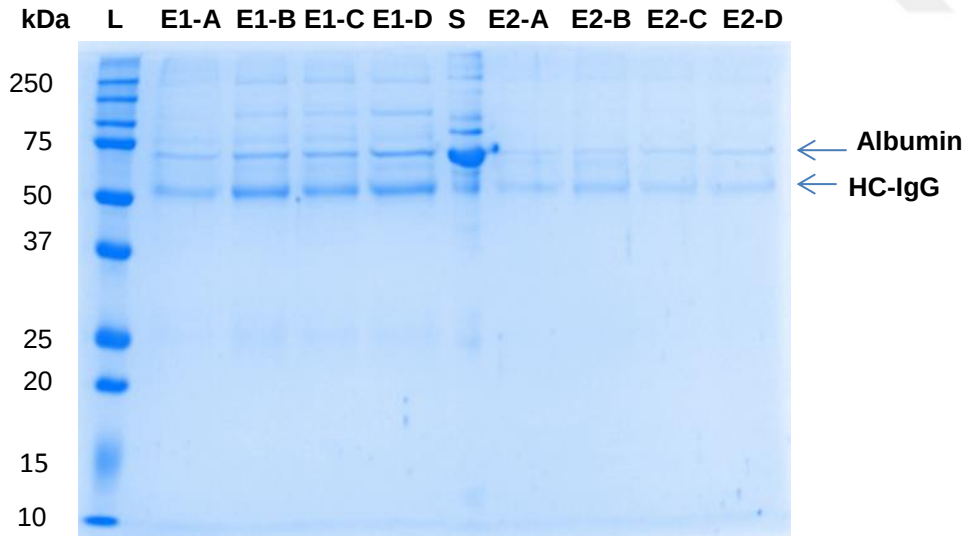

Figure 4.16 SDS-PAGE analysis of the effect of the non-specific protein suppress and enrichment of IgG glycoprotein from rabbit serum and with different NaCl concentration (A: 1M NaCl B: 0.5M NaCl C: 0.25M NaCl D: 0M NaCl) in wash buffer. Using 2 mg of sorbent in 0.1 mL of adsorption medium (50 mM HEPES pH 8.5) and 1 M Tris-Cl with 0.2 M NaCl elution buffer.

According to the SDS-PAGE image analysis, optimum results were obtained by using 0.05 M HEPES with 0.5 M NaCl as wash buffer. In elution bands belonging to 0.05 M HEPES with 0.5 M NaCl wash buffer; isolation yield of IgG glycoprotein increased, also non-specific proteins were suppressed the most with this condition.

4.8.2. The effect of sorbent mass for IgG purification process

By using different concentrations of APBA@MagSiO$_2$ microbeads, effects of sorbent mass on IgG adsorption capacity and isolation yield from complex media were investigated. For this purpose, six different concentrations of sorbent (1, 2, 5, 10, 20 and 40 mg) were used to adsorb same concentration of IgG in same adsorption buffer.

In here, according to initial protein concentration experiment set to suppress albumin adsorption effectively and increase the isolation yield of IgG glycoprotein, 1 mg/mL protein samples were used. The effect of sorbent mass on IgG glycoprotein adsorption capacity (mg IgG per g sorbent) under equilibrium conditions is shown in Figure 4.17(A). Adsorption capacity per unit sorbent was decreased with increasing amount of sorbent. Maximum adsorption capacity was observed as 46 mg IgG per g-sorbent with the lowest sorbent amount (i.e. 1 mg sorbent). Adsorption capacity decreased from 46 to 2 mg IgG per g sorbent with increasing sorbent mass from 1 to 40 mg.

When maximum isolation yield of IgG and minimum isolation yield of albumin to obtain more purified IgG were compared, optimized sorbent mass was found between 5 -10 mg interval.

In SDS-PAGE analysis, IgG purification level was determined colorimetricly according to sorbent mass variation. Calculated protein purification parameters via Image Lab 5.1 software showed that maximum purification of IgG was obtained with 5 mg sorbent. IgG was concentrated and albumin was diluted 4-fold each with this condition.

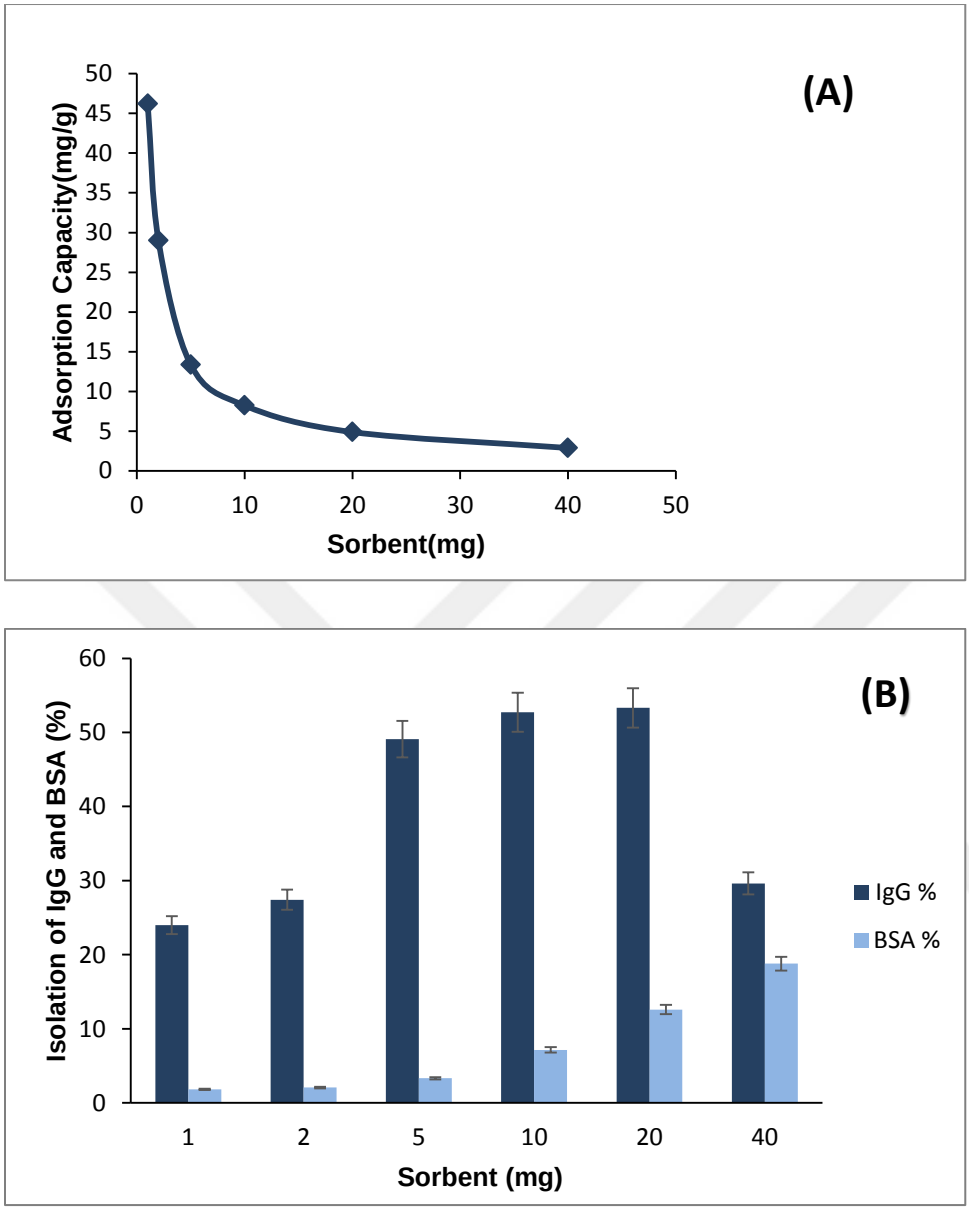

Figure 4.17 (A) Effect of sorbent mass to adsorption capacity of IgG glycoprotein, adsorption buffer 0.05 M HEPES pH 8.5, adsorption medium 0.5 mL

(B) Desorption and isolation yield change of IgG glycoprotein and albumin protein with different sorbent mass. Desorption buffer 1 M Tris-Cl with 0.2 M NaCl, desorption medium 0.1ml.

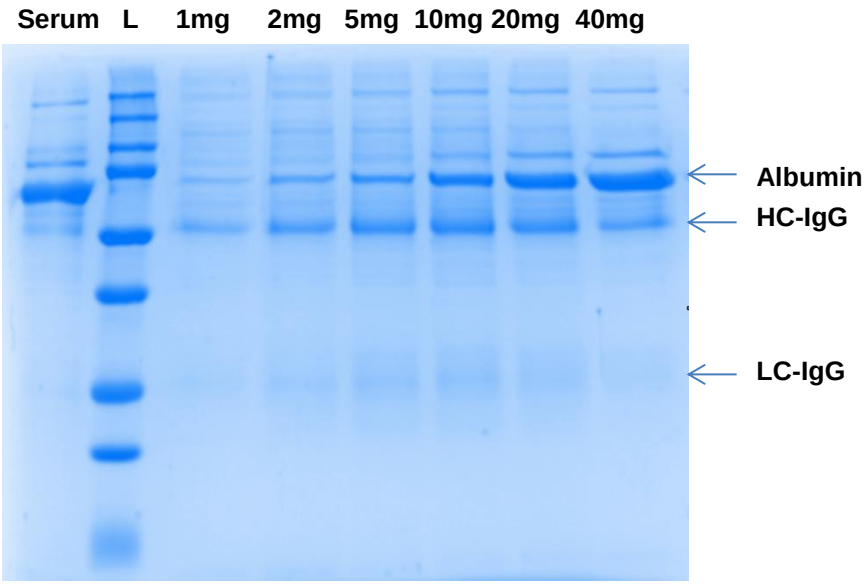

Figure 4.18 SDS-PAGE analysis of affinity purification steps of IgG glycoprotein from rabbit serum complex media using 1mg, 2mg, 5mg, 10mg, 20mg, 40mg of sorbent in 0.1 mL of adsorption medium(0.05 M HEPES pH 8.5) and 1 M Tris-Cl(pH:8.5) with 0.2 M NaCl elution buffer.

4.9. Reusability of Particle

In addition to adsorption/desorption yields, reusability of this particle is an important topic. Reusable particles offer a cost effective method. For this purpose, APBA functionalized magnetic silica microbeads reusability was investigated here, by performing five successful IgG glycoprotein isolations under the same conditions. The adsorption, desorption and isolation yields of IgG glycoprotein changes are given in Figure 4.19. Isolation yield of IgG almost did not change from the first to fifth use.

4.10. Desorption Yield of Proteins

Desorption yields of different adsorbed proteins on magnetic APBA functionalized silica microbeads, by using 1 M Tris-Cl buffer (pH 8.5) with 0.2 M NaCl are shown in Figure 4.20.

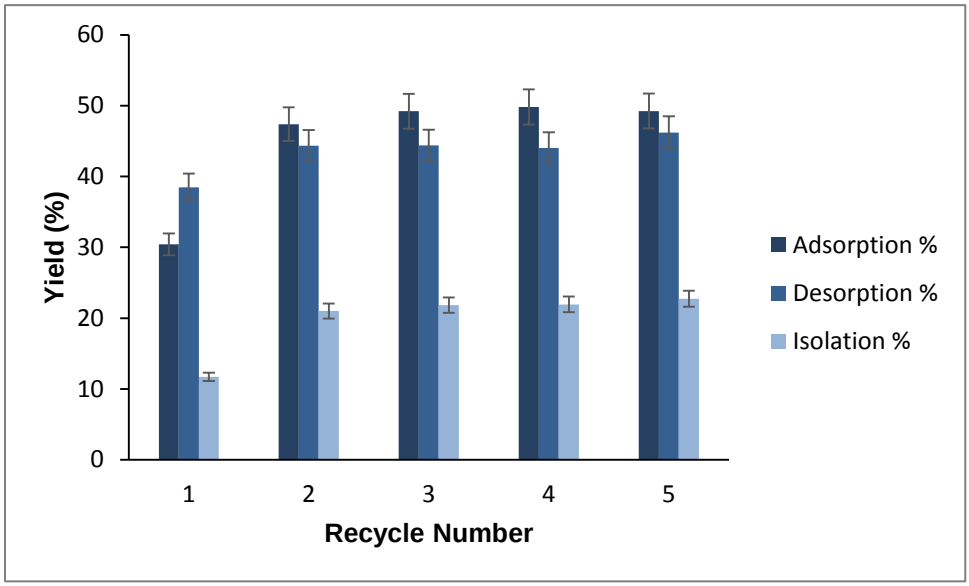

Figure 4.19 Reusability of APBA functionalized magnetic silica microbeads according to their adsorption/isolation yield with recycling times.

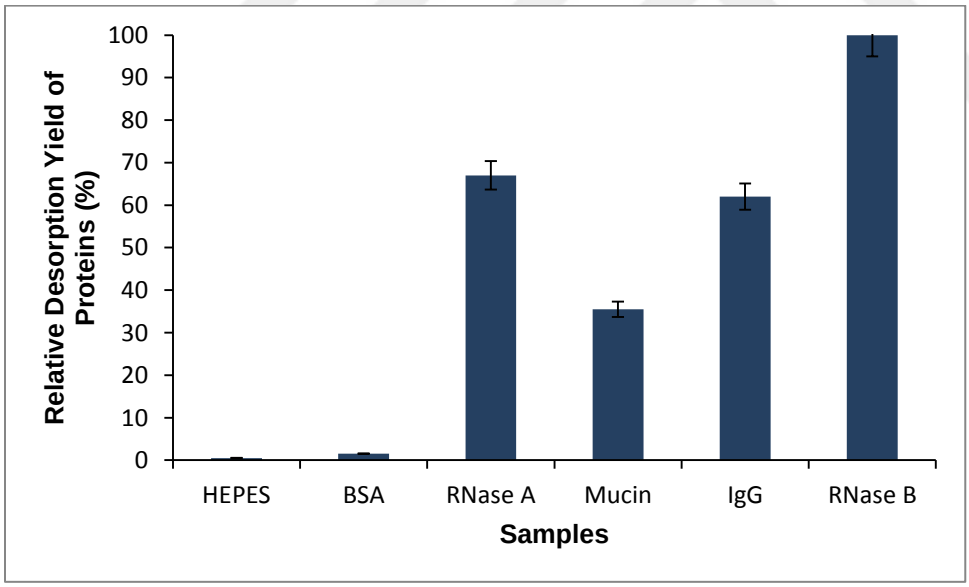

Figure 4.20 Desorption yield of equimolar glycoproteins (Mucin, IgG and RNase B) and non-glycoproteins (BSA, RNase A) from APBA functionalized magnetic silica microbeads with 1 M Tris-Cl buffer with 0.2 M NaCl, pH 8.5

In here, as BSA is a non-glycated protein and has no diol groups, it was neither adsorbed nor desorbed. Mucin, IgG and RNase B are glycoproteins so as expected, they were adsorbed by the particle. The maximum desorption yield was obtained with RNase B. RNase A is a non-glycated protein but has one diol group so it was adsorbed because of boronate affinity principle. RNase A and RNase B proteins structures are similar but distinctively RNase B has 6 sugar groups, thus RNase B was relatively adsorbed more. While SERS technique was studied for sensitive detection of adsorbed proteins on microbeads, these similar RNase A and RNase B model proteins were used to see efficiency of microbeads.

There are many studies about glycoprotein enrichment by using boronic acid functionalized particles. In Table 4.2, some examples in literature were summarized according to their adsorption capacity and they were compared with this study.

It is seen that, the selective enrichment of different type of glycoproteins were done by using boronic acid functionalized particles. In this study, IgG glycoprotein enrichment was realized by using APBA functionalized magnetic silica microbeads. Its maximum adsorption capacity was calculated as 84 $mg.g^{-1}$. This value is effective and average in comparison with others.

Table 4.2 Adsorption capacity comparisons of boronic acid functionalized particles in literature

Particle	Model Glycoprotein	Adsorption Capacity ($mg.g^{-1}$)	Reference
3-APBA functionalized magnetic silica microbeads	IgG	84	This study
4-FPBA functionalized magnetic molecularly imprinted nanoparticles (MMIPs)	Horseradish peroxidase(HRP)	62	[182]
GO-APBA/MIPs	OVA	278	[183]
3-APBA functionalized poly(glycidyl methacrylate-co-ethylene dimethacrylate) microspheres	Fetuin	337	[184]
3-APBA functionalized magnetic molecularly imprinted particles (MMIPs)	Horseradish peroxidase(HRP)	60	[185]
Binary 3-APBA functionalized attapulgite (ATTA-NH2-DBA)	Adenosine	21	[186]
4-vinylphenylboronic acid functionalized poly(glycidylmethacrylate-co-ethylenedimethacrylate) beads	OVA	31	[187]
APBA functionalized dextran coated MPs	IgG	170	[9]

4.11. SERS Analysis

RNase A and RNase B proteins have similar structure, only difference being the glycans in RNase B proteins. MPBA-Ag@MagPMMS has boronic acid, because of boronate affinity mechanism; this microsphere binds to diol groups. RNases have diol group but in RNase B protein diol groups are much more due to glycan structures available. SERS sensitive spectral detection method is useful to see this difference between proteins. Also with this method, according to the intensity of signal, determination of concentration of these proteins is also possible.

SERS spectras of RNase A non-glycosylated and RNase B glycosylated proteins at different concentrations are given in Figure 4.21. The same particle, MPBA-Ag@MagPMMS was used as SERS tag for two types of protein. The Raman bands at 698, 1000, and 1024 cm^{-1} were assigned to the bending of C−C ring/C−S stretching, C−C bending in the phenyl ring, and C−H bending in the phenylboronic acid group, respectively [188, 189]. The B−OH stretching of the same group should also contribute to the peak at 1070 cm^{-1} [190]. The SERS tag capturing RNase B and PATP/MPBA-functionalized Ag NPs displayed clear SERS peaks at 1436, 1390, and 1140 cm^{-1}. These peaks resulted from in situ-generated dimethylamino benzaldehyde (DMAB) from the photocoupling transformation of PATP on the Ag NPs under 785 nm laser irradiation [191]. Raman shifts at 1436 and 1390 cm^{-1} are related to the N=N stretching vibrations of DMAB [192]. In situ-formed DMAB should also contribute to the peak at 1070 cm^{-1} [191, 192]. On the other hand, the peak at 1574 cm^{-1} is related to the contributions from both MPBA and DMAB/PATP. The intensities of peaks at 1140 and 1436 cm^{-1} originating from the in situ-formed Raman reporter during the SERS measurement, DMAB, changed proportionally according to the RNase A and RNase B concentration in the sample mixture (Figure 4.21). RNase A has no glycan moieties but it contains a diol group, so binding to boronic acid functionalized SERS tag realized weakly. However, capturing of the RNase B glycoprotein was stronger and the SERS signal was more intensive compared to the one obtained for RNase A. Moreover, with increasing concentration of protein, peak area increased and RNase B concentration was determined over a broad range (0.1 to 1000 ng/mL). RNase B concentrations down to 0.1 ng/mL nearly 10^{-15} M could be detected with this method effectively.

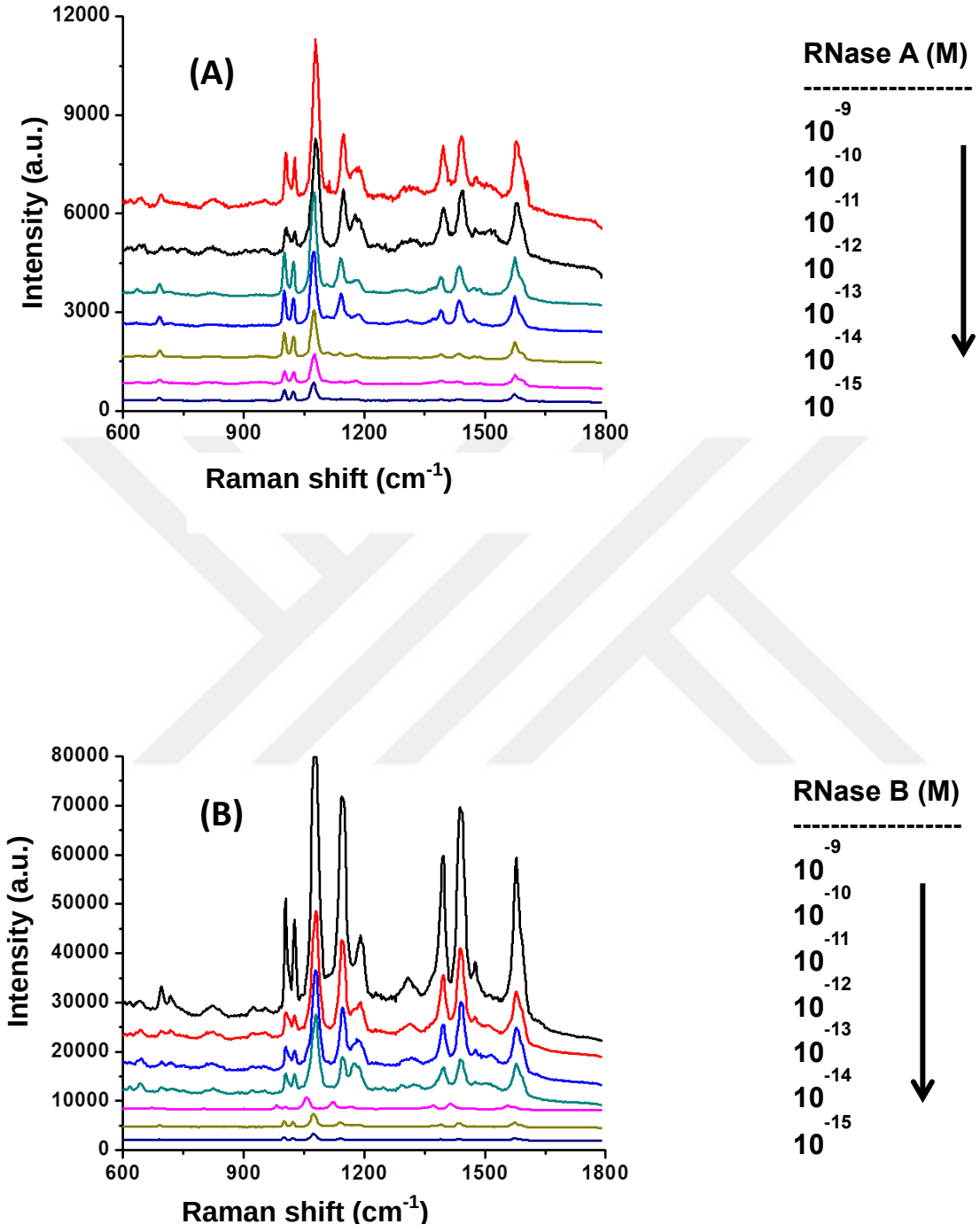

Figure 4.21 (A) SERS spectra of RNase A non-glycoprotein at different concentrations **(B)** SERS spectra of RNase B glycoprotein at different concentrations.

For observing the SERS behavior of this sandwich system with varying concentrations of RNase A and RNase B proteins, the peak area ratio from DMAB at 1436 cm^{-1} to 1070 cm^{-1} in SERS spectra of proteins were plotted against protein concentrations in Figure 4.22. Increasing RNase B concentration in the sample, resulted in a linear increase in SERS peak area ratio, because of boronic acid-glycan interactions, as expected. RNase A has no glycan in its structure, so peak area ratio stayed almost constant with varying concentration of RNase A. It is seen that, there is an important difference in peak area ratio between these two proteins SERS spectra; it also shows that this system substantially captured glycoproteins like RNase B.

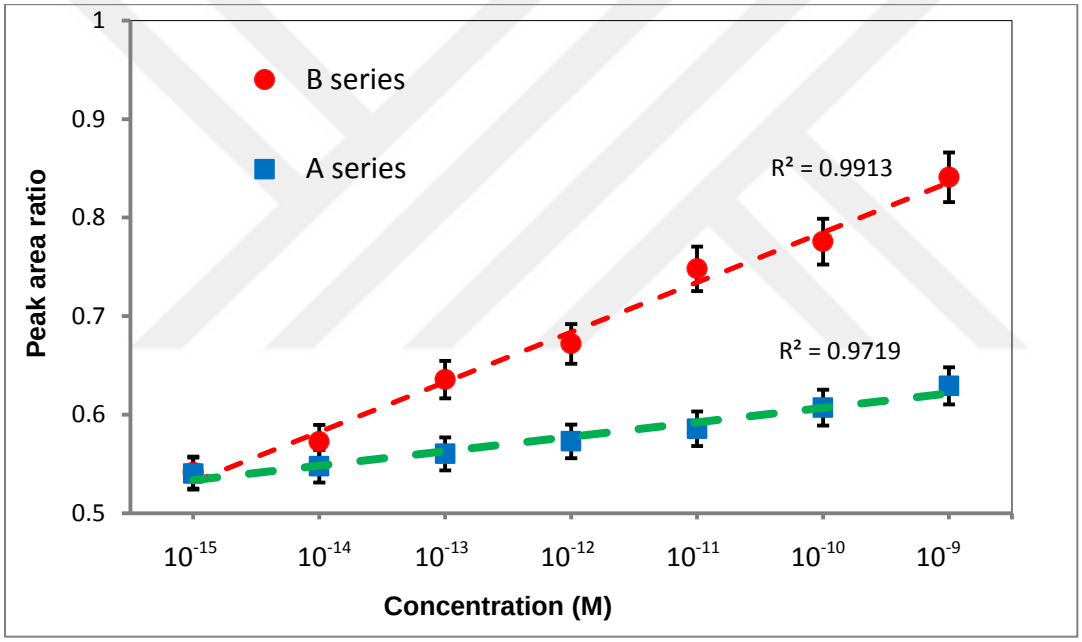

Figure 4.22 Calibration curves for RNase A and RNase B proteins determination in samples and trends of peak area ratio values of these proteins at different concentrations. The R^2 values are given on the plot.

In here, to analyze SERS behavior of the sandwich system in protein mixture which contains constant concentration of RNase A non-glycosylated protein and varying concentration of RNase B glycoprotein was plotted against protein concentrations in Figure 4.23.

It was shown that peak area ratio increased linearly with increasing concentration of RNase B. Besides, peak area ratio based on RNase A concentration nearly stayed constant because of constant concentration of RNase A protein, as expected.

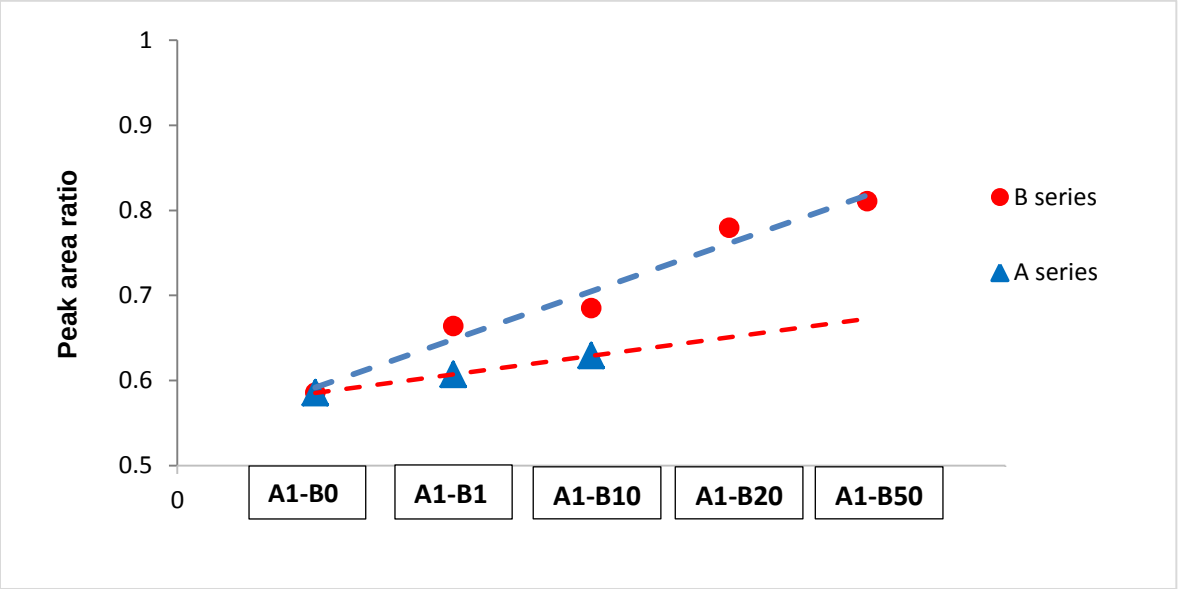

Figure 4.23 Calibration curves for RNase A and RNase B proteins with varying of RNase B concentration in RNase A-B mixture (RNase A concentration constant, 10^{-11} M) RNase A: 10^{-11}M - RNase B: 0, RNase A: 10^{-11}M - RNase B: 10^{-11}M, RNase A: 10^{-11}M - RNase B: 10^{-10}M, RNase A:10^{-11}M-RNase B:2x10^{-10}M, RNase A:$^{10\text{-}11}$M-RNase B:5x10^{-10}M, respectively.

In Table 4.3, several studies about low level detection of glycoproteins in literature are given. There are many detection techniques and application areas of glycoproteins. It is seen that clearly by using SERS technique, detection limit becomes lower. In fact, this study has highest sensitivity in comparison to other ones with 0.1 ng/mL detection level. It shows the effectivity of microspheres used.

Table 4.3 Comparisons of low level glycoprotein detection studies in literature

Usage Area	SERS	Detailed Information	Reference
Purification and sensitive determination of trace amount of glycoproteins	✓	• Phenylboronic acid-functionalized, Ag shell coated, magnetic, monodisperse polymethacrylate microspheres • Qualitative and quantitative analysis • RNase A and B model proteins • 0.1 ng/mL detection level sensitivity	This study
Quantitative determination of glycated hemoglobin (HbA1c) in diagnosis of diabetes.	✓	• Phenylboronic acid-functionalized, Ag shellcoated, magnetic, monodisperse polymethacrylate microspheres • ng/mL detection level sensitivity	[180]
Recognition of an intact glycoprotein and its characteristic fragments	✗	• MALDI TOF MS • MNP • lectin-like binding properties • RNase B glycan-imprinted MNPs • µM detection level sensitivity	[193]
Specific and sensitive determination of trace glycoproteins in complex samples	✓	• Boronate-affinity molecularly imprinted polymers (MIPs) • a-fetoprotein (AFP)model protein • ng/mL detection level sensitivity	[71]
Prostate cancerous cell detection(Elevated expression of sialic acid containing glycoprotein)	✓	• Confocal Raman microscope • Qualitative analysis • Lectin functionalized silver nanoparticle	[4]
Lectin type identification for diagnosis and developing effective therapeutics	✗	• GlycoAuNP's • LSPR • Qualitative analysis	[3]
With mimicking of specific lectin-glycan interaction, isolation and removal of *E. coli*	✗	• Magnetic NP's • Confocal Laser scanning microscopy	[25]
Quantification of blood glucose level in long-term history of glycemic control	✗	• DCDR • No calibration curve for glucose concentration vs Raman signal • µM detection level sensitivity	[6]
Determination of the glycosylation status of proteins and quantifying the relative concentrations of the RNase A protein and RNase B glycoprotein within mixtures	✗	• MALDI MS and Raman Spectroscopy • No calibration curve for glucose concentration vs Raman signal • µM detection level sensitivity	[8]

5. CONCLUSION

Glycoproteins are used as diagnostic tools for some diseases and forms major part of biopharmaceuticals. Thus glycoprotein purification and detection is an important topic nowadays. Within the scope of this thesis, some glycoproteins like IgG, RNase B etc. was purified by synthesized APBA functionalized magnetic silica microbeads in sample mixture. Also optimized purification conditions, effect of initial concentration of protein, sorbent concentration, binding buffer pH effects on adsorption mechanism and effect of ionic strength, molarity, pH and competitive ligand on elution mechanism were studied. Spectrophotometric detection and quantification, SDS-PAGE analysis of these proteins were performed. Also, using an ultrasensitive detection method, SERS technique, RNase A and RNase B proteins were analyzed and glycoprotein detection limit was determined.

In the first part, with the aim of purification of glycoproteins, APBA@MagSiO_2 microbeads kindly supplied by Prof. Dr. S. Ali Tuncel and Dr. Çiğdem Kip were used. Synthesized silica particles with paramagnetic properties were functionalized with 3-aminophenyl boronic acid (APBA). In this state, microbeads could bind glycan groups as pH-dependent. When these particles were interacted with sample containing glycoproteins and others, adsorption kinetic data shows that 30-40 minutes was sufficient to reach saturation. As binding buffer, optimum conditions were obtained with 0.05 M HEPES (pH: 8.5). Effect of initial protein concentration was also studied. It is seen that desired glycoprotein adsorption and purification in mixture increased with increasing concentration of protein, then at sorbent saturation point adsorption capacity became constant. IgG adsorption behavior was also observed and Langmuir model was found more suitable compared to others. It shows that adsorption has occurred as single layer and homogeneously.

After the washing step of sorbent, non-specific physical interactions were cleared away. For the washing process, to suppress non-specific interactions on sorbent ionic strength effect was investigated with different concentration of NaCl in washing buffer. As expected, with increasing NaCl concentration, non-specific

interactions decreased and optimum condition was obtained with 0.5 M NaCl in washing buffer.

Then, desorption process of glycoproteins was investigated. For this, pH, molarity, ionic strength and competitive ligand effects on desorption mechanism were studied. According to desorption yield, 1 M Tris-Cl buffer (pH: 8.5) was chosen. As ligand competitive, sorbitol effect was tried but with increasing sorbitol concentration in elution buffer, desorption yield decreased so sorbitol was not used in elution buffer in further experiments. Also to see ionic strength effect on desorption mechanism, different concentrations of NaCl in elution buffer was investigated and optimum NaCl concentration was found as 0.2 M.

Using optimum conditions determined, IgG glycoprotein purification in complex media was realized and SDS-PAGE analysis was performed. To see effect of sorbent concentration on adsorption capacity and isolation of IgG glycoprotein in serum sample, different amounts of sorbent were used (1, 2, 5, 10, 20, 40 mg). It was seen that with increasing amounts of sorbent, adsorption capacity per unit sorbent decreased. According to isolation yield of IgG glycoprotein, optimum sorbent amount was determined as 5 mg. Another important topic, reusability of particles was also examined. The reusability of APBA functionalized magnetic silica microbeads were studied by performing five successful IgG glycoprotein isolations under the same conditions. Isolation yield of IgG almost did not change from first to fifth iteration, so the particle is reusable.

In the second part of thesis, as an ultrasensitive detection of glycoproteins, SERS technique was used. For this detection method firstly, silver nanoshell-coated magnetic, monodisperse polymethacrylate (Ag@MagPMMS) microspheres were produced. To obtain pH dependent diol-sensitive system, microspheres were functionalized with 4-MPBA. As model proteins, much similar RNase B glycoprotein and RNase A protein were used. RNase A and B has similar structure, only difference is RNase B has between 6 and 10 sugar groups. Thus because of diol groups in RNase B, it is expected that only RNase B could attach to functionalized microbeads. RNase A was the negative control. RNase A and RNase B proteins separately and as mixture were interacted with MPBA-Ag@MagPMMS sorbent, on the other part synthesized PATP/MPBA@Ag NPs were bound onto the protein sample present on MPBA-Ag@MagPMMS and a

sandwich system was formed. SERS spectra of these proteins were obtained. When RNase B glycoprotein was bound to sorbent, SERS signal intensity became stronger than RNase A protein, which shows the glycoprotein specificity of the sorbent. According to specific peak area ratios, concentration of these proteins were calculated; in other words, calibration curves for RNase A and RNase B proteins according to concentration against peak area ratio values were obtained. RNase B curve was linearly increased with increasing concentration, but RNase A curve was nearly constant at different concentrations. With the aim of SERS method, RNase B concentrations down to 0.1 ng/mL, nearly 10^{-15} M, could be detected with this method easily. This detection limit will contribute to literature, as glycoprotein in femto-molar concentration levels can be detected easily with this method. Early diagnosis of diseases, characterization and quantification of glycoproteins in biopharmaceutics can be realized with this sensitive technique.

REFERENCES

1. Baker, J.L., E. Çelik, and M.P. DeLisa, Expanding the glycoengineering toolbox: the rise of bacterial N-linked protein glycosylation. *Trends in biotechnology*, **2013**. 31(5): p. 313-323.
2. Craig, D., et al., Formation of SERS active nanoparticle assemblies via specific carbohydrate–protein interactions. *Chemical Communications*, **2013**. 49(1): p. 30-32.
3. Jayawardena, H.S.N., X. Wang, and M. Yan, Classification of lectins by pattern recognition using glyconanoparticles. *Analytical chemistry*, **2013**. 85(21): p. 10277-10281.
4. Craig, D., et al., Confocal SERS mapping of glycan expression for the identification of cancerous cells. *Analytical chemistry*, **2014**. 86(10): p. 4775-4782.
5. Varki, A., Glycan-based interactions involving vertebrate sialic-acid-recognizing proteins. Nature, **2007**. 446(7139): p. 1023-1029.
6. Barman, I., et al., Raman spectroscopy-based sensitive and specific detection of glycated hemoglobin. *Analytical chemistry*, **2012**. 84(5): p. 2474-2482.
7. Dingari, N.C., et al., Raman spectroscopy provides a powerful diagnostic tool for accurate determination of albumin glycation. *PLoS One*, **2012**. 7(2): p. e32406.
8. Brewster, V.L., L. Ashton, and R. Goodacre, Monitoring the glycosylation status of proteins using Raman spectroscopy. *Analytical chemistry*, **2011**. 83(15): p. 6074-6081.
9. Dhadge, V.L., et al., Boronic acid-modified magnetic materials for antibody purification. *Journal of The Royal Society Interface*, **2014**. 11(91): p. 20130875.
10. Jain, E. and A. Kumar, Upstream processes in antibody production: evaluation of critical parameters. *Biotechnology advances*, **2008**. 26(1): p. 46-72.
11. Agrawal, A., T. Sathe, and S. Nie, Single-bead immunoassays using magnetic microparticles and spectral-shifting quantum dots. *Journal of agricultural and food chemistry*, **2007**. 55(10): p. 3778-3782.
12. Merkle, R.K. and R.D. Cummings, Lectin affinity chromatography of glycopeptides. *Methods in enzymology*, **1986**. 138: p. 232-259.
13. Ahmad, S., R.H. Khan, and A. Ahmad, Physicochemical characterization of Cajanus cajan lectin: effect of pH and metal ions on lectin carbohydrate interaction. *Biochimica et Biophysica Acta (BBA)-General Subjects*, **1999**. 1427(3): p. 378-384.
14. Bertok, T., et al., Ultrasensitive impedimetric lectin biosensors with efficient antifouling properties applied in glycoprofiling of human serum samples. *Analytical chemistry*, **2013**. 85(15): p. 7324-7332.

15. Gupta, G., A. Surolia, and S.-G. Sampathkumar, Lectin microarrays for glycomic analysis. *Omics: a journal of integrative biology*, **2010**. 14(4): p. 419-436.

16. Liu, L., et al., Hydrazide functionalized core–shell magnetic nanocomposites for highly specific enrichment of N-glycopeptides. *ACS applied materials & interfaces*, **2014**. 6(10): p. 7823-7832.

17. Zhang, H., et al., Identification and quantification of N-linked glycoproteins using hydrazide chemistry, stable isotope labeling and mass spectrometry. *Nature biotechnology*, **2003**. 21(6): p. 660-666.

18. Alvarez-Manilla, G., et al., Tools for glycoproteomic analysis: size exclusion chromatography facilitates identification of tryptic glycopeptides with N-linked glycosylation sites. *Journal of proteome research*, **2006**. 5(3): p. 701-708.

19. Gilar, M., et al., Characterization of glycoprotein digests with hydrophilic interaction chromatography and mass spectrometry. *Analytical biochemistry*, **2011**. 417(1): p. 80-88.

20. Selman, M.H., et al., Cotton HILIC SPE microtips for microscale purification and enrichment of glycans and glycopeptides. *Analytical chemistry*, **2011**. 83(7): p. 2492-2499.

21. Zhang, S., et al., Boronic acid functionalized magnetic nanoparticles via thiol–ene click chemistry for selective enrichment of glycoproteins. *New Journal of Chemistry*, **2014**. 38(9): p. 4212-4218.

22. Yao, G., et al., Facile synthesis of 4-mercaptophenylboronic acid functionalized gold nanoparticles for selective enrichment of glycopeptides. *Rapid Communications in Mass Spectrometry*, **2009**. 23(22): p. 3493-3500.

23. Springsteen, G. and B. Wang, A detailed examination of boronic acid–diol complexation. *Tetrahedron*, **2002**. 58(26): p. 5291-5300.

24. Huang, Y.-F., Y.-F. Wang, and X.-P. Yan, Amine-functionalized magnetic nanoparticles for rapid capture and removal of bacterial pathogens. *Environmental science & technology*, **2010**. 44(20): p. 7908-7913.

25. Behra, M., et al., Magnetic porous sugar-functionalized PEG microgels for efficient isolation and removal of bacteria from solution. *Biomacromolecules*, **2013**. 14(6): p. 1927-1935.

26. Marín, M.J., et al., Glyconanoparticles for colorimetric bioassays. *Analyst*, **2015**.

27. Hughes, J., et al., Ultra sensitive label free surface enhanced Raman spectroscopy method for the detection of biomolecules. *Talanta*, **2014**. 130: p. 20-25.

28. McAughtrie, S., K. Faulds, and D. Graham, Surface enhanced Raman spectroscopy (SERS): Potential applications for disease detection and treatment. *Journal of Photochemistry and Photobiology C: Photochemistry Reviews,* **2014**. 21: p. 40-53.

29. Wang, Y., et al., Nanomaterials in carbohydrate biosensors. TrAC Trends in *Analytical Chemistry*, **2014**. 58: p. 54-70.

30. Berg, J.M., J.L. Tymoczko, and L. Stryer, *Glycolysis and gluconeogenesis*. **2002**.

31. Zeng, X., et al., Carbohydrate–protein interactions and their biosensing applications. *Analytical and bioanalytical chemistry*, **2012**. 402(10): p. 3161-3176.

32. Varki, A., Biological roles of oligosaccharides: all of the theories are correct. *Glycobiology*, **1993.** 3(2): p. 97-130.

33. Sears, P. and C.-H. Wong, Toward automated synthesis of oligosaccharides and glycoproteins. *Science*, **2001**. 291(5512): p. 2344-2350.

34. Gagneux, P. and A. Varki, Evolutionary considerations in relating oligosaccharide diversity to biological function. *Glycobiology*, **1999**. 9(8): p. 747-755.

35. Dwek, R.A., Glycobiology: toward understanding the function of sugars. *Chemical Reviews*, **1996**. 96(2): p. 683-720.

36. Drickamer, K. and M.E. Taylor, Evolving views of protein glycosylation. *Trends in biochemical sciences*, **1998**. 23(9): p. 321-324.

37. Frey, A., et al., Role of the glycocalyx in regulating access of microparticles to apical plasma membranes of intestinal epithelial cells: implications for microbial attachment and oral vaccine targeting. *The Journal of experimental medicine*, **1996**. 184(3): p. 1045-1059.

38. Nakano, M., et al., Detailed structural features of glycan chains derived from α1-acid glycoproteins of several different animals: the presence of hypersialylated, O-acetylated sialic acids but not disialyl residues. *Glycobiology*, **2004**. 14(5): p. 431-441.

39. Bush, C.A., M. Martin-Pastor, and A. Imbery, Structure and conformation of complex carbohydrates of glycoproteins, glycolipids, and bacterial polysaccharides. *Annual review of biophysics and biomolecular structure*, **1999**. 28(1): p. 269-293.

40. Apweiler, R., H. Hermjakob, and N. Sharon, On the frequency of protein glycosylation, as deduced from analysis of the SWISS-PROT database. *Biochimica Et Biophysica Acta-General Subjects*, **1999**. 1473(1): p. 4-8.

41. Zielinska, D.F., et al., Mapping N-Glycosylation Sites across Seven Evolutionarily Distant Species Reveals a Divergent Substrate Proteome Despite a Common Core Machinery. *Molecular Cell*, **2012**. 46(4): p. 542-548.

42. Sethuraman, N. and T.A. Stadheim, Challenges in therapeutic glycoprotein production. *Current Opinion in Biotechnology*, **2006**. 17(4): p. 341-346.

43. Baker, J.L., E. Celik, and M.P. DeLisa, Expanding the glycoengineering toolbox: the rise of bacterial N-linked protein glycosylation. *Trends in Biotechnology*, **2013**. 31(5): p. 49-59.

44. Agard, N.J. and C.R. Bertozzi, Chemical Approaches To Perturb, Profile, and Perceive Glycans. *Accounts of Chemical Research*, **2009**. 42(6): p. 788-797.

45. Varki, A., *Essentials of Glycobiology*. Cold Spring Harbor Laboratory Press: Cold Spring Harbor, NY, **2009**.

46. Ghazarian, H., B. Idoni, and S.B. Oppenheimer, A glycobiology review: carbohydrates, lectins and implications in cancer therapeutics. *Acta histochemica*, **2011**. 113(3): p. 236-247.

47. Bucior, I. and M.M. Burger, Carbohydrate–carbohydrate interactions in cell recognition. *Current opinion in structural biology*, **2004**. 14(5): p. 631-637.

48. Yang, J., B.C. Furie, and B. Furie, The biology of P-selectin glycoprotein ligand-1: its role as a selectin counterreceptor in leukocyte-endothelial and leukocyte-platelet interaction. *Thromb Haemost*, **1999**. 81(1): p. 1-7.

49. Lasky, L.A., Selectin-carbohydrate interactions and the initiation of the inflammatory response. *Annual review of biochemistry*, **1995**. 64(1): p. 113-140.

50. Kaltner, H. and B. Stierstorfer, Animal lectins as cell adhesion molecules. *Cells Tissues Organs*, **1998**. 161(1-4): p. 162-179.

51. Orlean, P., Congenital disorders of glycosylation caused by defects in mannose addition during N-linked oligosaccharide assembly. *Journal of Clinical Investigation*, **2000**. 105(2): p. 131.

52. Freeze, H.H. and M. Aebi, Molecular basis of carbohydrate-deficient glycoprotein syndromes type I with normal phosphomannomutase activity. *Biochimica et Biophysica Acta (BBA)-Molecular Basis of Disease*, **1999**. 1455(2): p. 167-178.

53. Friedman, B.A., et al., A comparison of the pharmacological properties of carbohydrate remodeled recombinant and placental-derived beta-glucocerebrosidase: Implications for clinical efficacy in treatment of Gaucher disease. *Blood*, **1999**. 93(9): p. 2807-2816.

54. Rothman, R.J., et al., Antibody-dependent cytotoxicity mediated by natural-killer-cells is enhanced by castanospermine-induced alterations of IgG glycosylation. *Molecular Immunology*, **1989**. 26(12): p. 1113-1123.

55. LaTemple, D.C., et al., Increased immunogenicity of tumor vaccines complexed with anti-Gal: Studies in knockout mice for alpha 1,3galactosyltransferase. *Cancer Research*, **1999**. 59(14): p. 3417-3423.

56. Paleček, E., et al., Electrochemistry of Nonconjugated Proteins and Glycoproteins. Toward Sensors for Biomedicine and Glycomics. *Chemical reviews*, **2015**. 115(5): p. 2045-2108.

57. Parekh, R., et al., Association of rheumatoid arthritis and primary osteoarthritis with changes in the glycosylation pattern of total serum IgG. **1985**.

58. Tousi, F., W.S. Hancock, and M. Hincapie, Technologies and strategies for glycoproteomics and glycomics and their application to clinical biomarker research. *Analytical Methods*, **2011**. 3(1): p. 20-32.

59. Mechref, Y., et al., Identifying cancer biomarkers by mass spectrometry-based glycomics. *Electrophoresis*, **2012**. 33(12): p. 1755-1767.

60. Duffy, M.J., Carcinoembryonic antigen as a marker for colorectal cancer: is it clinically useful. *Clinical chemistry*, **2001**. 47(4): p. 624-630.

61. Kim, E.H. and D.E. Misek, Glycoproteomics-based identification of cancer biomarkers. *International journal of proteomics*, **2011**.

62. Lin, L., et al., A bioorthogonal Raman reporter strategy for SERS detection of glycans on live cells. *Angewandte Chemie*, **2013**. 125(28): p. 7407-7412.

63. Wang, H., et al., Simultaneous Capture, Detection, and Inactivation of Bacteria as Enabled by a Surface-Enhanced Raman Scattering Multifunctional Chip. A*ngewandte Chemie International Edition*, **2015**. 54(17): p. 5132-5136.

64. Luo, P.G., et al., Selective interactions of sugar-functionalized single-walled carbon nanotubes with Bacillus spores. *ACS nano*, **2009**. 3(12): p. 3909-3916.

65. Campuzano, S., et al., Bacterial isolation by lectin-modified microengines. *Nano letters*, **2011**. 12(1): p. 396-401.

66. Walsh, C.T., S. Garneau-Tsodikova, and G.J. Gatto, Protein posttranslational modifications: the chemistry of proteome diversifications. *Angewandte Chemie International Edition*, **2005**. 44(45): p. 7342-7372.

67. Hovatta, O., et al., European scientific, ethical, and legal issues on human stem cell research and regenerative medicine. *Stem Cells*, **2010**. 28(6): p. 1005-1007.

68. Scott, C.T., et al., Federal policy and the use of pluripotent stem cells. *Nature Methods*, **2010**. 7(11): p. 866-867.

69. Chen, G., S. Ha, and R.R. Rustandi, Characterization of glycoprotein biopharmaceutical products by Caliper LC90 CE-SDS Gel Technology, in Glycosylation Engineering of Biopharmaceuticals. **2013**, Springer. p. 199-209.

70. Schmaltz, R.M., S.R. Hanson, and C.-H. Wong, Enzymes in the synthesis of glycoconjugates. *Chemical reviews*, **2011**. 111(7): p. 4259-4307.

71. Ye, J., Y. Chen, and Z. Liu, A boronate affinity sandwich assay: an appealing alternative to immunoassays for the determination of glycoproteins. *Angewandte Chemie International Edition*, **2014**. 53(39): p. 10386-10389.

72. Campbell, M.P., et al., GlycoBase and autoGU: tools for HPLC-based glycan analysis. *Bioinformatics*, **2008**. 24(9): p. 1214-1216.

73. Haslam, S.M., S.J. North, and A. Dell, Mass spectrometric analysis of N- and O-glycosylation of tissues and cells. *Current Opinion in Structural Biology*, **2006**. 16(5): p. 584-591.

74. Petrescu, A.J., et al., The solution NMR structure of glucosylated N-glycans involved in the early stages of glycoprotein biosynthesis and folding. *Embo Journal*, **1997**. 16(14): p. 4302-4310.

75. Liu, Y., A.S. Palma, and T. Feizi, Carbohydrate microarrays: key developments in glycobiology. *Biological Chemistry*, **2009**. 390(7): p. 647-656.

76. Brooks, S., M. Dwek, and U. Schumacher, Functional and molecular glycobiology. **2002**: Bios scientific.

77. Ferrier, R.J., Carbohydrate boronates. *Advances in Carbohydrate Chemistry and Biochemistry*, **1978**. 35: p. 31-80.

78. Royle, L., et al., Detailed structural analysis of N-glycans released from glycoproteins in SDS-PAGE gel bands using HPLC combined with exoglycosidase array digestions, in Glycobiology protocols. **2007**, Springer. p. 125-143.

79. Fisher, A.C., et al., Production of secretory and extracellular N-linked glycoproteins in Escherichia coli. *Applied and environmental microbiology*, **2011**. 77(3): p. 871-881.

80. Dam, T.K. and C.F. Brewer, Multivalent protein–carbohydrate interactions: isothermal titration microcalorimetry studies. *Methods in enzymology*, **2004**. 379: p. 107-128.

81. Critchley, P., et al., Carbohydrate–protein interactions at interfaces: synthesis of thiolactosyl glycolipids and design of a working model for surface plasmon resonance. Organic & biomolecular chemistry, **2003**. 1(6): p. 928-938.

82. Taga, A. and S. Honda, Determination of association constant of carbohydrate-protein interaction, in Capillary Electrophoresis of Carbohydrates. **2003**, Springer. p. 275-284.

83. Jiménez-Barbero, J. and T. Peters, NMR spectroscopy of glycoconjugates. **2003**: Wiley-Vch.

84. Pei, Z., et al., Study of real-time lectin–carbohydrate interactions on the surface of a quartz crystal microbalance. *Biosensors and Bioelectronics*, **2005**. 21(1): p. 60-66.

85. Lee, Y.C., Fluorescence spectrometry in studies of carbohydrate-protein interactions. *Journal of biochemistry*, **1997**. 121(5): p. 818-825.

86. Bucior, I. and M.M. Burger, Carbohydrate-carbohydrate interaction as a major force initiating cell-cell recognition. *Glycoconjugate journal*, **2004**. 21(3-4): p. 111-123.

87. Mensch, C., et al., Studying the Glycan Moiety of RNase B by Means of Raman and Raman Optical Activity. *ChemPhysChem*, **2014**. 15(11): p. 2252-2254.

88. Kneipp, K., et al., Surface-enhanced Raman spectroscopy in single living cells using gold nanoparticles. *Applied Spectroscopy*, **2002**. 56(2): p. 150-154.

89. Zhao, J., et al., Localized surface plasmon resonance biosensors. 2006.

90. Zhou, H., et al., SERS detection of bacteria in water by in situ coating with Ag nanoparticles. *Analytical chemistry*, **2014**. 86(3): p. 1525-1533.

91. Alkilany, A.M., et al., Gold nanorods: their potential for photothermal therapeutics and drug delivery, tempered by the complexity of their biological interactions. *Advanced drug delivery reviews*, **2012**. 64(2): p. 190-199.

92. Craig, A.P., A.S. Franca, and J. Irudayaraj, Surface-enhanced Raman spectroscopy applied to food safety. *Annual review of food science and technology*, **2013**. 4: p. 369-380.

93. Huefner, A., et al., Intracellular SERS nanoprobes for distinction of different neuronal cell types. *Nano letters*, **2013**. 13(6): p. 2463-2470.

94. Neng, J., et al., A versatile SERS-based immunoassay for immunoglobulin detection using antigen-coated gold nanoparticles and malachite green-conjugated protein A/G. *Biosensors and Bioelectronics*, **2010**. 26(3): p. 1009-1015.

95. Hage, D.S. and J. Cazes, Handbook of affinity chromatography. **2005**: CRC Press.

96. Mallia, A.K., et al., Preparation and use of a boronic acid affinity support for separation and quantitation of glycosylated hemoglobins. *Analytical Letters, Part B: Clinical and Biochemical Analysis*, **1981**. 14(8): p. 649-661.

97. Sharon, N. and H. Lis, Lectins, 2nd edn. 454 p. **2003**, Kluwer Academic Publishers, Dordrecht, The Netherlands.

98. Masárová, J., et al., Novel peptide surface for reversible immobilization of concanavalin A. *Journal of biochemical and biophysical methods*, **2004**. 60(2): p. 163-170.

99. Oliveira, M.D., M.T. Correia, and F.B. Diniz, Concanavalin A and polyvinyl butyral use as a potential dengue electrochemical biosensor. *Biosensors and Bioelectronics*, **2009**. 25(4): p. 728-732.

100. Safina, G., M. van Lier, and B. Danielsson, Flow-injection assay of the pathogenic bacteria using lectin-based quartz crystal microbalance biosensor. *Talanta*, **2008**. 77(2): p. 468-472.

101. Shen, Z., et al., Nonlabeled quartz crystal microbalance biosensor for bacterial detection using carbohydrate and lectin recognitions. *Analytical chemistry*, **2007**. 79(6): p. 2312-2319.

102. James, T.D. and S. Shinkai, Artificial receptors as chemosensors for carbohydrates, in Host-Guest Chemistry. **2002**, Springer. p. 159-200.

103. Fang, H., G. Kaur, and B. Wang, Progress in boronic acid-based fluorescent glucose sensors. *Journal of Fluorescence*, **2004**. 14(5): p. 481-489.

104. Duggan, P.J., Fructose-permeable liquid membranes containing boronic acid carriers. *Australian journal of chemistry*, **2004**. 57(4): p. 291-299.

105. Yang, W., et al., The first fluorescent diboronic acid sensor specific for hepatocellular carcinoma cells expressing sialyl Lewis X. *Chemistry & biology*, **2004**. 11(4): p. 439-448.

106. Duggan, P.J. and E.M. Tyndall, Boron acids as protective agents and catalysts in synthesis. *Journal of the Chemical Society, Perkin Transactions 1*, **2002**(11): p. 1325-1339.

107. Patterson, S., B.D. Smith, and R.E. Taylor, Tuning the affinity of a synthetic sialic acid receptor using combinatorial chemistry. *Tetrahedron letters*, **1998**. 39(20): p. 3111-3114.

108. Sun, F., et al., Stealth Surface Modification of Surface-Enhanced Raman Scattering Substrates for Sensitive and Accurate Detection in Protein Solutions. *ACS nano*, **2015**. 9(3): p. 2668-2676.

109. Rahimi, M., et al., Langmuir, Freundlich and Temkin Adsorption Isotherms of Propranolol on Multi-Wall Carbon Nanotubes. *Journal of Modern Drug Discovery and Drug Delivery Research*, **2014**. 2: p. 18-20.

110. Dada, A., et al., Langmuir, Freundlich, Temkin and Dubinin–Radushkevich isotherms studies of equilibrium sorption of Zn2+ unto phosphoric acid modified rice husk. I*OSR Journal of Applied Chemistry*, **2012**. 3(1): p. 38-45.

111. Raman, C.V., A change of wave-length in light scattering. *Nature*, **1928**. 121(3051): p. 619-619.

112. Willard, H., et al., High performance liquid chromatography: Methods and applications. Instrumental methods of analysis. 7th ed. New Delhi: CBS publishers and distributors, **2001**: p. 614-629.

113. Kaur, H., Instrumental methods of chemical analysis. **2010**: Pragati Prakashan.

114. Jickells, S. and A. Negrusz. Clarke's analytical forensic toxicology. in Annales de Toxicologie Analytique. **2008**. EDP Sciences.

115. Das, R.S. and Y. Agrawal, Raman spectroscopy: Recent advancements, techniques and applications. *Vibrational Spectroscopy*, **2011**. 57(2): p. 163-176.

116. Parker, S.F. and P.B. Tooke, The effect of apodisation and finite resolution on Fourier transform infrared and Raman spectra. *Spectrochimica Acta Part A: Molecular and Biomolecular Spectroscopy*, **1997**. 53(13): p. 2245-2252.

117. Jeanmaire, D.L. and R.P. Van Duyne, Surface Raman spectroelectrochemistry: Part I. Heterocyclic, aromatic, and aliphatic amines adsorbed on the anodized silver electrode. *Journal of Electroanalytical Chemistry and Interfacial Electrochemistry*, **1977**. 84(1): p. 1-20.

118. Albrecht, M.G. and J.A. Creighton, Anomalously intense Raman spectra of pyridine at a silver electrode. *Journal of the American Chemical Society*, **1977**. 99(15): p. 5215-5217.

119. Dijkstra, R., et al., Raman spectroscopy as a detection method for liquid-separation techniques. *TrAC Trends in Analytical Chemistry*, **2005**. 24(4): p. 304-323.

120. Kambhampati, P., et al., On the chemical mechanism of surface enhanced Raman scattering: experiment and theory. *The Journal of chemical physics*, **1998**. 108(12): p. 5013-5026.

121. Kreibig, U. and M. Vollmer, Optical properties of metal clusters. 1995.

122. Moskovits, M., Surface-enhanced Raman spectroscopy: a brief retrospective. *Journal of Raman Spectroscopy*, **2005**. 36(6-7): p. 485-496.

123. Haynes, C.L., A.D. McFarland, and R.P.V. Duyne, Surface-enhanced Raman spectroscopy. *Analytical Chemistry*, **2005**. 77(17): p. 338 A-346 A.

124. Zeisel, D., et al., Near-field surface-enhanced Raman spectroscopy of dye molecules adsorbed on silver island films. *chemical Physics letters*, **1998.** 283(5): p. 381-385.

125. Sharma, B., et al., SERS: materials, applications, and the future. Materials today, **2012**. 15(1): p. 16-25.

126. Van Duyne, R., J. Hulteen, and D. Treichel, Atomic force microscopy and surface-enhanced Raman spectroscopy. I. Ag island films and Ag film over polymer nanosphere surfaces supported on glass. *The Journal of chemical physics*, **1993**. 99(3): p. 2101-2115.

127. Boltasseva, A. and H.A. Atwater, Low-loss plasmonic metamaterials. *Science*, **2011**.

128. Kosuda, K., et al., Nanostructures and surface-enhanced Raman spectroscopy. *Comprehensive nanoscience and technology*, **2011**. 3: p. 263-301.

129. El-Ansary, A. and L.M. Faddah, Nanoparticles as biochemical sensors. *Nanotechnology, science and applications*, **2010**. 3: p. 65.

130. Hudson, S.D. and G. Chumanov, Bioanalytical applications of SERS (surface-enhanced Raman spectroscopy). *Analytical and bioanalytical chemistry*, **2009**. 394(3): p. 679-686.

131. Alvarez-Puebla, R.A. and L.M. Liz-Marzán, SERS-based diagnosis and biodetection. *Small*, **2010**. 6(5): p. 604-610.

132. Zhou, C.-H., et al., Enzyme-induced metallization as a signal amplification strategy for highly sensitive colorimetric detection of avian influenza virus particles. *Analytical chemistry*, **2014**. 86(5): p. 2752-2759.

133. Boisselier, E. and D. Astruc, Gold nanoparticles in nanomedicine: preparations, imaging, diagnostics, therapies and toxicity. *Chemical Society Reviews*, **2009**. 38(6): p. 1759-1782.

134. Saha, K., et al., Gold nanoparticles in chemical and biological sensing. *Chemical reviews*, **2012**. 112(5): p. 2739-2779.

135. Eustis, S. and M.A. El-Sayed, Why gold nanoparticles are more precious than pretty gold: noble metal surface plasmon resonance and its enhancement of the radiative and nonradiative properties of nanocrystals of different shapes. *Chemical Society Reviews*, **2006**. 35(3): p. 209-217.

136. Niazov, T., et al., DNAzyme-functionalized Au nanoparticles for the amplified detection of DNA or telomerase activity. *Nano Letters*, **2004**. 4(9): p. 1683-1687.

137. Giljohann, D.A., et al., Gold nanoparticles for biology and medicine. *Angewandte Chemie International Edition*, **2010**. 49(19): p. 3280-3294.

138. Wang, Z. and L. Ma, Gold nanoparticle probes. *Coordination Chemistry Reviews*, **2009**. 253(11): p. 1607-1618.

139. Sapsford, K.E., et al., Functionalizing nanoparticles with biological molecules: developing chemistries that facilitate nanotechnology. *Chemical reviews*, **2013**. 113(3): p. 1904-2074.

140. Han, G., P. Ghosh, and V.M. Rotello, Functionalized gold nanoparticles for drug delivery. **2007**.

141. Rosi, N.L., et al., Oligonucleotide-modified gold nanoparticles for intracellular gene regulation. *Science*, **2006**. 312(5776): p. 1027-1030.

142. Maier, I., et al., Optical resonance-enhanced absorption-based near-field immunochip biosensor for allergen detection. *Analytical chemistry*, **2008**. 80(8): p. 2694-2703.

143. Turkevich, J., P. Stevenson, and J. Hillier, The size and shape factor in colloidal systems. *A General Discussion of the Faraday Society*, **1951**. 11: p. 55.

144. Frens, G., Controlled nucleation for the regulation of the particle size in monodisperse gold suspensions. *Nature*, **1973**. 241(105): p. 20-22.

145. Lattes, A., et al., Formamide, a water substitute in micelles and microemulsions xxx structural analysis using a diels-alder reaction as a chemical probe. *Tetrahedron*, **1987**. 43(7): p. 1725-1735.

146. Sohn, B.-H., et al., Directed self-assembly of two kinds of nanoparticles utilizing monolayer films of diblock copolymer micelles. Journal of the *American Chemical Society*, **2003**. 125(21): p. 6368-6369.

147. Chen, F., G.-Q. Xu, and T.A. Hor, Preparation and assembly of colloidal gold nanoparticles in CTAB-stabilized reverse microemulsion. *Materials Letters*, **2003**. 57(21): p. 3282-3286.

148. Mallick, K., Z. Wang, and T. Pal, Seed-mediated successive growth of gold particles accomplished by UV irradiation: a photochemical approach for size-controlled synthesis. *Journal of Photochemistry and Photobiology A: Chemistry*, **2001**. 140(1): p. 75-80.

149. Pol, V., A. Gedanken, and J. Calderon-Moreno, Deposition of gold nanoparticles on silica spheres: a sonochemical approach. *Chemistry of materials*, **2003**. 15(5): p. 1111-1118.

150. Henglein, A. and D. Meisel, Radiolytic control of the size of colloidal gold nanoparticles. *Langmuir*, **1998**. 14(26): p. 7392-7396.

151. Nakamoto, M., M. Yamamoto, and M. Fukusumi, Thermolysis of gold (I) thiolate complexes producing novel gold nanoparticles passivated by alkyl groups. *Chemical Communications*, **2002**(15): p. 1622-1623.

152. Bellapadrona, G., et al., Optimization of localized surface plasmon resonance transducers for studying carbohydrate–protein interactions. *Analytical chemistry*, **2011**. 84(1): p. 232-240.

153. Medley, C.D., et al., Gold nanoparticle-based colorimetric assay for the direct detection of cancerous cells. *Analytical chemistry*, **2008**. 80(4): p. 1067-1072.

154. Lee, P. and D. Meisel, Adsorption and surface-enhanced Raman of dyes on silver and gold sols. *The Journal of Physical Chemistry*, **1982**. 86(17): p. 3391-3395.

155. Chen, Y., et al., Electronic detection of lectins using carbohydrate-functionalized nanostructures: graphene versus carbon nanotubes. *ACS nano*, **2011**. 6(1): p. 760-770.

156. Chen, D., H. Feng, and J. Li, Graphene oxide: preparation, functionalization, and electrochemical applications. *Chemical reviews*, **2012**. 112(11): p. 6027-6053.

157. Chen, Y., A. Star, and S. Vidal, Sweet carbon nanostructures: carbohydrate conjugates with carbon nanotubes and graphene and their applications. *Chemical Society Reviews*, **2013**. 42(11): p. 4532-4542.

158. Cao, J.-T., et al., Quantum dots-based immunofluorescent microfluidic chip for the analysis of glycan expression at single-cells. *Analytical chemistry*, **2012**. 84(22): p. 10097-10104.

159. Sun, X., et al., Size-controlled synthesis of magnetite (Fe3O4) nanoparticles coated with glucose and gluconic acid from a single Fe (III) precursor by a sucrose bifunctional hydrothermal method. *The Journal of Physical Chemistry C*, **2009**. 113(36): p. 16002-16008.

160. Sun, S. and H. Zeng, Size-controlled synthesis of magnetite nanoparticles. *Journal of the American Chemical Society*, 2002. 124(28): p. 8204-8205.

161. Park, J., et al., One-nanometer-scale size-controlled synthesis of monodisperse magnetic Iron oxide nanoparticles. *Angewandte Chemie*, **2005**. 117(19): p. 2932-2937.

162. Chin, A.B. and I.I. Yaacob, Synthesis and characterization of magnetic iron oxide nanoparticles via w/o microemulsion and Massart's procedure. *Journal of materials processing technology*, **2007.** 191(1): p. 235-237.

163. Albornoz, C. and S.E. Jacobo, Preparation of a biocompatible magnetic film from an aqueous ferrofluid. *Journal of magnetism and magnetic materials*, **2006**. 305(1): p. 12-15.

164. Kim, E.H., et al., Synthesis of ferrofluid with magnetic nanoparticles by sonochemical method for MRI contrast agent. *Journal of Magnetism and Magnetic Materials,* **2005**. 289: p. 328-330.

165. Salazar-Alvarez, G., M. Muhammed, and A.A. Zagorodni, Novel flow injection synthesis of iron oxide nanoparticles with narrow size distribution. *Chemical engineering science*, **2006**. 61(14): p. 4625-4633.

166. Basak, S., D.-R. Chen, and P. Biswas, Electrospray of ionic precursor solutions to synthesize iron oxide nanoparticles: modified scaling law. *Chemical engineering science*, **2007**. 62(4): p. 1263-1268.

167. Cornell, R.M. and U. Schwertmann, The iron oxides: structure, properties, reactions, occurrences and uses. **2006**: John Wiley & Sons.

168. Gribanov, N., et al., Physico-chemical regularities of obtaining highly dispersed magnetite by the method of chemical condensation. *Journal of Magnetism and Magnetic Materials*, **1990**. 85(1): p. 7-10.

169. Sun, S., et al., Monodisperse FePt nanoparticles and ferromagnetic FePt nanocrystal superlattices. *Science*, **2000**. 287(5460): p. 1989-1992.

170. Lee, J.-H., et al., Artificially engineered magnetic nanoparticles for ultra-sensitive molecular imaging. *Nature medicine*, **2007**. 13(1): p. 95-99.

171. Haun, J.B., et al., Magnetic nanoparticle biosensors. *Wiley Interdisciplinary Reviews: Nanomedicine and Nanobiotechnology*, **2010**. 2(3): p. 291-304.

172. Yu, M.K., et al., Drug-loaded superparamagnetic iron oxide nanoparticles for combined cancer imaging and therapy in vivo. *Angewandte Chemie International Edition,* **2008**. 47(29): p. 5362-5365.

173. Arruebo, M., et al., Magnetic nanoparticles for drug delivery. *Nano today*, **2007**. 2(3): p. 22-32.

174. Dobson, J., Gene therapy progress and prospects: magnetic nanoparticle-based gene delivery. *Gene therapy*, **2006**. 13(4): p. 283-287.

175. Bao, F., J.-L. Yao, and R.-A. Gu, Synthesis of magnetic Fe2O3/Au core/shell nanoparticles for bioseparation and immunoassay based on surface-enhanced Raman spectroscopy. *Langmuir*, **2009**. 25(18): p. 10782-10787.

176. Sun, C., J.S. Lee, and M. Zhang, Magnetic nanoparticles in MR imaging and drug delivery. *Advanced drug delivery reviews*, **2008**. 60(11): p. 1252-1265.

177. Chertok, B., et al., Iron oxide nanoparticles as a drug delivery vehicle for MRI monitored magnetic targeting of brain tumors. *Biomaterials*, **2008**. 29(4): p. 487-496.

178. Cunningham, M., Microsuspension polymerization of methyl methacrylate. *Polymer Reaction Engineering*, **1999**. 7(2): p. 231-257.

179. Salimi, K., et al., Highly selective magnetic affinity purification of histidine-tagged proteins by Ni 2+ carrying monodisperse composite microspheres. *RSC Advances*, **2017**. 7(14): p. 8718-8726.

180. Usta, D.D., et al., A boronate affinity-assisted SERS tag equipped with a sandwich system for detection of glycated hemoglobin in the hemolysate of human erythrocytes. *ACS applied materials & interfaces*, **2016**. 8(19): p. 11934-11944.

181. Heraldy, E., Y. Hidayat, and M. Firdaus. The langmuir isotherm adsorption equation: The monolayer approach. in *IOP Conference Series: Materials Science and Engineering*. **2016**. IOP Publishing.

182. Sun, X.-Y., et al., Boronate-affinity based magnetic molecularly imprinted nanoparticles for the efficient extraction of the model glycoprotein horseradish peroxidase. *Microchimica Acta*, **2017**. 184(10): p. 3729-3737.

183. Luo, J., et al., Double Recognition and Selective Extraction of Glycoprotein Based on the Molecular Imprinted Graphene Oxide and Boronate Affinity. *ACS Applied Materials & Interfaces*, **2017**. 9(8): p. 7735-7744.

184. Zhang, J., et al., Novel functionalized poly (glycidyl methacrylate-co-ethylene dimethacrylate) microspheres for the solid-phase extraction of glycopeptides/glycoproteins. *Journal of separation science*, **2017**. 40(5): p. 1107-1114.

185. Hao, Y., et al., A facile and general approach for preparation of glycoprotein-imprinted magnetic nanoparticles with synergistic selectivity. *Talanta*, **2016**. 153: p. 211-220.

186. Li, H., et al., Binary boronic acid-functionalized attapulgite with high adsorption capacity for selective capture of nucleosides at acidic pH values. *Microchimica Acta*, **2016**. 183(5): p. 1779-1786.

187. Zhang, J., Y.l. Ni, and X.l. Zheng, Preparation of poly (vinylphenylboronic acid) chain grafted poly (glycidylmethacrylate-co-ethylenedimethacrylate) beads for the selective enrichment of glycoprotein. *Journal of separation science*, **2015**. 38(1): p. 81-86.

188. Driskell, J.D., C.G. Larrick, and C. Trunell, Effect of hydration on plasmonic coupling of bioconjugated gold nanoparticles immobilized on a gold film probed by surface-enhanced Raman spectroscopy. *Langmuir*, **2014**. 30(22): p. 6309-6313.

189. Ouyang, L., et al., A surface-enhanced Raman scattering method for detection of trace glutathione on the basis of immobilized silver nanoparticles and crystal violet probe. *Analytica chimica acta*, **2014**. 816: p. 41-49.

190. Sun, X., et al., Functionalized aligned silver nanorod arrays for glucose sensing through surface enhanced Raman scattering. *RSC Advances*, **2014**. 4(45): p. 23382-23388.

191. Severyukhina, A.N., et al., Nanoplasmonic chitosan nanofibers as effective SERS substrate for detection of small molecules. *ACS applied materials & interfaces*, **2015**. 7(28): p. 15466-15473.

192. Huang, Y.-F., et al., Surface-enhanced Raman spectroscopic study of p-aminothiophenol. *Physical Chemistry Chemical Physics*, **2012**. 14(24): p. 8485-8497.

193. Bie, Z., et al., Boronate-Affinity Glycan-Oriented Surface Imprinting: A New Strategy to Mimic Lectins for the Recognition of an Intact Glycoprotein and Its Characteristic Fragments. *Angewandte Chemie International Edition*, **2015**. 54(35): p. 10211-10215.

CURRICULUM VITAE

Credentials

Name, Surname : Büşra Bilgiç

Place of Birth : Fatih / İstanbul

Marital Status : Single

E-mail : busra.bilgic@tubitak.gov.tr

Address : Hacettepe University, Chemical Engineering Department, Research Laboratory 17, Beytepe, Ankara, Turkey

Education

High School : Nermin Mehmet Çekiç Anatolian High School, Ankara (2005-2009)

BSc. : Hacettepe University, Chemical Engineering Department, Ankara (2009-2014)

BA : Anadolu University, Business Administration, Open Education, Eskişehir (2012-2016)

MSc. : Hacettepe University, Chemical Engineering Department, Ankara (2014-2018)

Foreign Languages

English : Advanced

Italian : Moderate

German : Beginner

Work Experience

August 2015 – *: Quality Assurance Engineer, Research Engineer,* TÜBİTAK SAGE

June 2012 *: Intern,* Knauf Insulation Isolation, Industry and Trade Inc., Ankara

Areas of Experiences

Biochemical and Bioprocess Engineering

Affinity Chromatography

Adsorption Kinetics and Isotherms

Quality Assurance

Quality Management System

Defense Industry

System Engineering

Projects and Budgets

-

Publications

Büşra Bilgiç, Khaliunsarnai Tsogtbaatar, Çiğdem Kip, Ali Tuncel, Eda Çelik, “Selective enrichment of Immunoglobulin G from complex media using boronic acid functionalized magnetic SiO_2 microspheres” *(in preparation)*

Oral and Poster Presentations

Büşra Bilgiç, Kouroush Salimi, D. Deniz Usta, Eda Çelik, Ali Tuncel “ Low Level Detection of Glycoproteins by Boronic Acid Functionalized SERS Tag” (*in preparation*)

HACETTEPE UNIVERSITY
GRADUATE SCHOOL OF SCIENCE AND ENGINEERING
THESIS/DISSERTATION ORIGINALITY REPORT

HACETTEPE UNIVERSITY
GRADUATE SCHOOL OF SCIENCE AND ENGINEERING
TO THE DEPARTMENT OF CHEMICAL ENGINEERING

Date: 11/02/2018

Thesis Title / Topic: Selective Enrichment of Glycoproteins Using Magnetic Microspheres And Their Sensitive Detection with Surface Enhanced Raman Spectroscopy

According to the originality report obtained by myself/my thesis advisor by using the *Turnitin* plagiarism detection software and by applying the filtering options stated below on 11/02/2018 for the total of 63 pages including the a) Title Page, b) Introduction, c) Main Chapters, d) Conclusion sections of my thesis entitled as above, the similarity index of my thesis is 10 %.

Filtering options applied:

1. Bibliography/Works Cited excluded
2. Quotes included
3. Match size up to 5 words excluded

I declare that I have carefully read Hacettepe University Graduate School of Sciene and Engineering Guidelines for Obtaining and Using Thesis Originality Reports; that according to the maximum similarity index values specified in the Guidelines, my thesis does not include any form of plagiarism; that in any future detection of possible infringement of the regulations I accept all legal responsibility; and that all the information I have provided is correct to the best of my knowledge.

I respectfully submit this for approval.

11.02.2018
B. Bilgiç
Date and Signature

Name Surname:	Büşra Bilgiç
Student No:	N14122218
Department:	Chemical Engineering
Program:	Chemical Engineering - Master of Science
Status:	☒ Masters ☐ Ph.D. ☐ Integrated Ph.D.

ADVISOR APPROVAL

APPROVED.

Asst. Prof. Dr. Eda Çelik Akdur
(Title, Name Surname, Signature)